

Doctoral Dissertation

Mohd Ruzeiny Bin Kamaruzzaman

15 December 2023

Laboratory for Cyber Resilience
Graduate School of Science and Technology
Nara Institute of Science and Technology (NAIST)

Air Traffic Control (ATC) Resilient Response Model Amid Automatic Dependent Surveillance-Broadcast (ADS-B) Ghost Aircraft Spoofing Cyberattack

Mohd Ruzeiny Bin Kamaruzzaman

A Doctoral Dissertation
submitted to Graduate School of Science and Technology,
Nara Institute of Science and Technology (NAIST)
in partial fulfilment of the requirements for the degree of
Doctor of Engineering

Mohd Ruzeiny Bin Kamaruzzaman

Thesis Committee:
Professor Youki Kadobayashi (Supervisor)
Professor Shoji Kasahara (Co-supervisor)
Professor Yuichi Hayashi (Co-supervisor)
Associate Professor Yuzo Taenaka (Co-supervisor)
Associate Professor Doudou Fall (Co-supervisor)

Abstract

As Automatic Dependent Surveillance-Broadcast (ADS-B) is being mandated by more Air Navigation Service Providers (ANSP) globally, the unchanging openness and unencrypted nature of the system pose a constant significant threat of cyberattack in the form of false message injection to the air traffic surveillance system. Among the attack types within the category of false message injection which is easy to launch and potentially causing high negative impact to Air Traffic Management (ATM), is the Ghost Aircraft Spoofing (GAS) attack that can be easily launched via a software-defined radio device targeting a ground station. It is considerably less complex and does not require a high level of skills for effective execution. This attack type aims to create confusion to the Air Traffic Controller (ATC) by exploiting the already degraded air traffic surveillance capability. The immediate impact of this attack is delayed aircraft arrivals and departures in the context of flight operations. This situation happens when legit real aircraft flying near the ghost aircraft will need to fly away or change its flightpath to avoid mid-air collision and other hazards. Changing flightpath or slowing down will certainly incur additional time to the flight, resulting in imminent delay. Moreover, prolonged attacks will cause greater impact, disrupting airport operations related to ground movement for taxiing-in and taxiing-out. ATC will suspend departures not just because of the posed risk and threat to climbing aircraft, but also to make way for landing aircraft. Uncertainties from GAS will make the departures continue to be suspended and the total number of aircraft affected on the airport ground will rise.

To mitigate this incident, this dissertation first, analyze the immediate impact to the arriving aircraft which are in descent phase, and later the cascading effects it brings to the departure operations and aircraft ground movement in quantitative terms of accumulation of delay time and number of affected aircraft. The methodology used for quantification is through statistical data from formation of First-In-First-Out (FIFO) queues representing pertinent queuing functions applied by the ATC in the entire Arrival-Ground Movement-Departure (AGMOD) dynamics. After the impact and cascading effects have been identified and proven, this dissertation proposes two types of mitigation plan based on possible ATC responses to reduce the delay time for arriving and departing aircraft. The arriving aircraft will be guided with a tactical framework to continuously explore ideal deviational flight path that is shortest at that point of time and with less to no interference by other aircraft. The second proposed response plan focuses on the departure sequencing by countering uncertainties optimistically through synchronous aircraft movement for taxiing-out. The proposed approach records

positive results with more aircraft at several designated taxiway zones close to the runway compared to conventional approaches which permit departures based on original schedule time prior the GAS attack or based on prioritization for aircraft closest to the runway to move ahead of others.

This dissertation demonstrates the advantages of the application of 'best shortest path' theory in the arriving aircraft scenario and customized queueing engine to facilitate the taxiing-out movement. In both scenarios, delay time managed to be reduced compared to the conventional approaches that would be taken by the ATC. In overall, the proposed ATC response as elaborated by this dissertation promotes resilient ATM and in line with the main objective of the ATC, which is to facilitate safe and smooth movement of air traffic.

Keywords:

ghost aircraft spoofing, aircraft arrival, aircraft ground movement, aircraft departure, air traffic control, air traffic management, tactical maneuvering, trajectory benchmarking, modulated synchronous taxiing, departure sequencing, cyberattack

Contents

1. Introduction	7-12
1.1 Background.....	7-9
1.2 Problem Statement.....	9-10
1.3 Research Objectives and Contributions.....	11-12
1.3.1 Research Objectives.....	11-12
1.3.2 Research Contributions.....	12
2. Related Works	13-17
2.1 Queue Formation as Impact Assessment Methodology.....	13-14
2.2 Risk of Mid-Air Collision.....	14-16
2.3 Elements of Uncertainties.....	16-17
3. GAS – High-Impact Attack Scenario from the ATC’s Perspective	18-24
3.1 High Impact Attack Scenario.....	18-24
4. GAS and its Cascading Effects to AGMOD Dynamics	24-36
4.1 ATC Responses to GAS.....	24-26
4.2 Simulation of ATC Responses.....	26-31
4.3 Analysis of Simulation Results.....	31-35
4.4 Discussion.....	35-36
5. Reducing Delay in Flights Arrival	36-42
5.1 Scenario Background.....	37-38
5.2 Simulation of Tactical Trajectory Benchmarking.....	39
5.3 Simulation Results.....	40-42
5.4 Discussion.....	42
6. Reducing Delay in Departure	42-67
6.1 Synchronous Taxiing Approach and Discrete Events Modelling.....	43-51
6.2 Attack Based Simulation of MSTA, T-P and L-P.....	51-56
6.3 Simulation Results and Analysis.....	56-62
6.4 Discussion.....	63-67

7. Future Works	67-71
7.1 Minimizing Impact to AGMOD.....	67-69
7.2 Enhancing Implementation of MSTA.....	69-71
8. Conclusion	71-72
9. References	73-80
10. Appendices	81-102

1. Introduction

1.1 Background

The introduction of ADS-B for flight surveillance protocol in the early last decade was due to the recognition of it as an emerging technology that could help to instill reliability and cost efficiency in managing air traffic [1]. The effectiveness of ADS-B in complementing the legacy systems that mainly depend on radar coverage for aerial lateration has encouraged many ANSPs to make it as a standard to be fulfilled by aircraft flying over their regulated airspace by certain time in the future [2]. However, the advantages that are driving its worldwide implementation are shadowed by a few shortcomings as open and unencrypted channels have made ADS-B vulnerable to certain types of cyberattacks. For example, a spoofing type of attack - ghost aircraft injection, which is targeting the ground station, possesses the capability to cause sheer disruption to the air traffic management despite its easy execution [3]. ADS-B based attacks are mainly trying to confuse ATC by compromising the broadcasts' confidentiality, integrity, and availability [4]. Impact from such attacks theoretically can be as common as flight delays or at worst, as catastrophic as mid-air collisions [5].

To probe further the claim on how these ADS-B based attacks are disrupting the ATM, particularly in propagating delays to 'Arrivals-Ground Movement-Departures' (AGMOD) dynamics, this dissertation analyzes key discrete events during AGMOD by quantifying delays in metrics of numbers of affected aircraft and amount of time step delays. These calculations are made with the assumption that ADS-B spoofing is launched during time of emergencies where surveillance capabilities such as radar detection and lateration techniques are unavailable, causing data fusion's blackout. Whenever such a grave situation happens, the air traffic controls would have to revert to the procedural control in guiding aircraft in the affected sector with safety concern as the upmost priority.

For that purpose, this research collaborated with the Civil Aviation Authority of Malaysia (CAAM) in assessing the cascading impact of the GAS attack and then forming mitigations to reduce the occurred delay in both arrival and departure. For reducing delay in arrival, this research proposes a framework that assesses the trajectory of a ghost aircraft and the risks of collision with a real aircraft which is heading towards an airport to begin approach procedures. By using the ADS-B data provided by CAAM, this research can demonstrate how real traffic is impacted by ghost aircraft occurrence. After learning the immediate

impact, this dissertation discussed a maneuvering framework for descending aircraft with safety and efficiency as its clear quality objectives.

This research also discussed the possible optimization to the perturbed states of AGMOD dynamics. The scope of optimization is an ATC response technique or approach that should not become too dependent on technological advancements such as machine learning and data fusion algorithms as the main problems discussed in this paper. These systems capabilities are greatly affected by the cyberattacks and subsequently would leave us with limited capabilities and options. Nevertheless, we all agree on the type of capability that would be able to provide adequate Situational Awareness (SA) of the current air traffic during cyber incidences. It would be a more desired contingency plan in ensuring the ATM's operational resiliency. Only a few have explored the operational resilience of ATM through an effective contingency plan whenever hit by cyberattacks. ATM relies heavily on electronic systems for processing a huge amount of data [6]. Therefore, disruptions to its capability to execute its critical function would eventually disrupt the flow of air traffic. A compromised cyber-physical system would be devastating as public safety and national economy would also face serious impact as described in [7]. Furthermore, research on radar or other surveillance systems jamming technologies, for instance [8] and [9], is being highly pursued by certain quarters in the name of ensuring public safety and security. There are possibilities that if these technologies are manipulated by adversarial entities, they could cause havoc, even to the extent of causing physical damages to the critical infrastructures and leading to human casualties. These consequences have become the motivation for this research to identify impact of such attacks, to understand their immediate impact on ATM, and to explore viable mitigation techniques to prevent such catastrophic event from happening.

Besides that, although numerous studies such as [10] and [11] have shown how GAS attack bring chaos to ATC's surveillance system, studies that explored the problem from the context of aircraft ground movement dynamics, such as taxiing for departure are still lacking. Even though there were studies done on occurred perturbations during aircraft movement on taxiway in [12] and [13], the studied disruptions were not caused by cyberattack. Therefore, we took the initiative to analyze the gap in the knowledge to find measures to mitigate disruptive impact caused by ghost aircraft spoofing in the ADS-B-In system. For this purpose, the collaboration with Civil Aviation Authority of Malaysia (CAAM) has been extended into formulating a taxiing approach for departure operations at the Kuala Lumpur International Airport (KLIA) to identify possible technique to cut delay originating from GAS.

As part of the achievement out of the collaboration with CAAM, this dissertation has come out with the Modulated Synchronous Taxiing Approach

(MSTA) algorithm. The outcome of the done research was encouraging as the approach managed to bring more aircraft to the Pre-Runway Queue (PRQ) compared to conventional First Come First Serve (FCFS) sequencing technique during the ongoing spoofing incidence. Therefore, this dissertation will elaborate how the proposed mitigations can help to reduce delay caused by the GAS during period of uncertainties by using official ADS-B data supplied by CAAM and publicly available departure sequencing schedules published by Malaysia Airport Holdings (Limited).

1.2 Problem Statement

GAS attack on ADS-B ground station in an integrated attack scenario which is also experiencing degradation of radar surveillance and multilateration sensors will cause serious confusion to the ATC especially in managing air traffic close to the terminal airspace involving flight arrivals and departures. The confusion experienced by the ATC will trigger standard response by requesting airport-inbound flights to reduce speed and maintain safe separation with other surrounding aircraft including the ghost aircraft. Creating impromptu separation as between a legit and the ghost aircraft, in most cases, will add extra flying time either in climbing or descending phase. In more serious situations, the ATC must reroute affected inbound flights to alternative airports for safety and economic reasons.

Although the current emergency procedures provide guidance to deal with uncertainties arose from GAS attack, its impact on the overall traffic management especially when both flight arrivals at and departures from the affected airports will be substantially delayed. The delay incurred will vary, depending on the current airport situation by looking at its ground movement dynamics. The overall ground movement dynamics consists of aircraft moving on the taxiway either arriving or departing and aircraft which are currently parked or occupying a gate. Thus, GAS attacks will not only be affecting the arrival and departure phase but will also disrupt the movement and lead to congestion at certain parts of the taxiway. Event of disruption to the entire airport Arrival-Ground Movement-Departure dynamics (AGMOD) can be viewed as a series of cascading effects that first concurrently disrupting the arrivals and departures and later building up congestion on the airport ground due to increased gate occupancy and halted departure movement of taxiing-out aircraft. As GAS prolongs, the uncertainties surrounding the ATM will increase as certain airspace sectors are closed to alleviate safety risks. During this phase, the ATC will relentlessly try to verify validity of the threats to flight operations by monitoring the surveillance system and conducting visual checks which is also assisted by landing aircraft pilots. Duration of this process depends

heavily on the complexity of the GAS attack and existing air traffic volume that needs to be handled. Even though the ATC might be able to assist the arriving aircraft to safely land at the airport during this cyber incident, it is the opposite for aircraft on the taxiway that are trying to takeoff. Suspension of departures indefinitely will worsen the AGMOD dynamics with congestion build-ups starting the gates right to the taxiway for taxiing-out and up till the runway entrance.

Today's solutions for false message injection type of attack are more into preventive approach which require modifications and updates to the fusion algorithm. Studies such [14] as focused on detection of anomalies in the broadcasted data for possible intrusion injection. There are also studies which experiment encryption as a preventive method to secure the open channel transmission that ends up becoming a private channel, inhibiting cross validation by other data sources from different surveillance techniques. While most previous studies, such as [15] and [16] demonstrated how GAS attacks can bring chaos to ATC's surveillance system, only a few have explored the operational resilience of ATM through an effective contingency plan whenever hit by cyberattacks. ATM relies heavily on electronic systems for processing a huge amount of data [17]. Therefore, disruptions to its capability to execute its critical function would eventually disrupt the flow of air traffic. The cyber-physical system of the ATM domain would experience a huge blow if any of its cyber components such as the ADS-B surveillance system are compromised as described in [18].

Only a small amount of research investigated reactive or response-type approaches to the GAS attack. [19] is among the research that analyzed the impact of GAS attack and proposed an ATC's response plan which is engineered based on queuing dynamics. Despite both preventive and reactive solutions being proposed to deal with ADS-B intrusions, research that investigates the ATM's resiliency during and post attack is still lacking. As flight operations consist of arrival and departure, contingency measures are highly needed to mitigate the impact to the flight path and trajectory. The same goes for the ground movement of aircraft for departure, delays due to uncertainties affecting airspace regions. A specific approach is required to handle the GAS attack impact on departures as current existing procedures may not be effective in handling the uncertainties arose from airspace regions closure and not yielding the optimum results in the context of impact mitigation to the departure operations resiliency.

1.3 Research Objectives and Contributions

The objective of this dissertation is to analyze quantitatively GAS attack impact to the airport arriving aircraft and the cascading effects to the AGMOD dynamics. The analysis helps to determine the magnitude of the impact based on delay time incurred to the entire AGMOD dynamics and how many aircraft affected based on current system state. After determining the occurred impacts, this dissertation proposes mitigation techniques through two dedicated ATC response procedures. First, for affected aircraft during descent phase (prior entering approaching phase). This response plan's framework consists of air safety element that maintains the mandatory separation minima of 5 nm laterally and two thousand feet vertically. The underlying principle is for the ATC to safely guide the affected aircraft to evade the ghost aircraft flying path while at the same time, consistently exploring linear shortest path with least interference as its deviational trajectory. This tactical response aims to avoid unnecessary and excessive deviations that will increase arrival time delay. Second, this dissertation focuses on reducing aircraft departure delay time by demonstrating the efficiency of modulated synchronous taxiing movement during the GAS attack. This approach is crafted to specifically capitalizes the available 'safe window' (a brief period) whereby certain air space region is free from GAS occurrence and relatively safe to allow flight takeoffs and for aircraft to climb through these air space regions.

The summary of our objectives and contributions is as follows:

1.3.1 Research Objectives:

- i. to analyze the impact and existence of cascading effects of GAS quantitatively through statistics recorded by queues representing pertinent points and phases along the entire AGMOD system dynamics.
- ii. to determine impact magnitude in different scenarios, particularly in a baseline scenario (no GAS), low density attack (little GAS occurrence), and high-density attack (more GAS and at higher frequency).
- iii. to study the characteristics and behavior of high impact GAS attack through expert inputs from the ATC.

- iv. to propose a mitigation technique to reduce delay time in arrival by preventing excessive deviation from the original path due to occurrence of ghost aircraft through an ATC level tactical response plan.
- v. to propose a mitigation technique to reduce delay time in departure sequencing by considering the findings on (iii) above.
- vi. to craft the mitigation technique of (v) above to be more flexible and has high adoptability by different types of airports.

1.3.2 Research Contributions:

- i. a GAS impact assessment methodology using accumulative delay time and number of affected aircraft as quantification metrics.
- ii. determination of GAS impact magnitude based on differently parameterized scenarios.
- iii. identification of characteristics of high impact GAS attack that can be studied in various aspects.
- iv. a mitigation technique to reduce delay time in arrival through the ATC tactical level response plan's framework that benchmarks the ghost aircraft trajectory whilst maintaining safe separation and linear shortest path with little interference as the recommended deviation.
- v. a mitigation technique to reduce delay time in departure through the modulated synchronous taxiing that capitalizes on the available time of inexistence of the GAS attack.
- vi. mitigation algorithm of (v) above that is crafted based on time taken by each aircraft to reach the designated physical zones to practically measure progression on the taxiway towards the runway.

2. Related Works

2.1 Queue Formation as Impact Assessment Technique

According to [20], Message Injection - Ground Station Ghost Inject is categorized as an attack type with low complexity but with high severity, thus the risk posed by this attack type is far higher than other attack types and should be addressed appropriately. This type of attack purposely broadcasts fake ADS-B messages containing data resembling a genuine ADS-B message, for example speed, location, trajectory, and aircraft identifier code, with the intention to confuse ATC [21]. In response, ATC is anticipated to adhere to the Standard Operating Procedures (SOP) in handling such irregularities. Previous research attempted to demonstrate ADS-B based attacks' impact on the en-route aircraft, flying over specified air sectors [19]. The methodology used was based on a 'dynamic network of queues' approach after a rescheduling action has taken place using formal methods and furthermore extended with a graph level vulnerability metrics to assess how the affected air sector suffers from the route manipulations. [19] also compared three different threat scenarios and which one would cause greatest delay. In the simulated attacks, the author concluded that spoofing has turned out as the one causing the longest delay. Although [19] and our study had similar objective which is to quantify threat impacts and leveraging queues functionalities, we adopted different 'queue-server' deployment design, approached the problem through AGMOD dynamics and used different areas for quantification.

As part of a holistic approach to enhance capability of cyber security risk analysis, having the capability to assess possible emerging developments during and post incident would be advantageous in drafting effective mitigation plans [22]. On selecting the methodology to construct the timeline in cascading effects, [23] showed how modelling of cascading events is preferred to be based on the blending of deterministic and probabilistic approaches in handling human influences. Besides that, the existing dynamic dependencies within the model must be accounted for to accommodate unforeseen circumstances. Apart of the researches in this dissertation contains similarities on recognizing roles played by human agents which is in the context of AGMOD dynamics and ATC responses in verifying legitimacy of the air traffics are key events to be analyzed. Another method that solely investigated airport delay propagation is based on ripple effects experienced by congested airports during specific period. The combination

of a queue engine and an algorithm has enabled the model to respond to the stochastic events of supply and demand availability at the macro level [24].

In AGMOD Dynamics, queueing mechanics is aspired by current practice of a 'close-to-real' air traffic control approach. Basically, during emergency situations, the ATC under structured guidance has the discretion on how to realign the queues which is by evaluating priorities of each aircraft. This is among the main attributes of a resilient ATC model, incorporating ATC possible responses in the event of emergencies. In finding tenable solutions to delay propagation problems, several previous studies had focused on optimizing ground movements while waiting for traffic build ups to ease for a clear takeoff. [25] did some comparison on a few optimization strategies encompassing the pre-tactical and tactical phase of flight operations. The authors simulated a ground-based delay for the pre-tactical and as for the tactical phase, an en-route delay was analyzed. The results vary between the optimization techniques which were based on different types of stakeholders' interests. Another study [26] has proposed a model for optimizing dynamics of ground movement by cutting short the time taken for taxiing out aircraft. It applied a scenario based on a real airport and in the end, introduced a back pressuring algorithm to minimize costs especially on taxiing time. Looking at both literature and others which are quite similar, none have explained how the dynamics can be improved during incidences caused by disrupted systems and emergencies such as cyberattacks. Most of today's solutions including machine learning algorithms for intrusion detection might be able to counter cyberattacks but what if the outages are massive which also affect the capabilities for data fusion. Moreover, cyberattacks on ATC such as spoofed ADS-B is relatively something new and could lead to more catastrophic events jeopardizing public safety and national security.

2.2 Risk of Mid-Air Collision

Numerous previous studies have proposed risk assessment frameworks to assess hazards in air traffic flow. One of the notable frameworks is the Collision Risk Model (CRM) that assesses the probability of mid-air collisions through the consideration of multiple factors such as flight trajectories, ground speed and traffic in the surrounding airspace. Figure 2 below shows the closest point right before aircraft get into a collision mid-air. We adopted the idea presented in [27] by applying the concept of risk modelling for mid-air collision and framed the entire problem in the context of an ADS-B message injection attack. It is interesting to see how the turn of events during the attack incident can be analyzed in depth through a discrete approach. The appearance of a ghost aircraft should be taken

seriously due to the limited knowledge at that point in time. As safety is paramount, risks to flights when in mid-air require resolution as early as possible before the situation worsens.

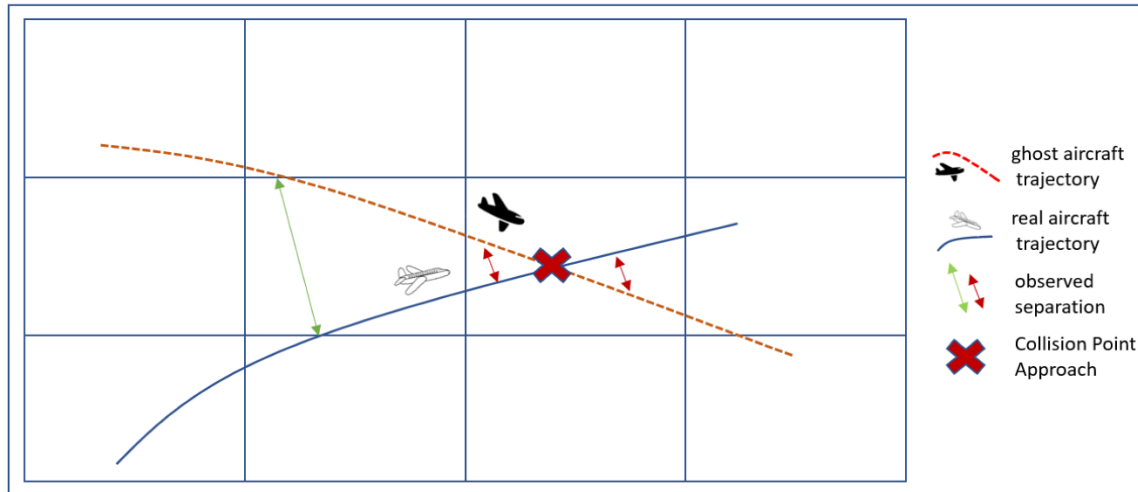


Figure 1. Closest Point of Approach (CPA) between two aircraft prior to an imminent collision between a real aircraft and a ghost aircraft based on an adaptation of CRM [27].

The ATC plays an important role in incident mitigation. Numerous studies discuss ATC's involvement in mitigations of cyber incidents. One of them is [28]. The idea for this study was to rebuild the progression queues of en-route aircraft from certain air space sectors after they were hit by cyberattacks. In the experiments, ATC would be manipulating the queues using a specific algorithm to minimize the impact of certain attack types. As the simulation in this study only involving a single aircraft, the only thing in common with our study is the importance of time progression in the context of critical events that take place once intervention is carried out by ATC. Despite manipulating arrival queues, we provided a tactical solution and close guidance for a single aircraft. Another study by [29] analyzed the impact of ADS-B ghost aircraft spoofing and how the impact can be quantified in terms of delay in arrivals and the number of affected aircraft. The study clearly mentioned ATC's responses in handling unidentified aircraft—ghost aircraft—by slowing down the traffic flow due to the verification procedures of the ghost aircraft. In this dissertation's proposed framework, it is clearly mentioned that delays induced by the ATC response through diverting the flight path due to risks of mid-air collision with the ghost aircraft. The time delay for arriving aircraft may be different from one another based on several factors such as current traffic load and ease of approaching. Even though, the delay magnitude is constant in [30], the model is relevant to be referred to as its flexibility for

parameter tuning enables this dissertation to research further on reducing the time delay through practical novel frameworks.

2.3 Optimization of Taxiway and Runway Utilization

In general, recent studies on taxiway and runway optimization focus on the throughput rate and delay minimization using modified and enhanced algorithms. This can clearly be found in [30] whereby the authors analyzed the total time taken for a makespan against the operation time on runway of a group of aircraft. The optimization proposed by this study is through the branch and bound technique using best first search that aims to minimize each makespan. Best first search is quite like the approach that is used in this research. The difference between our research and [30] is the deployment technique and the output of the approach in quantifying the properties for justifying the reliability and efficiency of the proposed solution.

Another approach that looks similar to ours but uses greedy and dynamic programming approach has been explored by [31]. In general, the study applied purely mathematical formulations to compute optimized solutions based on early simulations using inputs of unequal ready-times, target times and deadlines. The scenario seemed straightforward with consideration given to heavy traffic volume. Although the algorithmic approach is quite similar with the one used in this research, the dynamics were far different as the crafted spoofing incident in this research causes different type of perturbations and the applied parameters were totally different. In brief, the above studies on taxiway optimization explicitly discussed different problems compared to ours. Even though concepts such as 'best first search' and usage of 'shortest job first' technique are well transpired in this research, the set of problems were analyzed using methods and techniques that exclusively deep dived onto perturbations to the ground movement caused by ADS-B GAS attacks in the airspace region and how factor of uncertainties within a short time span should be treated with a technique that can provide relieve to the airport ground movement situation which has already been plagued by uncertainties.

2.4 Elements of Uncertainties

Among the major influential factors of a taxiway rescheduling operation is the existence of uncertainties which was described in depth in [32]. Considering

heuristics principles, the authors computed the proposed solution using the FCFS approach to obtain a clear and fast solution. Meanwhile, [33] studied elements of uncertainties in depth by defining several objective functions beginning as early as an aircraft is under pushback and begins movement on the taxiway. This research's crafted scenario shows occurrence of perturbations and uncertainties delaying the target time to reach certain points along the taxiway up to the runway. However, our scenario's spoofing attack perturbations are exclusively crafted to demonstrate impact on the ground departures with logical time scale and magnitude. We carefully defined the attack parameters as close as they would be in the context of real aircraft departure operations based on inputs from a civil aviation authority. There is also a study which was brief but meaningful in determining the state of taxiway at certain time points, as explored by [34]. Simulation results clearly showed the physical location of aircraft along the taxiway at certain time points. However, no objectives for optimization were defined as the study only provided supporting information for decision makers in coming up with robust flight plans.

3. GAS – High-Impact Attack Scenario from the ATC's Perspective

The scenario-based analysis in this dissertation does not involve real attack executions either physically or through electronic means. Even though the scenario-based analysis was developed qualitatively, they were discussed thoroughly with CAAM and received input from the perspective of a national aviation regulatory body, regarding the features and characteristics of a high impact message injection attack. Next, this dissertation discusses possible mitigation techniques that can be undertaken to address the incident. For this purpose, the conceptual framework was developed, and the performance of the technique was tested through simulations using ADS-B data officially obtained from CAAM. Like most of the research that defines parameters and the scope of their work, this research is also bound to specific assumptions to ensure the scope of work is realistic and close to the real-would-be scenarios while the identified objectives can be fulfilled accordingly.

3.1. High Impact Attack Scenario

An attacker who knows how ATC would respond to the launched attacks would be able to launch the most disruptive attacks. A previous study by [35] predicts the decision-making process carried out by an attacker targeting a CPS through attack tree analysis and its probable consequences. Even though the study did not specifically touch on any kinds of aviation CPS, the main takeaway is that a well-prepared attacker might craft a devastating attack on the ADS-B system through actions in series of events. Each event leads to another and as the stages progress, the consequences of disruption to the ATM become greater and greater. Now there are several available open sources of ADS-B data, enabling the live tracking of flights across the globe. This free and accessible information could somehow nurture understanding on the frequently used routes, and how a normal flight profile should look when flying over a certain air space. Knowledge on normalcy in air traffic can be used negatively by anyone with ill intent.

The notably changing pattern of spoofing over several time periods creates prolonged confusion and broadens uncertainties experienced by the ATC. Whenever emergency situations affecting approaching flights occur, priority will absolutely be given to the airport inbound flights to ensure safe landing. Therefore, arrangements on the ground will need to accommodate this objective to the extent of departure suspension and allocation of specific runway and taxiway for smooth landing and arrival. Inspired by the hostility of such situations and at the same time trying to apply immersive thinking on how a cyber attacker would launch a high-impact attack, we crafted attack scenarios to test our approach with multiple aircraft taxiing-out sequence scheduler. This is vital so that results can be analyzed by comparing simulation outcomes of the tested schedules discreetly to determine the effectiveness of our approach.

We discussed further with CAAM and tried to assimilate into the mind of an attacker which has sole objective of disrupting the ATM at the worst level. A thoughtful attacker who knows how ATC would respond, he or she would pose high level threat. The main takeaway is that a well-prepared attacker might craft a devastating attack on ADS-B system through actions in series of events. Each event leads to another and as the stages progress, the consequences of disruption to the ATM escalate. Attack on Aviation CPS draws high likelihood due to existence of extensive level of sophistication throughout the systems to enable communications, navigation, and surveillance such as demonstrated in [36].

In a closely connected technical area, studies such as [8] and [9] have proven whilst radar jamming technologies are being improved for security purposes, it also can be manipulated for malicious goals. This proves that the risks posed by

cyber attackers are valid and real. Meanwhile, **Figure 2** depicts concept of an integrated attack that can create a high impact attack scenario as a basis to our analysis. Upon radar system jamming, fusion localization capability degrades substantively while synchronously, false ADS-B messages are being injected or

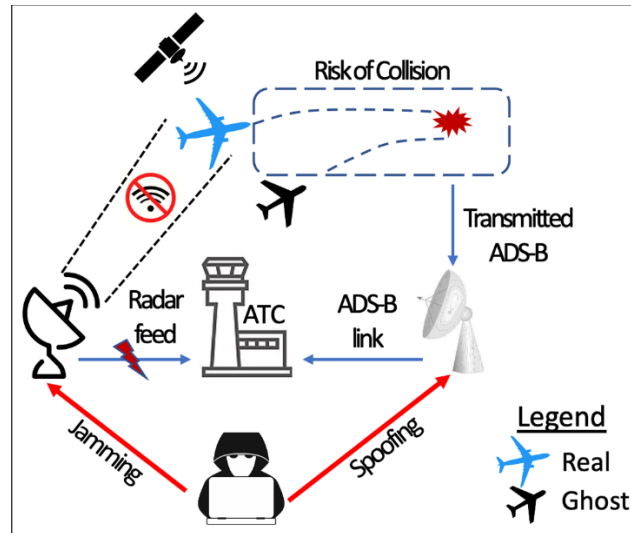


Fig.2. Coordinated Attack in a High-Impact Attack Scenario

broadcasted into the ADS-B ground receiver and linked to the ATC surveillance system. When this happens, radar sensing would not be visible on the screen and with only ADS-B link is available, the ATC would be relying totally on this sole surveillance system whilst trying to observe the entire situation as best as possible. The situational awareness that existed up to this level will be the basis for determining the type of departure realignment technique that would be able to mitigate the attack. The expected response by the ATC's based on emergency procedures would be to monitor vigilantly while trying to verify the authenticity of the anonymous aircraft through radio checks and other available means. This entire chain of events beginning from attack detection through ADS-B as sole surveillance system, until deciding for suspension of departure and later recommencement of departure amid uncertainties are depicted as in **Figure 4**.

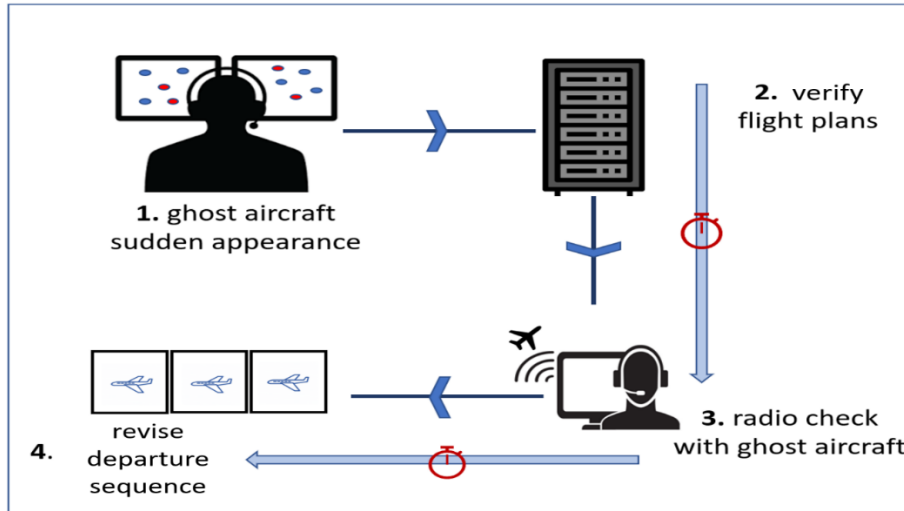


Fig.3. Model of The ATC's Responses for Arrival and Departure

Based on CAAM's ATC expert opinion, we explored characteristics of a high-impact ghost aircraft spoofing attacks that would disrupt ATM tremendously. An integrated attack may amplify the impact severity depending on the level of situational knowledge possessed by the attacker and number of technical preparations. Today, there are available open sources of ADS-B data, enabling live tracking of flights across the globe. Open access information could somehow nurture understanding on the frequently used routes, and how a normal flight profile should look like when flying over certain air space. The established knowledge can be used negatively by anyone with ill intent. An attacker capability was demonstrated in [37] through the structural attack launch with the objective of maximum damage infliction to the air traffic management. Considering the criticality of possible impacts that can be caused by GAS attacks, this dissertation explained three researches that adopted three primary criteria that have been verified by CAAM. First are the tangible impacts analyzed in to the AGMOD operations [29] and in [21] that probed impact to en-route aircraft. Another criteria is as mentioned in a recent study on tactical flight diversion for mitigating risks of ADS-B GAS [38].

3.1.1 Targeted Location for GAS

[38, 39, 40] all explained how location of spoofing incident determines the type of response that should be taken by the ATC. Through series of consultations with CAAM, a busy airspace especially the terminal airspace such as the Lumpur Terminal Maneuvering Area (TMA) in **Figure 5** [41] is most likely to experience the highest impact from irregular flying activities or noncompliance to the enforced local rules and regulations as listed on [42]. However, ghost aircraft

spoofing activities within TMA itself can be extremely disruptive in the early stage but could only last for just a brief period. This is due to the ability of independent optical verification by the ATC tower or from situational updates by landing or passing by aircraft. In contrast, spoofing attacks at the outer side but near to TMA borders takes more time to be verified. Therefore, distance of GAS attack which can evade physical check but yet, appear in a busy airspace region plays an important factor in maximizing the disruptive impact to the ATM.

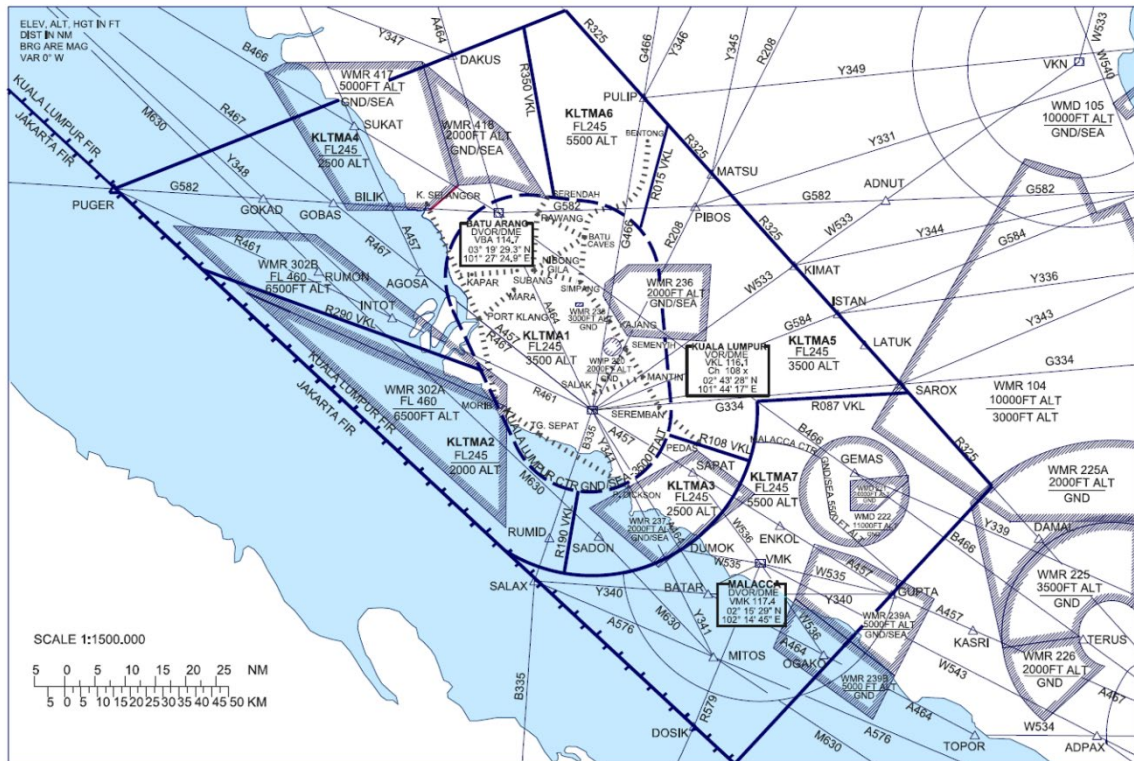


Fig.5. Lumpur Terminal Maneuvering Area (TMA)

3.1.2 Ghost aircraft behavior

Besides location, [40] also explained the behavioral trait of a ghost aircraft in the ATC responses. A skillful attacker would launch a ghost aircraft that resembles an aircraft with a legit flying profile in terms of its trajectory, speed and altitude that correlates with its current location or flying phase. Ghost aircraft that merely are just trying to disrupt the airspace without proper disruptive trajectories for example, random movements at unnatural flying routes and frequent changes in heading could be identified sooner as spoofing. This can be detrimental to the objective of the attack in maximizing the disruption to inbound flights.

3.1.3 Attack Magnitude or Density

The third criterion mentioned by [40] that is vital in creating a high impact attack is the magnitude or density of the attack. The occurrence of more than just one ghost aircraft that displays characteristics as discussed above will cause more serious repercussions than a single ghost aircraft. However, the appearance of excessive ghost aircraft might be unrealistic. CAAM is of the opinion that the right combination of number and frequency will determine the impact and looks more real. The direct impact to the ATM is duration of flight delays and number of affected real aircraft, as demonstrated by [29]. **Figure 6** shows how the three discussed criteria becomes highly disruptive in a major attack scenario.

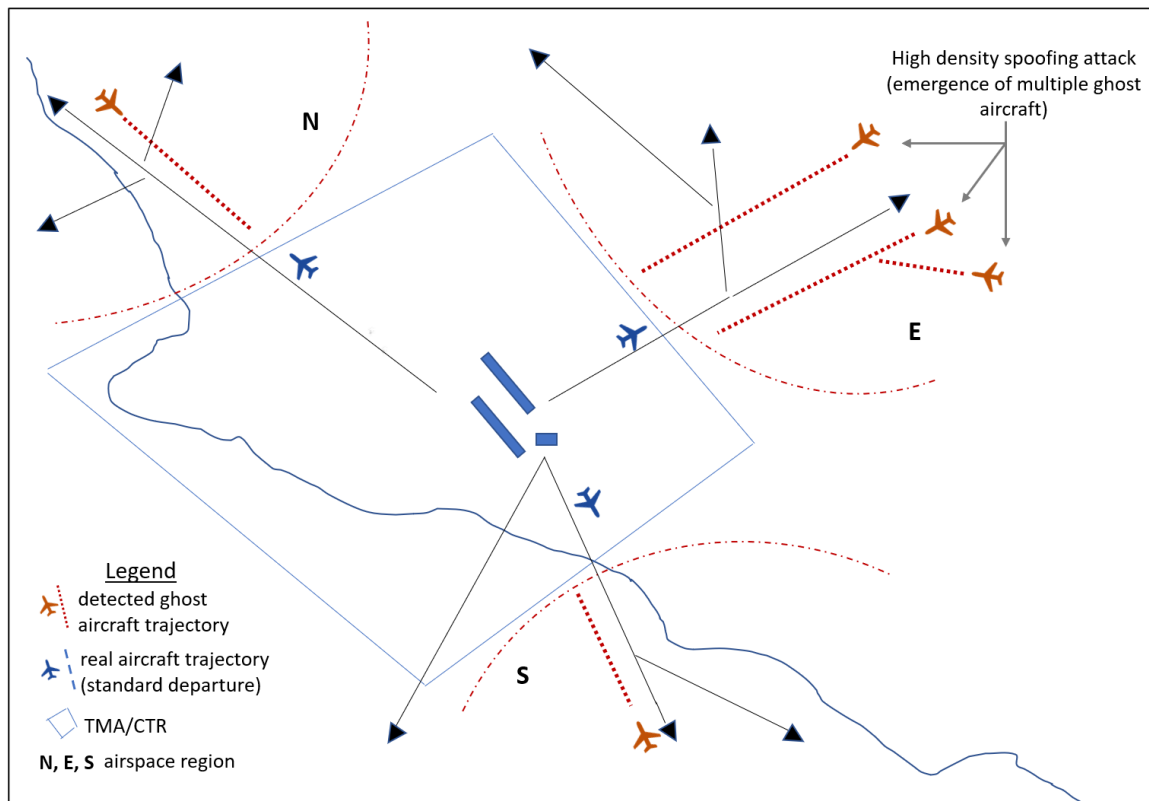


Fig.6. Model of Attack Scenario Near to TMA

In the context of the climbing phase by aircraft originating from KLIA through standard departure instrument of KLIA, appearance of ghost aircraft with trajectory profile resembling a legit aircraft in approach would cause serious confusion to ATC and disrupt smooth climbing phase of departed aircraft. Confusion experienced by the ATC might get deeper if spoofed ghost aircraft trajectories are purportedly crafted to look like an aircraft in descent phase, heading towards KLIA for landing but of course they are not responding to

communications initiated by ATC and neglecting traffic rules and safety regulations. Moreover, if the attack incidents persist in a time range that is neither too short, nor too long, for example within a period of thirty to forty minutes, it is within the period which ATC would still be scrambling to verify legitimacy of the ghost aircraft. These types of attacks will consume ATC's time and trigger their huge effort trying to resolve the incidents. Critical developments would peak during this period. Successful alleviation by the ATC could bear some results right after this period passes. Higher impact can be anticipated when two ghost aircraft are detected, for example in the case of multiple GAS attack which occurs in the eastern airspace region. Continuous or subsequent attacks within the critical period would create longer disruption to the departures for aircraft heading towards this airspace region. However, according to CAAM, too many spoofed ghost aircraft might be verified as false targets sooner and would jeopardize the entire attack.

3.1.4 Attacker Creativity in Evading Electromagnetic Interference Countermeasures

A knowledgeable attacker will be aware of the risks of getting caught once the authorities have detected the radio wave transmitted by the Realtek Software-Defined Radio (RTL-SDR) device used to inject the false ADS-B to the targeted ground station. As this kind of device operate on low power consumption, it is however able to transmit radio signals within the range of 500kHz to 1.75GHz. Thus, transmission in 1090MHz could be handled without problem with its latest capability. At a certain time point during the attack, the authorities would manage to detect the source of the rogue radio frequency interference using techniques such as mentioned in [43] by applying cognitive radio spectrum monitoring technology analysis. The research studied the correlation coefficient differences between two sets of ADS-B sources and identified a clear difference in the threshold. Meanwhile [44] proposed the physical layer countermeasures by examining the signal source range and direction-of-arrival. The researcher used the angular feature of the receiver antenna and proposed architectural enhancement for the system to calculate directional signal interrogations to determine authenticity of the received signals. As its application is focused on ADS-B In features in aircraft, ground station verification is not covered and still remains vulnerable to ground-based attacks. Even though there are traditional techniques such as 'Transmitter Foxhunting' explained by [45] in its equipment developmental specifications and as described by [46] which uses radio doppler to find the source of radio wave, all of these equipment and techniques will still

rely on the deployment of physical search mission to apprehend the attacker. Moreover, if the attacker possesses a delicate mobility advantage such as having a drone that is equipped with the transmitter dongle to execute attacks, the process on locating the attack source will definitely require substantive amount of time. For the ATC that operates on critical real time systems, they shall not jeopardize safety and cannot afford waiting for the end result of the foxhunting operations. A resilient model is still the needed answer by the ATC to ensure safety to all aircraft regardless of the flight phases they are currently in.

4. GAS and its Cascading Effects to AGMOD Dynamics

4.1 ATC Responses to GAS

In message injection attack type, an attacker injects false data into the air traffic communications. Theoretically whenever a perturbation occurs in the air traffic flow, it will likely cause a chain of reactions to the AGMOD Dynamics. This attack can be carried out either to the aircraft or to the ADS-B ground stations. Once the attacker is successful in injecting fake flights information, the ANSP systems responsible for designated air space regions will detect the 'ghost aircraft' mimicking attributes of legitimate ones. If this really happens, then the attacker's objective has been successfully achieved. Due to the relatively easy execution and possible high negative impact, the assessment method is broken down into two potential key connecting events which are:

a. ATC responses to spoofing attack:

Anticipated responses by the ATC, whenever unidentified aircraft (referring to the spoofed ADS-B) got into their display.

b. Dynamics of AGMOD during attack:

Quantification of impacts (cascading effects) on the airport inbound and outbound phases.

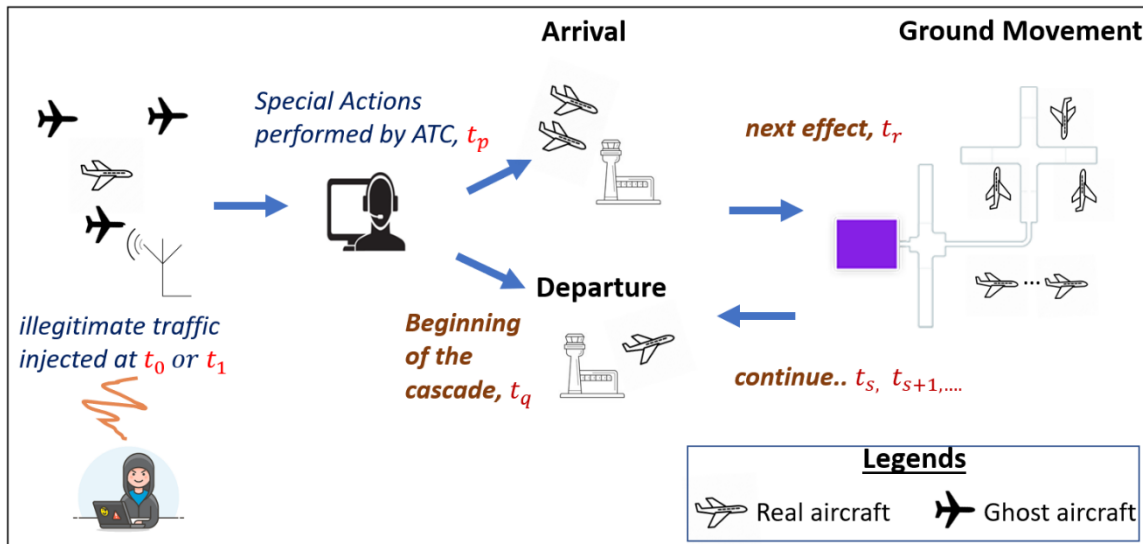


Fig.7. Propagation of Delay Caused by ADS-B GAS Cyberattack

It is unlikely that ghost injection and any kinds of spoofing attacks are targeting the airport tower controller due to minimal airspace threshold that it monitors and the ability to optically confirm the presence of aircraft and other flying objects within its range, thus making it a less favorable target.

4.1.1 The Chain of Cascading Effects of GAS

To further explain the possible cascading effects, this research observed a flight delay propagation as the outcome of perturbed AGMOD dynamics caused by the spoofing attacks as shown in **Figure 7**. The possible sequence of cascading effects is anticipated in the following phases:

1) Invocation of Procedural Response by the ATC

Upon realizing anomalies on the system's display, ATC shall take actions according to the Emergency Standard Operating Procedures (E-SOP). The First action is to validate aircraft's flight plan by checking the aircraft ID with its filed flight plan. This step is likely to be automatic as the ATC's system is supposedly able to monitor aircraft according to their filed flight plan or at least there is a manual procedure that should quickly verify an aircraft's flight plan. An aircraft with no flight plan will trigger an alarm that necessitates further probe. The ATC will try to establish communications with the flagged aircraft, attempting to radio-check the pilot of the unidentified aircraft to solicit prudent responses. During emergencies with limited to no radar coverage, the priority is to ensure airport approaching aircraft in the Terminal Maneuvering Area (TMA) and Controlled

Traffic Region (CTR) to evade the 'ghost aircraft' by maintaining or even increasing the separation rule so that the risks of collision can be avoided. In the phase of descent for landing, clearly all aircraft queuing behind the interrogated ghost aircraft must slow down and maintain distance. The duration taken for validating traffic within the queue for arrival which can be up to few minutes per ghost aircraft will induce accumulated delay in the landing schedule. The ATC will act based on procedures to provide guidance and assistance until the aircraft has safely landed.

2) Delays in Arrival:

Delays on arrival will occur due to the time spent by the ATC on verifying unidentified aircraft. Only the degree of delay has yet to be determined, which would depend on the time taken for verification.

3) Halt in Ground Movement:

Concurrently, the situation on the airport runway and taxi area will also be affected with aircraft having to adjust their schedule, especially those that are leaving the airport. Pushback and taxiing out to the runway are not allowed or take longer time than usual. While on the taxiway, the pilots can assess the ongoing situation either to wait for clearance to proceed or request to return to previous gate upon approval by the airport ATC.

4) Delays in Takeoff:

Delays in Takeoff are the synchronous result of the late arrivals and abrupt stop of ground movement of the aircraft. In this stage, pilots shall wait further instruction before being allowed to proceed to the runway to make way for incoming aircraft to land.

4.2 Simulation of ATC Responses

4.2.1 Attack Scenario

To make the attack scenario close to real, this dissertation tries to immerse into the mind of an attacker. [47] enlists the key factors for profiling a credible attacker's attributes which include the goals and motivations in committing a cyberattack. An attack can be so devastating, for instance the system is being flooded with ghost aircraft, which has a clear intent to cripple the ATC monitoring capabilities. The magnitude

would be obviously massive. Based on operational standards, this attack would be easily categorized as a large scale cyberattack. Immediate responses would be taken to quickly alleviate the attacks. However, if an attack were in small scale, slow in pace but consistently launched into the environment, it might persistently trouble the incident response team. In the short term, the impacts would be low but in a longer period, it could turn out to be devastating. For example, a type of 'frog boiling' attack, that seems to blend into the normalcy but continuously confusing and inflicting more hardship and tensivity on the targets [48].

Based on these immersive thoughts and inputs from a national air traffic regulator, the Civil Aviation Authority of Malaysia (CAAM), this research proposed a model which is based on adaptation of an airport inbound-outbound phases and designed two spoofing attack scenarios that would be most likely desired by attackers in creating a more realistic simulation. The attack scenario described above was then refined into two types of attack scenarios. Attack Scenario A encompassed a light scale attack whereby a single spoofed ADS-B is launched in a fixed inter generation time step while Attack Scenario B was with larger magnitude with larger magnitude of GAS generated into the traffic nearby the TMA. Both scenarios simulated only the dynamics of the cascading effects quantitatively without launching any kinds of systemic cyberattacks.

4.2.2 Discrete Events Modelling and Simulation Parameters

The description of the simulation phases is as follows:

1) Attacks Initiation

During this phase, several ghost aircraft will be injected into the ADS-B infrastructure, on top of the generation of legit aircraft. Whenever ghost aircraft are inducted, the ATC will request for servers at push back, taxiing out and taking off to temporarily paused. This action is taken to clear the airport airspace and runways so that airport approaching aircraft could land safely. These situations will cause further delays to departing aircraft. Besides for simplicity and practicality, response by ATC is assigned with value of a specific time duration called as 'service time' due to the close-to-real situation whereby the ATC would take an average of five minutes trying to determine the legitimacy of a ghost aircraft in the system. Due to this factor, the 'service time' with the value of '5' is assigned to the ATC in verifying ghost aircraft in the queue. Identified ghost aircraft which did not

respond to interrogation by the ATC were sent to the elimination bin. This process was made possible by assigning attribute value to the ghost aircraft which differed from the attribute value of the legit aircraft. In our model, an entity separator reads these values on aircraft emerging from 'Arrival Queue 1' and specifies which route to forward these aircraft, based on their attribute value.

Moving forward, the same value of '5' 'service time' was also applied to the succeeding legit aircraft coming into the queue as this was for mimicking the enforced separation rule between verified and non-verified aircraft in the TMA. We named the ATC system for this stage in the model as 'Air Traffic Management System-I (ATMS-I)'.

2) Arrivals

During this phase, ATMS-I has already realigned 'Arrival Queue 2' from 'Arrival Queue 1' that consists of a legitimate aircraft making final approach in sequence. Aircraft in this queue are then handed over to 'Air Traffic Management System-II (ATMS-II) for landing. ATMS-II will begin handling airport 'Ground Movement' phases starting with aircraft entering the Taxiway queue after being served 'Landing Control ATMS-II' server. This is where statistics for Arrivals are recorded.

3) Ground Movement-Inbound

After the Arrivals, this phase in the model is comprised of 'Taxiway In' queue, 'Taxiing In' server, and 'Parking' queue that resemble aircraft moving towards the gate.

4) Gates

Once aircraft reach this phase, they will halt for a service time equal to '15-time steps', resembling disembarkation and embarkation process based in real time situation. In addition to the inbound flow of aircraft, five aircraft will be generated at the start of simulation time from the gates. These, especially pre-loaded aircraft were meant as aircraft that have already parked at gates during simulation startup, ready to move outwards.

5) Ground Movement – Outbound

This phase is represented through four discrete event system servers that comes with pause and resume functions, namely the 'Pushback',

'Taxiing Out', 'Runway Out' and 'Taking Off'. These servers will pause from forwarding the aircraft into the next queue if they receive a pause command from the command generator that is triggered based on events of ghost aircraft attack, experienced by the ATC's 'Verification' server in ATMS-I. Meanwhile the queues in this phase are 'Pushback Queue', 'Taxiway Out', 'Runway Out' and 'Departure Queue'. Statistics of aircraft movement are collected along these queues. The ATC response and AGMOD Dynamics discrete events model was developed using Matlab's Simulink Sim events which is as in **Figure 8**.

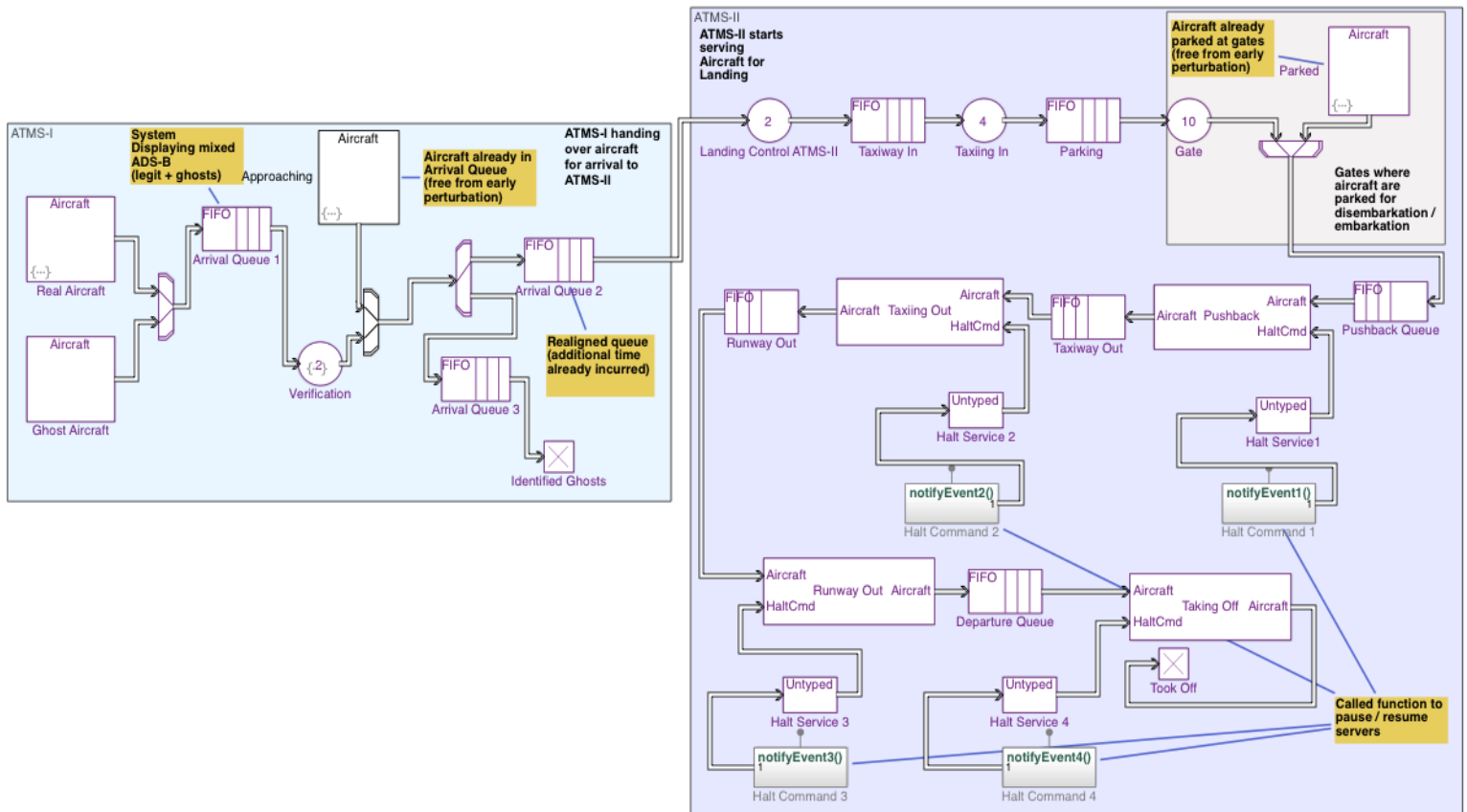


Fig.8. Discrete Events Model of AGMOD Dynamics

Algorithm 1 explains the procedural flow of the model.

Algorithm 1 ATC's Response and AGMOD Phases Under GAS Attack

Input:

A list of aircraft and their arrival time (aircraftlist).

Output:

Number of Aircraft and their arrival time at queues within AGMOD Phases (statistics).

```

1: initialization
2: queue ← getlistofAircraftsWithIntervalTime(aircraftlist)
3: for aircraft in queue do
4:   response ← aircraft interrogation(aircraft)
5:   if (response is aircraft have flightplan) then
6:     arrivalqueue2.add(aircraft)
7:     proceed to Taxiway In(aircraft)
8:     proceed to Parking (aircraft, delay)
9:     proceed to Pushback Queue(aircraft)
10:    proceed to Taxiway Out(aircraft)
11:    proceed to Runway Out(aircraft)
12:    proceed to Departure Queue(aircraft)
13:    proceed to Took Off(aircraft)
14:  else if response is radio check then
15:    proceed to Halt Pushback()
16:    proceed to Halt Taxiing Out()
17:    proceed to Halt Runaway Out()
18:    proceed to Halt Taking Off()
19:    compute delay at the departure()
20:    compute delay at the arrival()
21:  if no response after 5 minutes then
22:    queue.remove(aircraft)
23:    queue.update()
24:  end if
25: end if
26: end for

```

A Series of simulations were run using the parameters stated in **Table I**. Ghost aircraft were generated based on fixed intergeneration times specified in the table. Baseline (normal traffic flow without ghost aircraft) simulation run was done as the benchmark for comparing between non perturbed and perturbed AGMOD phases.

Simulation Run	Generated Entities and Intergeneration Time	ATMS-I Verification Server Service Time
Baseline (no ghost aircraft)	1 Legit aircraft at every 3 time steps	1
Light Attack	1 Legit aircraft at every 3 time steps 1 Ghost aircraft at every 5 time steps	5
Heavy Attack	1 Legit aircraft at every 3 time steps 5 Ghost aircraft at every fixed intervals of 5 time steps <i>i.e.</i> : $t_0 = 5, t_5 = 5, t_{10} = 5$	5

Table I-A. Simulation Parameters for Runtime of $T=60$

4.3 Analysis of Simulation Results

4.3.1 General Findings

During baseline run, verification server in ATMS-I was set to the value of '1' service time step as it did not have to spend longer time to verify incoming traffic into the TMA since no ghost aircraft were inducted. All queues and servers then proceeded normally without having any delays including the discrete event systems servers in the outbound phases. However, for Scenario A and B, induction of ghost aircraft into the ATMS-I's 'Arrival Queue 1' had compelled the ATC to run verification on the ghost aircraft and all following aircraft with a value of '5' service time step. Simultaneously the four servers for outbound phases were also halted upon the arrival of the first ghost aircraft. Representation of different service time step values in this model can be observed as the longer stretch of horizontal line in the projected graphs.

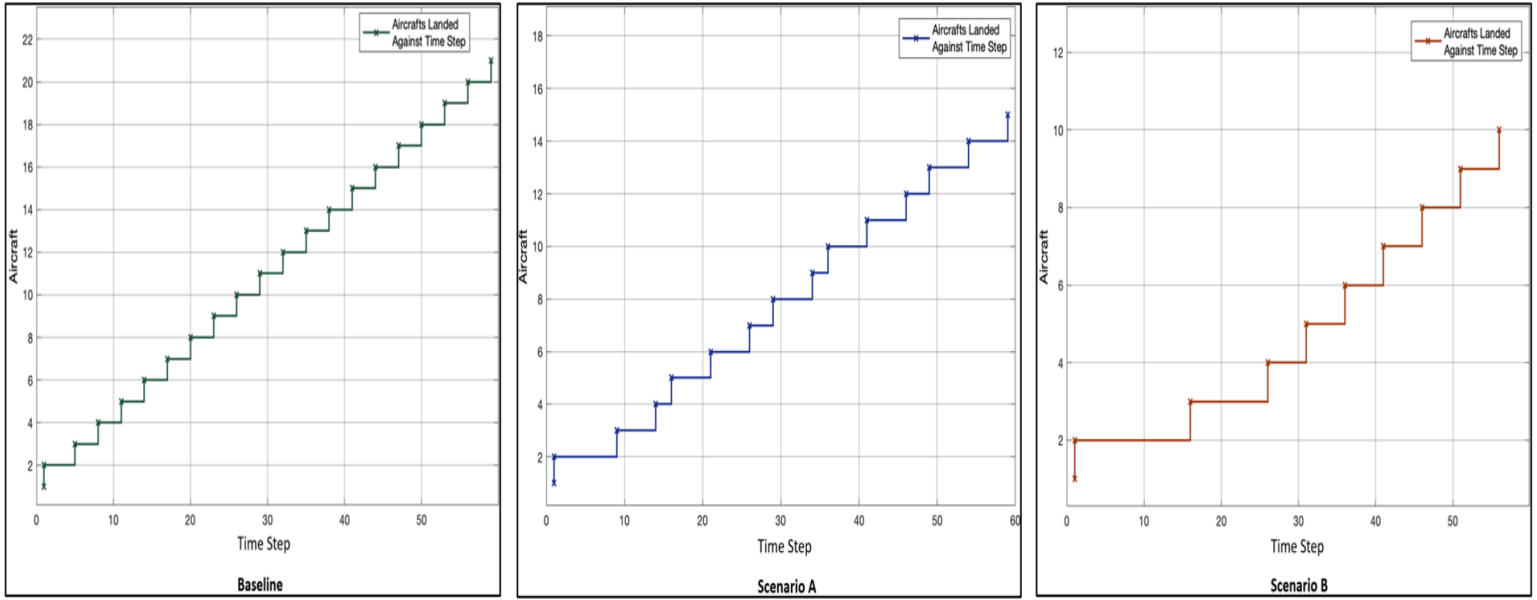


Fig.9. Comparison of Aircraft Arrival Times Between Three Different Scenarios

4.3.2 The Cascading Effects Within AGMOD Dynamics

We observed the results and managed to identify statistical differences between the three simulated scenarios. These differences displayed the quantified cascading effects of the AGMOD Dynamics in these following phases:

i) Arrival

In **Figure 9**, the left most graph (Baseline) shows that under the nonexistence of spoofing attacks, 21 aircraft had landed until the simulation arrived at the time steps of $t=59$. The middle graph (Scenario A) shows the arrivals under light attack with results showing 15 aircraft arrived within the entire simulation run time. Meanwhile, the rightmost graph (Scenario B) shows that only 10 aircraft had arrived in the same simulation run time. This is a difference of more than half of the number of aircraft that should have arrived if there were no spoofing attacks.

ii) Gate

In **Figure 10**, the Baseline graph shows up to 21 aircraft had parked at the gates during the entire simulation run time which was without any spoofing disruptions. However, Scenario A recorded those 15 aircraft had parked during the entire simulation under

light attack. In Scenario B, the numbers of parked aircraft during the entire simulation were correlated with the numbers recorded in the previous key phase which is the arrival. Only 10 aircraft parked at the gates, which is again, slightly less than half of the numbers from the baseline simulation in the same phase.

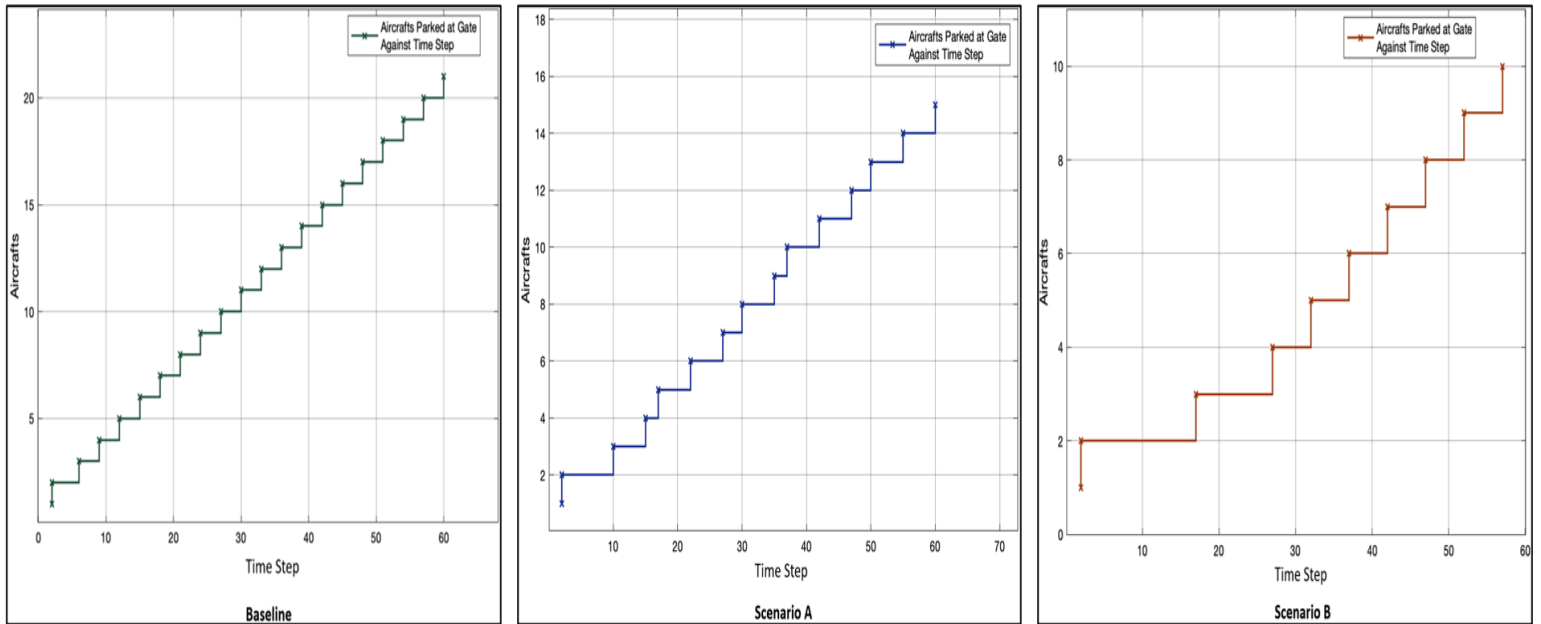


Fig.10. Comparison of Aircraft Parked Times Between Three Different Scenarios

iii) Pushback

Moving on to the next phase, 'Pushback' as depicted in **Figure 11**, pre-loaded aircraft were successfully pushed back in regular manner and then started to be followed by aircraft which had been parked for 15 service time steps. A steady pattern of 'Pushback' was recorded in the Baseline graph with existence of consistent 3-time steps of intervals after the first aircraft that originated from ATMS-I jurisdiction was successfully pushed back. In Scenario A, the 'Pushback' was stopped at $t=30$ with only 9 aircraft while the same number of aircraft managed to be pushed back in Scenario B, but with a longer time span of $t=42$. Both Scenarios A and B were experiencing paused services in the outbound phases due to concurrent spoofing attacks faced by ATMS-I. This situation explains why the numbers of 'Pushback' for both scenarios were substantively hampered.

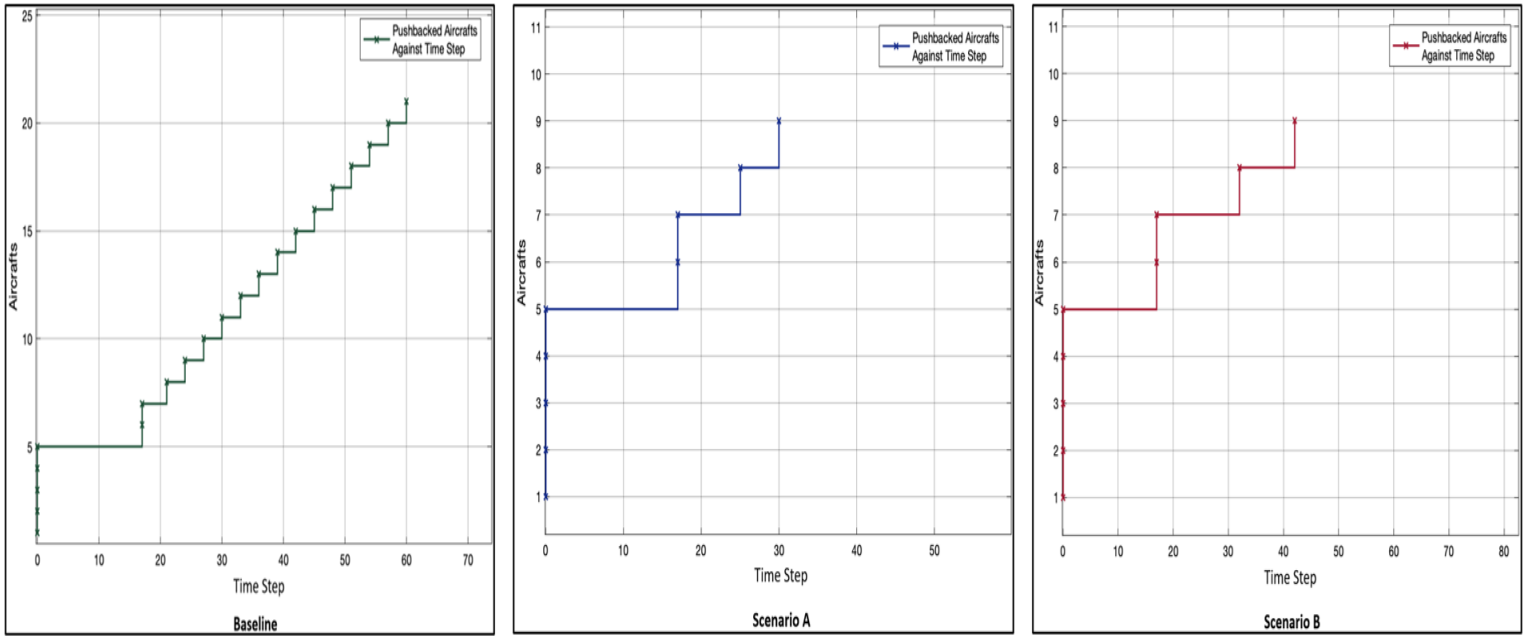


Fig.11. Comparison of Aircraft Pushback Times Between Three Different Scenarios

iv) Takeoff

Figure 12 shows the final outbound phase which is 'Takeoff' with as many as 19 aircraft that managed to takeoff from the airport until the point of $t=58$ under the 'no attack' scenario. However, in both Scenario A and B, which were experiencing continuous spoofing attacks, only 5 takeoffs were recorded for Scenario A at the point of $t=8$ while only 2 aircraft had managed to take off in Scenario B at the point of $t=5$. This is clear evidence that the cascading effects in both Scenario A and B, that had begun since the 'Arrival' phase also happened in the later stages of the AGMOD Dynamics, particularly in the 'Takeoff' phase with so little aircraft were allowed for takeoff. This delay in takeoff was also propagated by the ATC's policy of not allowing any takeoff while GAS persisted. Directly, this means that queues for taxiing-out aircraft are full and congestion on the airport aircraft is growing. Usually, this situation is tolerable up to the extent of the airport reaching its maximum ground capacity to accommodate aircraft. Otherwise, alternative airport shall be considered to cater upcoming arrivals. The summary of pertinent statistics recorded from the simulation runs of the key AGMOD phases can be referred to **Table II**.

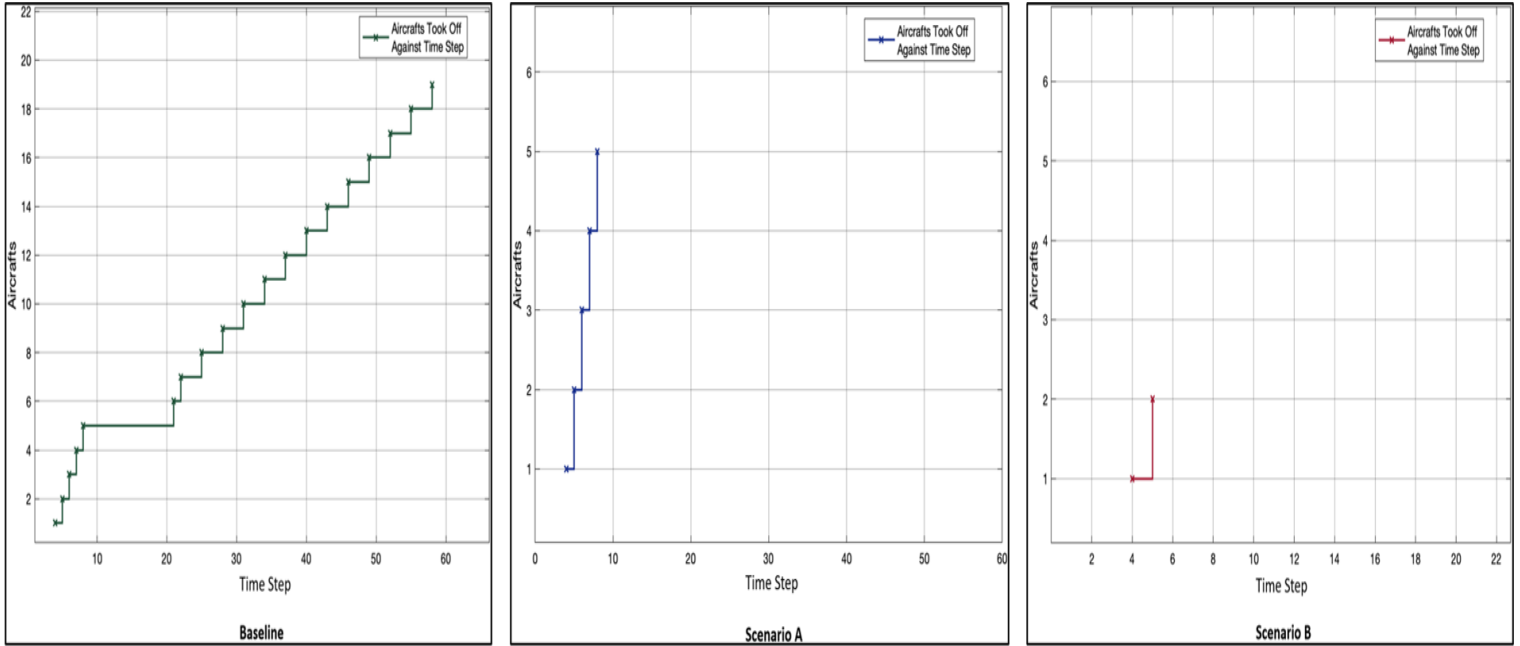


Fig.12. Comparison of Aircraft Takeoff Times Between Three Different Scenarios

Simulation Type	Results			
	Arrival	Gate	Pushback	Takeoff
Baseline (no GAS)	21 at $t=59$ m	21 at $t=60$ m	21 at $t=60$ m	19 at $t=58$ m
Attack Scenario A (Light)	15 at $t=59$ m	15 at $t=60$ m	9 at $t=30$ m	5 at $t=8$ m
Attack Scenario B (Heavy)	10 at $t=57$ m	10 at $t=57$ m	9 at $t=42$ m	2 at $t=5$ m

Table I-B. Summary of Simulation Results

4.4 Discussion

4.4.1 Other Relevant Findings

We noticed that progression from Arrival to Gate phase in all three scenarios did not record a substantive difference in time steps taken. The little difference is due to the servers representing the Ground Movement-inbound phase not being assigned any specific value for their 'service time'. In our model, we defined this phase as normal without any perturbations to the overall AGMOD dynamics,

as in close-to-real time situation, supposedly there would be no occurrence of delaying events. Thus, without specifically tuning the servers, aircraft flow from Arrival to Gate with regular service time of `1'. In contrast, the Ground Movement-outbound phase shows sheer differences due to the servers were being halted following spoofed ADS-B detected in ATMS-I's `Arrival Queue 1' which lasted until the end of simulation run time.

4.4.2 Factor of Fixed Variables and Laid Assumptions during Simulations

In running this simulation, the scenario applies fixed arriving aircraft intervals of 3 and 5 seconds. It helps to simplify the calculation process and produced a clean result at the end of the cascade, which is the temporary departure server downtime. The downtime of the departure server that represents the suspended departures by the ATC then determined the number of aircraft which managed to takeoff prior to the GAS attack. The aircraft arriving intervals which has been defined as a short span of time of 3 and 5 seconds causes a continuous downtime of the departure server and disallow departure for any aircraft to resume departure once the phase has been suspended by the ATC.

Simulation 1 has also applied several assumptions such as constant movement speed on the ground for taxiing-out aircraft. Without fluctuation of movement speed for the entry/exit of an aircraft (entity) into the formed queues regardless of aircraft types are standardized and eliminate any consideration for uncertainties of ground movement process during the simulation. Besides that, the simulation also assumed that aircraft that managed to takeoff during the initial stage of the attack were not affected by the presence of the ghost aircraft.

5. Reducing Delay in Flights Arrival

For this purpose, inputs from Civil Aviation Authority of Malaysia (CAAM) were used in forming a framework that assesses the trajectory of a ghost aircraft and the risks of collision with a real aircraft which is

heading towards an airport to begin approach procedures. By using ADS-B data provided by CAAM, this dissertation demonstrates how real traffic is impacted by a single ghost aircraft occurrence. After learning the immediate impact, this dissertation proposes a tactical maneuvering framework with safety and efficiency as its clear quality objectives.

5.1 Scenario Background

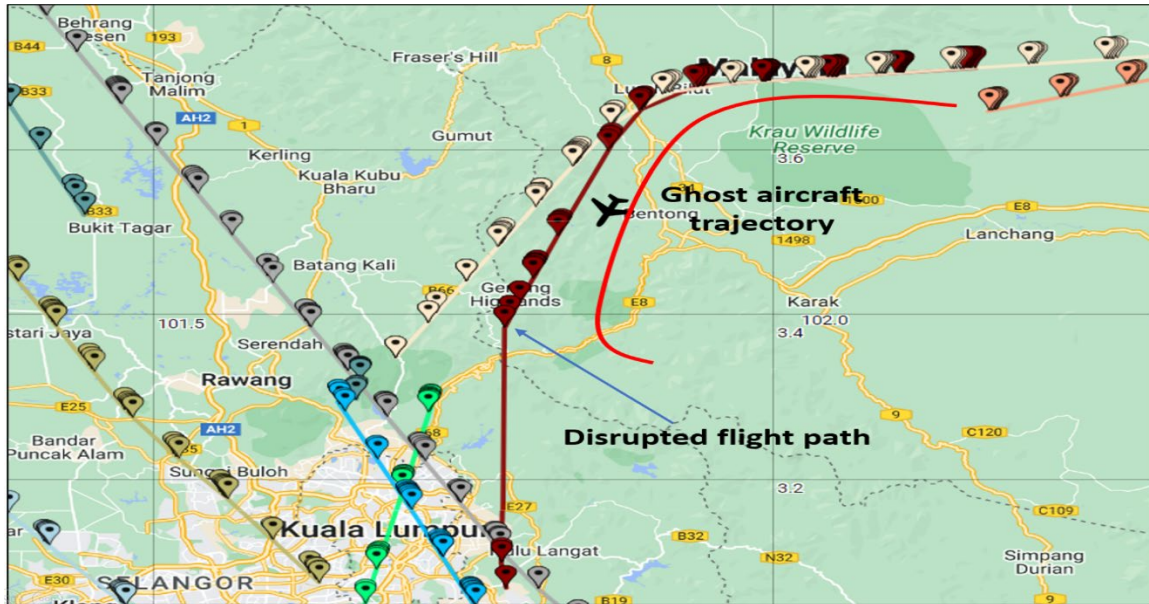


Fig. 13. GAS Conflicting Trajectory with Other real Legit Aircraft's Flight Path

Figure 13 depicts an attack scenario of injection of ghost aircraft trajectory interfering with the normal trajectory of an aircraft that has begun descending towards Kuala Lumpur International Airport (KLIA) based on official ADS-B data on 1000H until 1005H on 6 January 2020. The ghost aircraft (red trajectory) was injected theoretically in the scenario-based analysis near the Eastern border of the Lumpur TMA. When the ATC detected a possible collision, and after trying to verify the ghost aircraft but to no avail, the ATC would take standard preventive actions by alerting the legitimate aircraft and to slow the affected aircraft down and divert its route. The appearance of a ghost aircraft at the TMA border and flying towards the TMA would catch the serious attention of ATC, as shown as the red curvy trajectory closing into the real legit flight represented by the dark red ADSB track heading south. Both tracks were used to model and simulate the proposed benchmarking trajectory in addressing this attack. There were also other TMA-inbound flights as depicted in peach, beige,

grey and fluorescent green ADS-B tracks. However, these flights were not interrupted. Once the ADS-B surveillance system detects that a ghost aircraft is closing in on the TMA, ATC will divert other conflicting flights not to fly too close to the unverified ghost aircraft. When the ATC detected a possible collision and after trying to verify the ghost aircraft but to no avail, the ATC would take standard preventive actions by alerting the legitimate aircraft and to slow the affected aircraft down and divert its route.

Meanwhile, the attacker will try to prevent his strings of ghost aircraft attack from being verified by the ATC through visual observation of the airport control tower. Broadcasting the false messages in the TMA area or too close to airport airspace would trigger the tower and, with the help of bypassing pilots, they could conclude the actual non-existence of the ghost aircraft. This is why maintaining anonymity of not being able to be scrutinized through optical equipment or physical check as long as possible is important to ensure attack persistence and brings maximum impact.

Besides that, several assumptions were applied throughout the simulation which are as follows:

- a. This scenario is declared as an emergency due to other surveillance methods such as radar and multi-lateration also being suppressed and jammed by adversarial actions. Only the ADS-B system was available and running.
- b. The tactical maneuvering technique was not influenced by the presence of the surrounding traffic. This was mainly due to the real traffic conditions based on the tested data. The weather was fine with no warnings issued by Notice to Air Men (NOTAM) or any other communication lines.
- c. A non-standard descent procedure was simulated due to emergency status.
- d. The injected ghost aircraft used the same descent profile as the real aircraft except its trajectory was designed with one less way point for simulation purposes.

5.2 Simulation of Tactical Trajectory Benchmarking

The main principle of the proposed framework is constantly benchmarking the trajectory of the ghost aircraft. The tactical diversion adheres to 6 nautical miles (6nm) lateral separation minima including a tactical threshold of 1 nm buffer airspace. In the event of further incursion inwardly by the ghost trajectory, the tactical diversion will move further away from the ghost trajectory. At the time this event is happening, the separation minima are still more than or equal to 5 nm. The existence of buffer airspace is also meant to accommodate non-instantaneous processing by the aircraft's pilot based on recommendations given by the framework. The concept of the proposed framework is as shown in **Figure 14**.

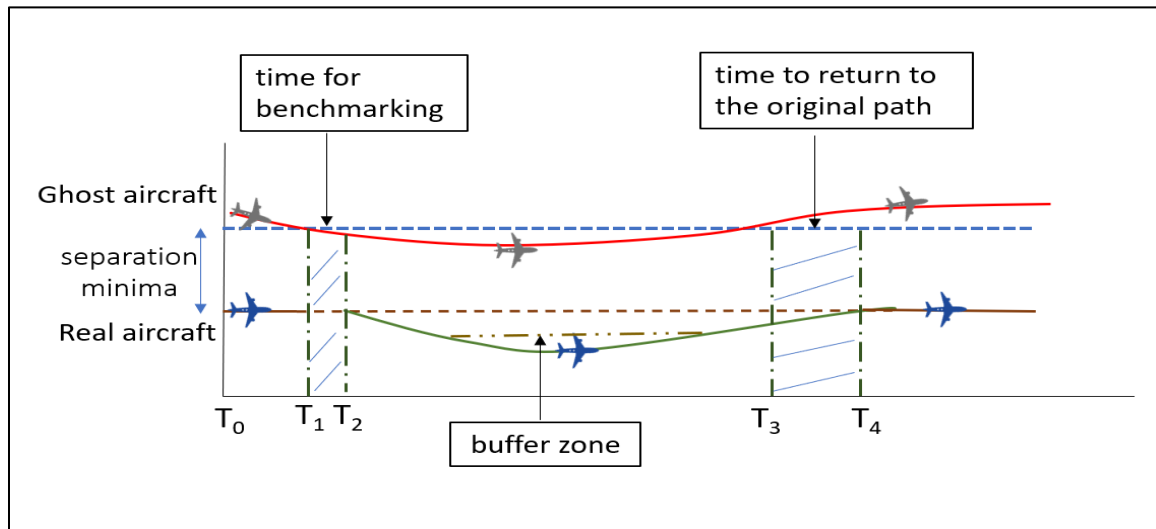


Fig.14. Framework for the Tactical Diversion

To populate the required data to run the simulation in Matlab fusion application, we converted the lat-long data obtained from the ADS-B file and converted it into XY coordinates before plotting it on a cartesian plane. The same was performed for the ground speed, which was converted from knots to meters per second and altitude, which was from feet to meters. Trajectory data for the real aircraft and the ghost aircraft are as shown in **Table III in Appendix 1-A** and **Table IV in Appendix 1-B**. Meanwhile our proposed tactical diversion trajectory and the conventional simplistic diversion trajectory data can be referred to in **Table V** and **Table VI** in **Appendix 1-C** and **1-D** respectively.

5.3 Simulation Results

Based on the simulation results as shown in **Figure 15**, the proposed ATC level tactical maneuvering— $T1c$ which started at coordinate $x = -5464$ m, $y = -952$ m—took 352.3 s to close in to the track of the original trajectory— $T1a$, which began at coordinate $x = -122.2$ m, $y = -14.0$ m. Throughout the entire simulation, the plotted trajectories adhered to the separation minima rule whilst both the ghost aircraft and the legitimate aircraft continued to descend with a similar profile. The benchmarked tactical maneuvering was triggered when the ATC spotted that the ghost aircraft was closing into the real aircraft’s path and eventually arrived at a location less than 6nm away at $E1a$ from coordinate $T1b$, which is $x = -2572$ m and $y = -9577$ m. At the time the real flight trajectory arrives at the finishing point at $t = 300$ s, the simplistic deviation, $T1d$ only managed to reach the location of $T2d$ at coordinate $x = -43,672$ and $y = -18,045$, approximately 66.7% from its full trajectory course. Comparatively, this location is farther away than the distance of the aircraft guided under the proposed benchmarking framework, $T2b$ from the supposed location under the original trajectory. At the end of the simulation, the simplistic deviation took a total of 423 seconds to arrive at the end of its trajectory.

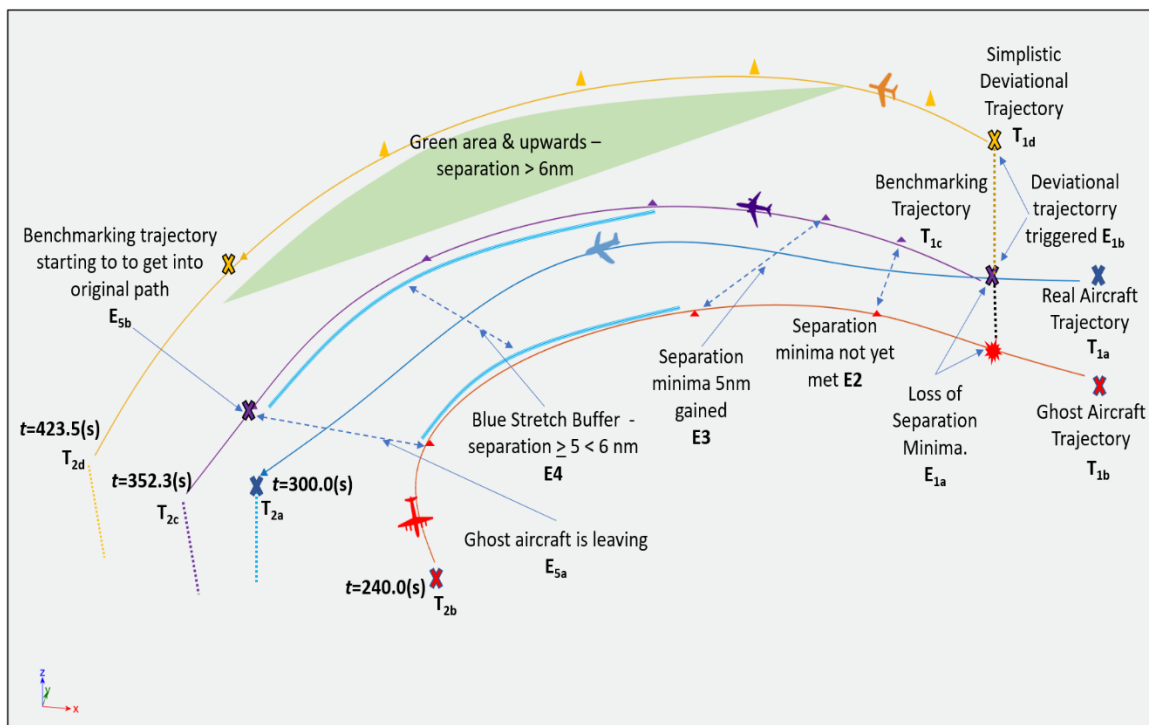


Fig.15. Simulation Results—Performance of Tactical Maneuvering Against Conventional Simplistic Deviation

Apart from the time taken by both compared trajectories to finish their course, other readings, such as trajectory data, are shown in **Table III** and **Table IV** accordingly. The state of the tactical maneuvering trajectory framework can be described as:

The current state of each of the trajectories is as per the progression of the trajectory at the inferred time, $S_n (T_n)$. Properties for a trajectory, T, at any state

$$= \{latitude, longitude, altitude, course, speed, descent(rate), roll, pitch, yaw\}$$

Based on the proposed tactical maneuvering framework's linear separation, e , at n state,

$$S_n = e(Tc_n) \geq 5nm \geq e(Tb_n)$$

with Tc is the proposed tactical trajectory for deviation and Tb is the ghost aircraft trajectory.

Based on the results, it is obvious that the conventional simplistic deviation trajectory requires more time to reach the location close to the tactical benchmarking trajectory. A visual observation of the end state of the simplistic deviation trajectory suggests a substantive distance to fly before being able to join the original flight path. We can also infer that the distances travelled by each trajectory differ from each other based on their time of arrival through comparison with the original real aircraft's trajectory as the focal point. The difference between $T2a$ and $T2c$ (at endpoint) is more than 52.3 s as of $t = 300$ s. This is primarily due to the tactical benchmarking trajectory having flown longer distance and at lower speeds. Meanwhile, the difference between the coordinates of $T2a$, $T2c$ and $T2d$ is more than 1 nm apart from a fixed angle. This tells us that, with a faster speed profile, there is a possibility that tactical benchmarking and a simplistic deviation trajectory would be able to get closer to the real trajectory by covering more distance, thus be able to complete its designated path within the simulation run time.

However, this argument is still inconclusive as the original ADS-B data that were used were insufficient to produce a clear projection of each of the trajectories into airport airspace. Nevertheless, based on the findings of 300 to 423.5 s of the simulation run, the tactical benchmarking trajectory provides a guided trajectory that is safe and quicker to merge with the original trajectory compared to the simplistic deviation trajectory resulting

from a generic and unguided action by the ATC. Furthermore, the analysis of discrete events within the proposed framework always looks for the optimal state by safely and quickly finding an updated path to join the original trajectory depending on several conditions such as current surrounding air traffic and consideration of existence of meteorological factors.

5.4 Discussion

The benchmarking trajectory simulation applied assumptions in the context of no interference from non-conflicting surrounding traffic. Therefore, this simulation does not have to consider any other traffic except the only traffic that consists of a single legit real aircraft and occurrence of a GAS attack. This is purposely done to demonstrate the benchmarking framework in its basic form without having to consider other variables that would make the trajectory benchmarking simulation wider. The simulation also assumed that the ATC is totally guiding the aircraft in assisting the approach phase of the arriving aircraft with no further options for the pilot to select or request alternative fixes to pursue the approach phase. At all times during the entire simulation, the proposed trajectory benchmarking and simple diversion is constantly compared against the original trajectory (without ghost aircraft incursion) as we assumed the original trajectory is always the best trajectory for landing approach. The simulation is also done based on assumptions that KLIA remains as the intended landing airport.

As a fixed variable, the movement of the ghost aircraft swayed from the real legit aircraft as per event E5_a in the simulation and did not close in again after that. It was done in that way for simplicity and to demonstrate the basic form of the workability of the proposed benchmarking trajectory framework.

6. Reducing Delay in Departure

Apart from coming up with an alternative flight path in evading spoofed airspace, the takeoff procedure which begins from the taxiway or the gates, would require a specific method that can complement and support the overall process for safe takeoff. After a temporary halt of

departures, the situation on the airport ground may have changed substantively with more flights wanting to depart as soon as possible. Some airlines together with the ATC may have reassessed their priorities either to try to takeoff or prefer to remain on the ground. Managing these changing priorities could not be a simple straightforward implementation of a First Come First Serve (FCFS) sequence.

6.1 Synchronous Taxiing Approach and Discrete Events Modelling

During emergencies including in ADS-B based spoofing attack incident, ATC's priority is to ensure airport approaching aircraft to safely land. The ATM would be full of uncertainties that require impromptu decision making. As [18] has modeled the ATC's response and the cascading effects that have occurred, movements on the ground were limited to arrivals and taxiing-in while pushback, taxiing-out and takeoff were put on hold. This incident is directly caused by the degradation of other surveillance systems such as radar failure. When the attacks have subsided or the situation has started to improve and gradually getting back to normal, the ATC at this point may decide to resume departure. However, if there are still ongoing attacks, a special procedure is required to ensure unaffected aircraft can takeoff safely and smoothly without experiencing further delay and avoiding possibility of a long waiting time, stalled at the taxiway during the taxiing-out.

In mitigating the above problem, this dissertation proposes taxiing approach primary objective as to assist the ATC in resuming departure amid ongoing ADS-B spoofing incidence. It is carried out through three key components or phases which are the establishment of situational awareness of the current spoofing pattern and the aircraft sequencing jobs in hand, selection of aircraft cluster for taxiing-out, and cluster switching while taxiing-out. The entire approach is modeled based on discrete events progression which is comprised of set of events that would alter the dynamics on the taxiway through inducement of perturbations and disruptions to the flow of the taxiing-out process.

6.1.1 Modelling Kuala Lumpur International Airport (KLIA) for Ground Movement Dynamics

This dissertation adopts KLIA as the airport model and adheres to assumptions which are as follows:

- 1) The developed scenario is referring to an attack incident occurred during emergency whereby no other aircraft surveillance methods are available.
- 2) Types and movements of aircraft in terms of speed and velocity on the ground are equal and consistent.
- 3) Sampling across simulation run time is uniformly distributed.
- 4) All aircraft agree in advance with the selection basis performed by ATC.
- 5) Simulation is inspired by a major airport controlled by an authority that operates on parallel runways and has authority over sizeable airspace.

This research is collaborated with Civil Aviation Authority of Malaysia (CAAM) by getting expert opinion and advice on several aspects of ground movement optimization under emergencies. We were guided by an experienced ATC officer on how situation on the ground would be in real world. To make our attack scenario even closer to real, the Kuala Lumpur International Airport (KLIA) taxiway which is shown in **Figure 16-A**, has been chosen to be tested with the proposed sequencing algorithm. As a medium sized airport that is servicing hundreds of domestic and international flights daily, KLIA is among Southeast Asian region's important air gateway. The taxiway is later represented in zones **Figure 16-B** to determine distance from a particular point.

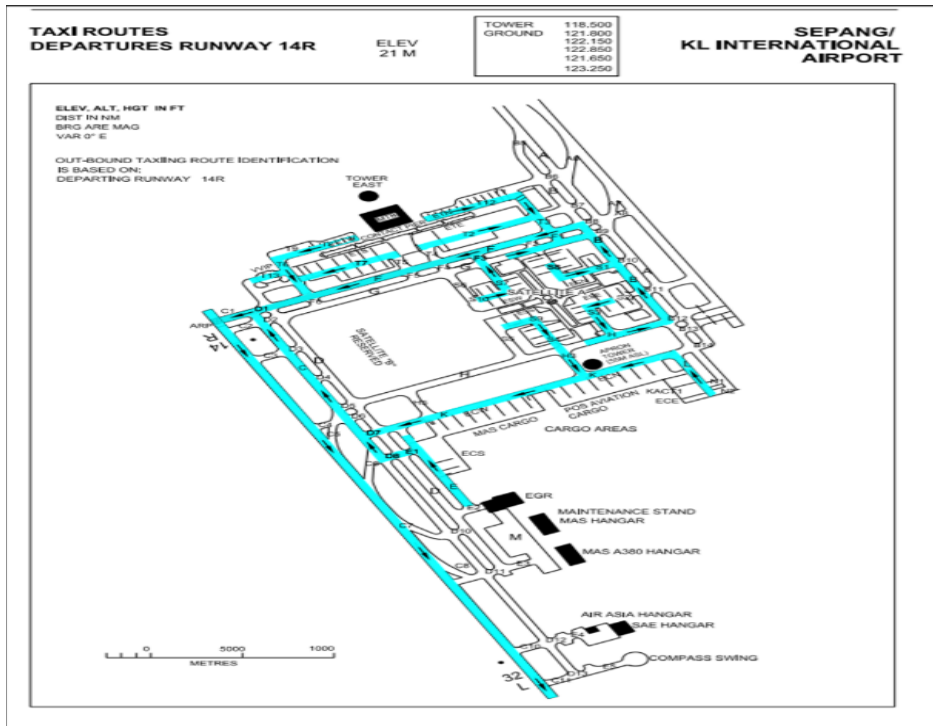


Fig. 16-A. Departure Flow Diagram Through 14R KLIA

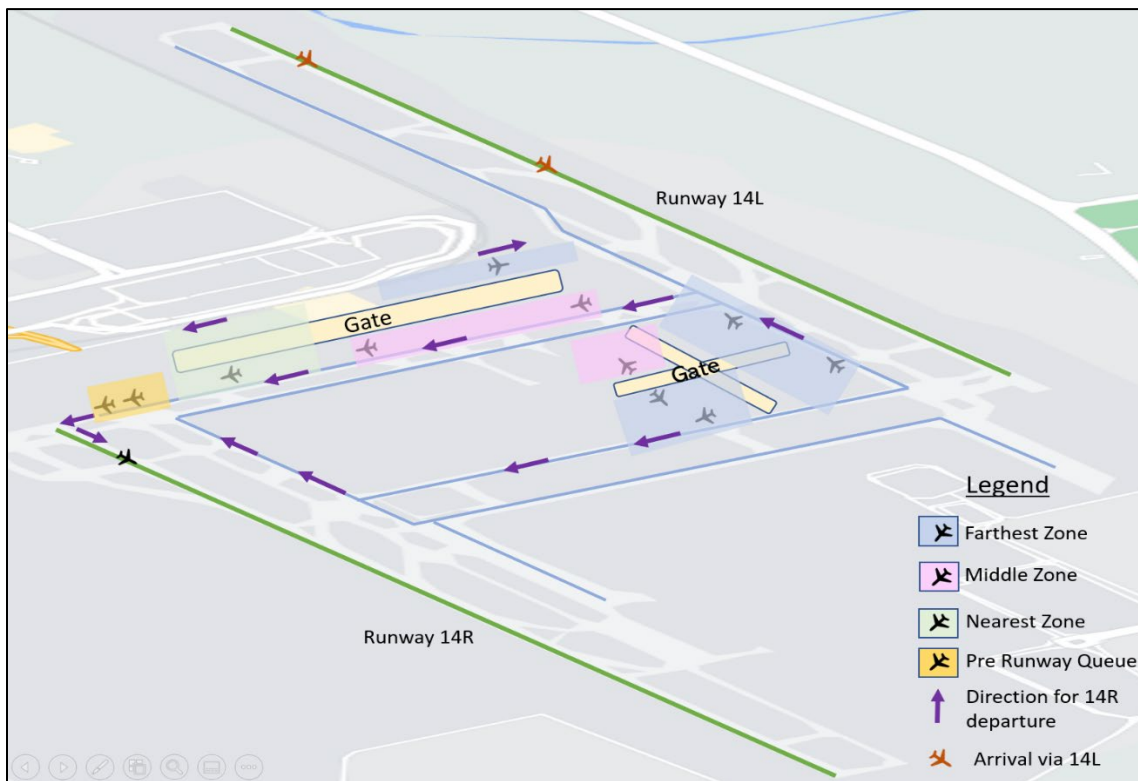


Fig. 16-B. KLIA Taxiway with Zonal Identifier (modified from Google Maps)

6.1.2 Formation of Concurrent Queues

The standard time taken to progress to the runway at KLIA from a specific gate is viewed as a variable that can represent the current state of the entire departure queue. The departure queue is a composition of sequence from 7 concurrent queues formed for each minute from six minutes to two minutes distance to the runway, the Pre-Runway Entrance Queue (PreQ) and the runway server. This sequence can be indicated as:

$$\{q_n\}, 0 < n \leq 7$$

The total number of aircraft filling a specific queue at a designated zone can be noted as

$$\frac{x}{q_n}$$

with x refers to the current number of aircraft in the queue, which at a normal capacity,

$$x \leq M_n$$

M is the maximum capacity of queue n . Thus, the state function to represent the number of aircraft attempting to taxi out for departure at KLIA's taxiway is

$$\sum_n^7 \frac{x}{q_n}$$

Queues for taxiing-out are being reassessed each time the spoofing attack changes into another airspace region. This dynamically interchanging pattern fits with the queue formation as discussed in several research on intelligent transportation systems such as [49] and [50].

To gauge the performance of a taxiing-out approach, we applied a customized zonal queuing mechanism to demonstrate the statistical formation during the entire taxiing process till simulation end time. As shown in **Figure 16**, the 7 specified queues in designated zones are formed through the standard progression time to the runway. In our simulation, these queues are also programmed to record the number of aircraft that have entered and passed through them. At the end of the simulation, the

statistics recorded by these queues formed parts of the entire statistics for measuring the performance of the taxiing-out approach.

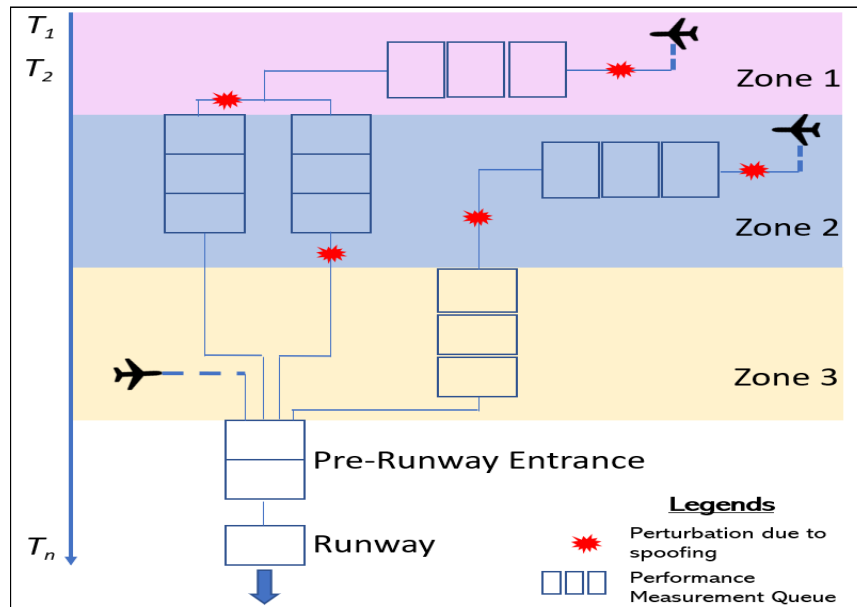


Fig.16-C. Example of Perturbations on the Ground and Queue Formations During Taxiing-out

6.1.2 Algorithmic Flow

Figure 17 describes the three core components of our proposed synchronous movement approach. The first component is the assessment of vital information about location of parked aircraft, standard time that would be taken by each aircraft to reach the runway and ghost aircraft spoofing pattern attack. Spoofing attacks behavior will determine which aircraft cluster may proceed with departure and which should wait at their respective gates. After a period of observation and departure suspension, the ATC may arrive at a decision to recommence departure operations. Information gathered since the beginning of the incident and reaching the tolerable risk level might allow the departures to resume. In relation, the middle section in **Figure 17** are the applied algorithms for departures, in which aircraft are released synchronously with Shortest Job First (SJF) leading the clusters to the runway.

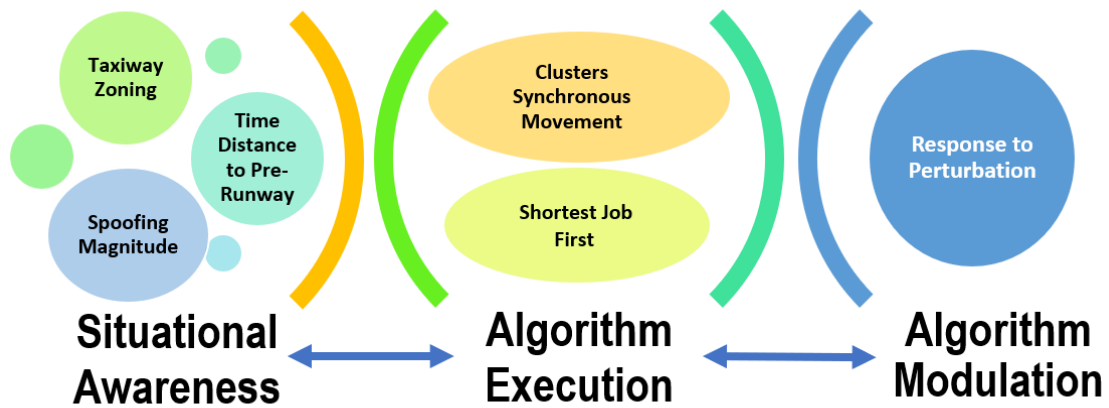


Fig.17. Three Phases Process in the Modulated Synchronous Taxiing Approach

Figure 18 explains the flow of our model in administering the departure sequence amid the ongoing spoofing attack. First and foremost, cyberattack incidents are assessed by ATC and which air space sector is affected. At the same time ATC establishes pivotal information regarding aircraft on the ground and where they are located. This step will provide a rough picture of which aircraft would not be able to proceed to takeoff due to the spoofing activities in the airspace that these aircraft must fly through. Unaffected aircraft will be allowed to get into taxiway out and head to the runway for takeoff. As these aircraft move towards the runway, the sequencer driving algorithm guides iterative checks for change in spoofing pattern and if there is a change of affected air space, the sequencer would only allow the unaffected aircraft to proceed while the affected ones remain at their gates or temporarily halted at the taxiway, allowing other aircraft to bypass.

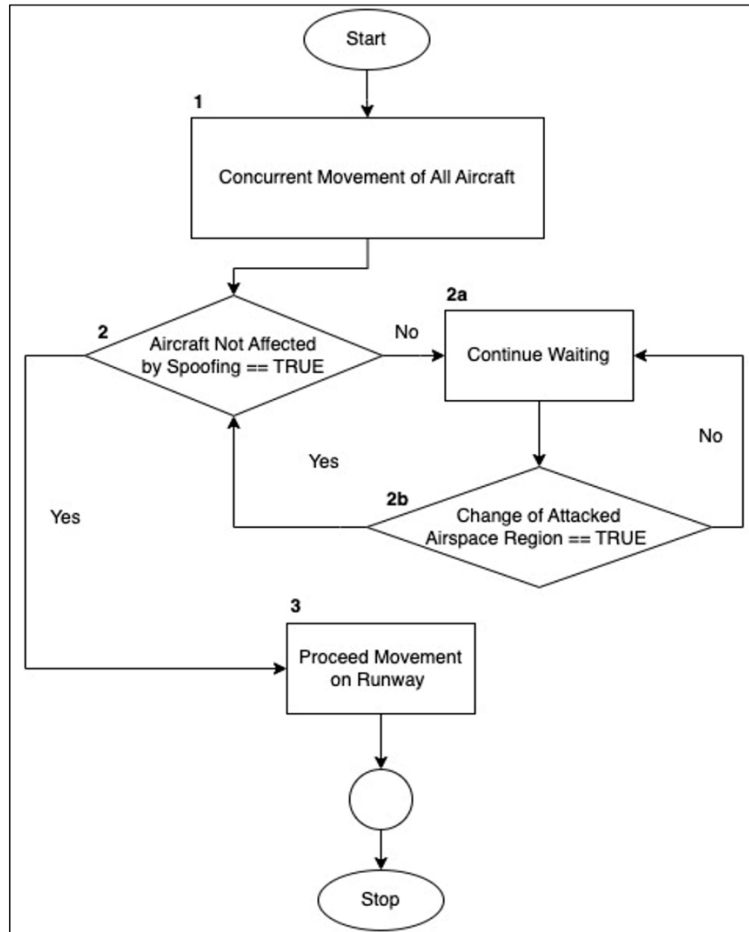


Fig.18. Example of Perturbations on the Ground and Queue Formations During Taxiing-out

Meanwhile the middle flow on the right side is the part in which the modulation is being executed by making the 'Algorithm Execution' phase responsive and adaptive to the perturbations. The changes are tracked and monitored by the model and updates the synchronous movement based on affected airspace region of aircraft clusters as per the current ongoing spoofing patterns. We name it as the 'Algorithm Modulation' phase which describes its adaptability with changes in the spoofing scenario. The modulation is confined to the algorithm that is being used to guide departure operations. For instance, changes in spoofing pattern, magnitude and time will make the current algorithm allow progression of clusters on the taxiway only if the airspace is free of ghost spoofing.

Among the existing practices by the ATC in sequencing taxiing for departure is based on the original time schedule before the occurrence of delaying events. The flow in **Figure 19** represents two types of conventional sequencing which is the Time-Prioritization (T-P) and Location-Prioritization (LP) approach.

T-P is a practice whereby the ATC prioritizes aircraft takeoff by allocating the next available departure time as per the order in the original schedule. It is also normal for the ATC to allocate a separation time between 1 to 1.5 minutes for aircraft to start taxi and head to the runway, depending on traffic flow of the surrounding airspace. The separation time to start taxiing is usually prescribed as a mean to avoid congestion at the Pre-Runway Entrance Queue (PReQ) and to prevent possibility of idling during taxiing-out.

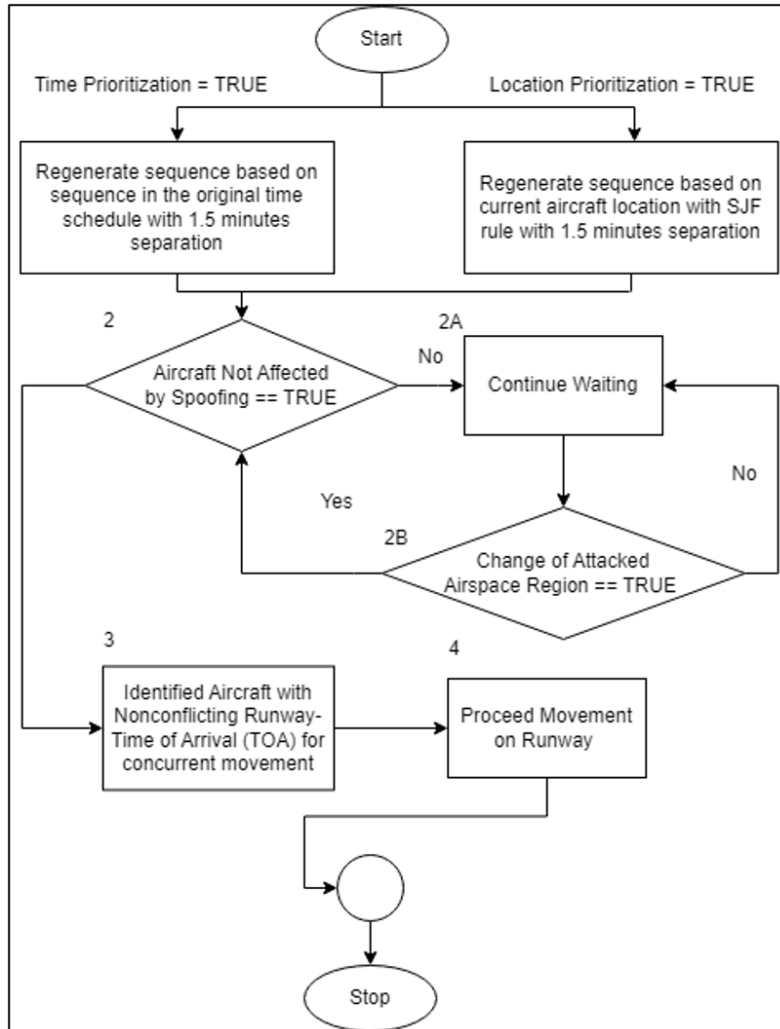


Fig.19. Example of Perturbations on the Ground and Queue Formations During Taxiing-out

In the case of uncertainties arising from perturbation events caused by ghost spoofing, the ATC would execute the time-prioritization schedule during this incident with the current available knowledge of which airspace region is clear and safe for takeoff. Aircraft that intend to fly through affected airspace will still be put on hold at their respective gates.

However, while taxiing takes place, a sudden change in the attacked air space region would see the affected aircraft to be halted at their current locations, whether at the gates or on the taxiway. The ATC then needs to revise the time-prioritization schedule once again to identify which aircraft in line can proceed for taxiing. The ranking based on original schedule remains although sequence is being revised. Aircraft clusters that are allowed to proceed for taxiing are getting switched repeatedly based on the spoofing conditions, until the attacks are clearly resolved.

Besides the T-P schedule for recommencing departures, the ATC may also opt for Location-Prioritization (L-P) departure under certain circumstances. One possible situation that this approach is used for recommencing departure is due to the long waiting time experienced by certain clusters of aircraft which have moved from their originating gates. Any delaying events which could also include our cyberattack scenario, aircraft recommencement might be done based on their current position to facilitate quicker takeoffs.

The flow of L-P differs from T-P from the beginning. The sequence for takeoff is built based on the SJF criterion to assure little waiting time for aircraft which are located close to the runway. Whenever the spoofing attack changes as per in our crafted attack scenario, alternate clusters will be selected for taxiing and the ones which are closer to the runway continue to be given priority to move first. The separation of 1.5 minutes between aircraft would also take effect to avoid congestion. This approach aims to expedite takeoffs by simply choosing aircraft which are already close to the runway.

6.2 Attack Based Simulation of MSTA, T-P and L-P

According to consultation with CAAM, in general there are three designated airspace regions for climbing after takeoff at KLIA, which are Northern (N), Eastern (E) and Southern (S). In our crafted attack scenario, these airspace regions are being alternately attacked with ghost aircraft spoofing. The first attack instance spans for 3 minutes, from $T=0$ minute (m) till $T=2.9$ m. This attack targeted the S airspace region. Next, the attack shifts to E region beginning at $T=3.0$ m till $T=5.9$ m. Lastly the attack focused on N region, and it is defined a bit longer from $T=6.0$ m till $T=10.0$ m. In accordance with the discussed attack qualities of a high-impact scenario, occurrence of a single ghost aircraft spoofing attack is already enough to coerce the ATC to suspend departures. Thus, our simulation is

designed based on a single ghost aircraft spoofing, occurring during the designated period in a specified airspace region. We assume movement speed is always consistent for all aircraft and no other traffic intervention on taxiway except for this taxiing-out simulation. According to CAAM, the earlier stage when the ATC decided to recommence departure is the period with the highest volatility. A slight perturbation will trigger the effect of uncertainties. This is the reason why we change the attacked airspace regions throughout the simulation by creating three attack periods. The entire attack duration and the affected air space regions are summarized in **Table VII** as in **Appendix 2-A**.

6.2.1 Attack During Peak Period

This research adopted the departure schedule on October 18, 2022, from 0900 till 0950 hours at KLIA 1 as per **Table VII** as in **Appendix 2-A** to simulate attack during a busy departure period. This schedule is among the schedules that contains the greatest number of departures within an hour time frame. We limit the number of aircraft to a total number which have been delayed for the past one hour as based of CAAM's feedback, the ATC would supposedly take up to an hour before deciding on using MSTA. This schedule consists of 17 aircraft's allocated time of departure. Next, we simulated the data using our model of discrete events of perturbations on the taxiing-out during departure. Besides MSTA, we also computed the reshuffled sequence of the peak time schedule using the conventional T-P and L-P approaches for performance comparison.

i) Discrete Events Model for MSTA

Figure 20 is the proposed MSTA model for simulating the peak schedule as in **Table IX** in **Appendix 3-A**. The model, which was developed using Matlab Simulink's SimEvents®, replicate the entire taxiing-out sequence comprise of the 'Farthest', 'Middle', 'Nearest' and 'PRQ' zones including the perturbations caused by ghost aircraft spoofing attacks that occur during the taxiing-out simulation run time of $T = 10.0$ minutes. Changes to the state of the system dynamics are statistically recorded across the model.

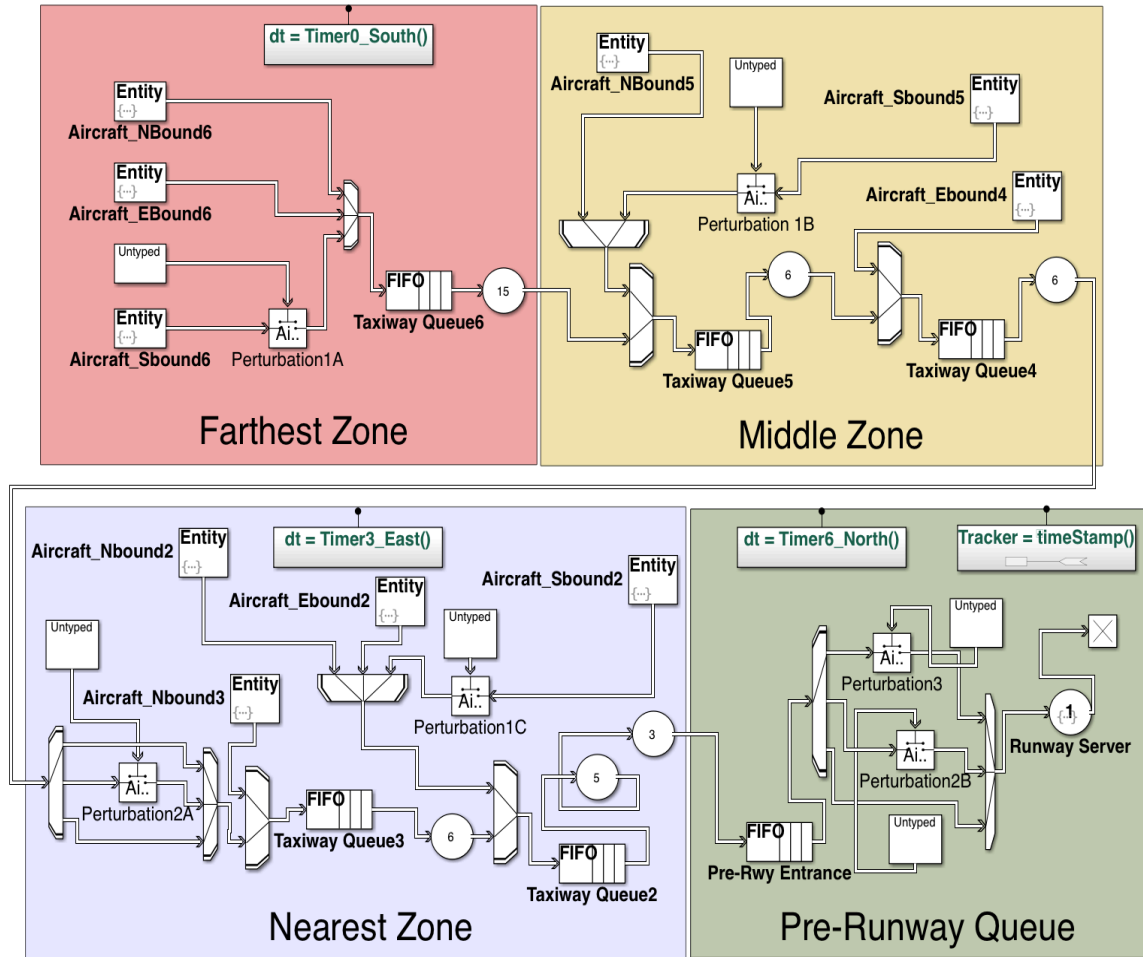


Fig.20. Discrete Events model of MSTA (peak schedule)

ii) T-P and L-P Sequencing Simulation

Sequencing approach order for T-P is based on whichever aircraft is listed first in the original schedule. This condition is similar to 'First-In-First-Out (FIFO) scheme. **Table XI** as in **Appendix 4-A** shows the simulated results of the sequencing. We deliberately keep the simulation in tabular form to highlight the order in the schedule and to demonstrate which aircraft was prioritized over others. The ATC will assess the entire job as a whole and determine the planned time for each aircraft to enter the runway. Time for an aircraft to begin movement depends on the time it is expected to reach the runway from its current position.

iii) A color-coded scheme is adopted to visualize the aircraft movements and to mark spoofing event occurrences. Red

columns representing spoofing events mean no movement. Aircraft that were allowed to proceed for taxiing-out during the first attack period are columns in light yellow. Aircraft that began movement during the second attack period are assigned with blue color while for aircraft that began to move during the third attack period is in purple column. The specific color code which represents an aircraft progression is maintained till the end of the simulation, unless the aircraft has managed to enter the runway, which will turn into green column. For blanks with dashes, these were the aircraft that were not selected for taxiing even though the airspace region that they intended to fly through were not affected by the ongoing spoofing incident. On top of that, there are colorless columns with dashes that supersede the green ones horizontally, meaning that no movement is required as the aircraft has reached the runway. Some aircraft theoretically were allowed to move but their respective 'Time to begin movement' and 'Planned time to enter runway' details were not disclosed as the changes in the spoofing attack period made the projected sequence obsolete and requires a revision by the ATC. The movement column for these aircraft is also blank with dashes. The same color-coded procedure was also applied in L-P simulation as in **Table XII** in **Appendix 4-B**.

In L-P, prioritization of aircraft that is closest to the runway make the sequence predictable from the beginning of every attack period. Despite its difference with T-P in aircraft selection, both approaches practice the commencement of concurrent movement for aircraft that have non-conflicting 'Planned time to enter the runway'. Its selection basis may see major changes of aircraft location, starting from the area close to runway and gradually followed by aircraft in the subsequent zones.

6.2.2 Attack During Non-Peak Period

A non-peak schedule is adopted for departures from 1800 till 1850 hours on the same date and airport which is as in **Table X** in **Appendix 3-B**. A special DEM which is as **Figure 21** is built to simulate the proposed MSTA. It is almost similar to the Peak-Time DEM but way simpler as it comprises only 47 percent load of the peak schedule entities. The Farthest Zone comprises of 3 aircraft located 6 minutes from the PRQ Zone. In

Middle Zone, one aircraft is parked 5 minutes from the PRQ Zone, while in the Nearest Zone, one aircraft is located 3 minutes from the PRQ Zone and there are two aircraft which are 2 minutes from PRQ Zone. We maintained the attack scenario and pattern of three periodic attacks but swapped S airspace with N as the first airspace to experience spoofing attacks. E airspace came second while S airspace was attacked in the last period. Total simulation run time remains 10.0 minutes. The parameters for the attack scenario duration coupled with the affected airspace are as per **Table VIII** in **Appendix 2-B**.

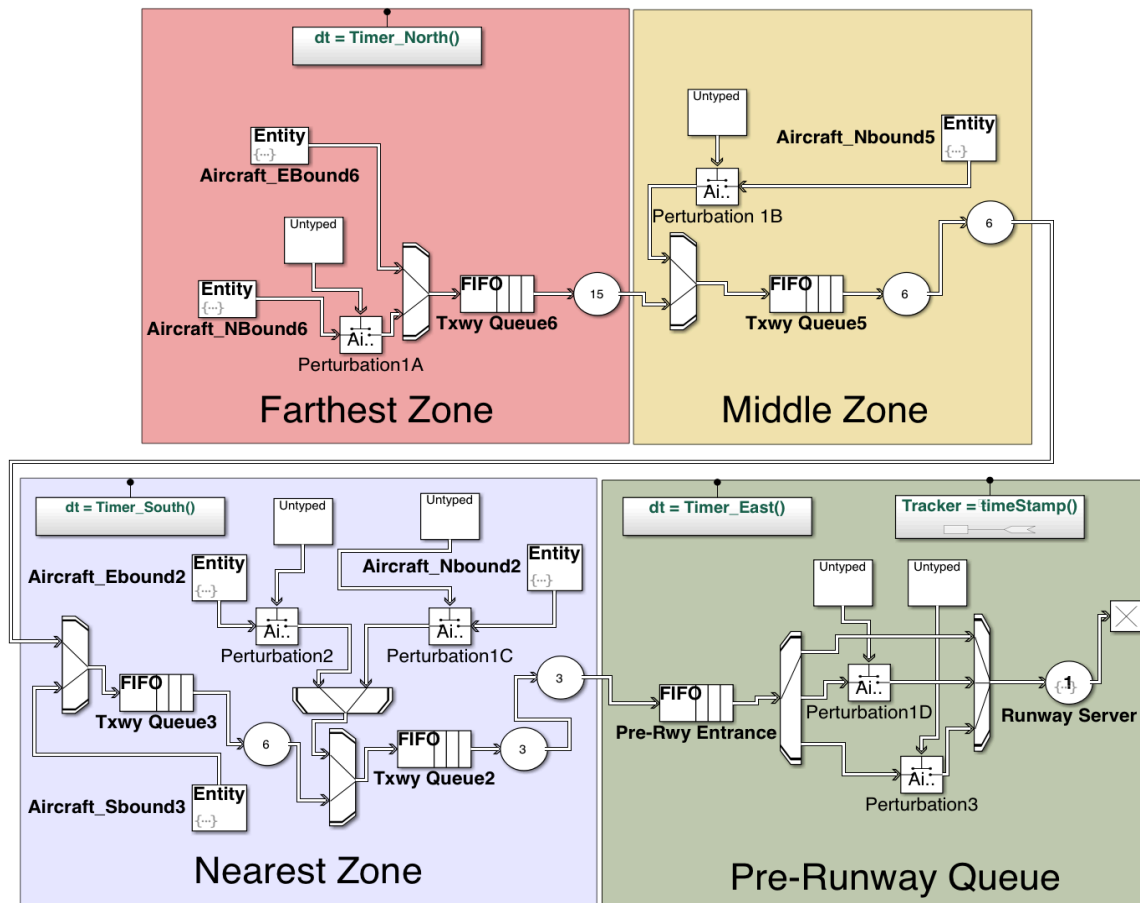


Fig.21. Discrete Events model of MSTA (non-peak schedule)

After MSTA model was simulated for the non-peak schedule, the non-peak sequence was also simulated based on the respective algorithms by using aircraft movement diagram because of the limited number of aircraft has enabled simple movement tracking of aircraft to be plotted directly. Simulated movement diagrams are in for T-P approach and for L-P approach are as **Figure 22** in **Appendix 5-A** and **Figure 23** in **Appendix 5-B** respectively. Both figures show numbered sequences, tracks for each

aircraft that moved, delimited dashed lines representing border of the zones on taxiway and time from there to reach the PRQ and recorded time for aircraft that entered runway.

6.3 Simulation Results and Analysis

6.3.1 Peak Period

i) Runway

First, the performance of the three simulated approaches based on number of progressive aircraft at four different zones and the runway were evaluated. As seen in **Figure 24-A**, MSTA records five aircraft in the runway, starting from the first one at $t = 3.5$ seconds (s), while the following four aircraft consistently arrived within 1.5 minutes (m) intervals. This shows the SJF algorithm by selecting aircraft that are close to the runway has taken advantage of the available time and airspace. The same result can also be seen with the location-prioritization scheme in **Figure 24-B**, whereby this approach adopts sjf too. Identical results were recorded in both MSTA and L-P. Meanwhile, the number of aircraft entering the runway is lower with T-P approach as only two aircraft recorded within the same simulation run time as recorded in **Figure 24-C**. At the end of the simulation, the closest aircraft to enter the runway is at the runway server, finishing its final checks with remaining preparation time of 0.5 m before entering the runway.

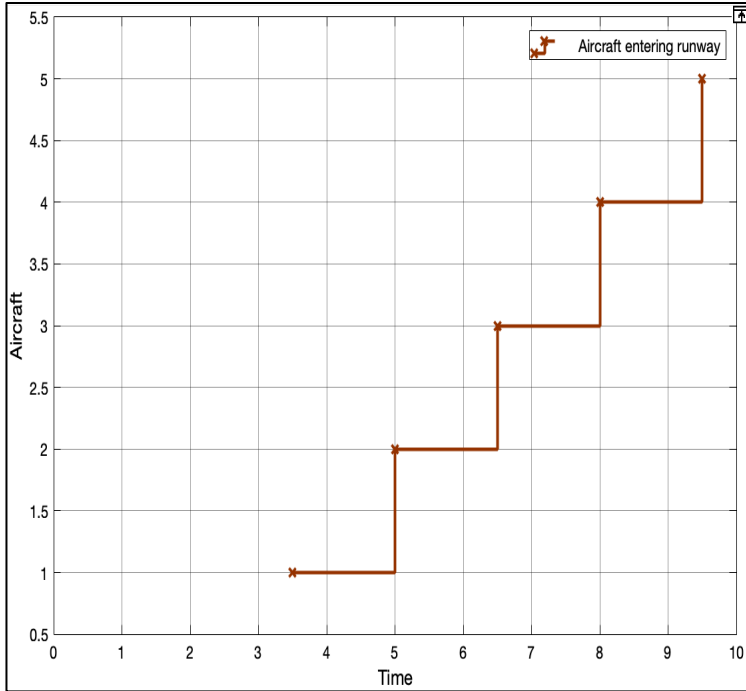


Fig.24-A. MSTA (aircraft entering runway)

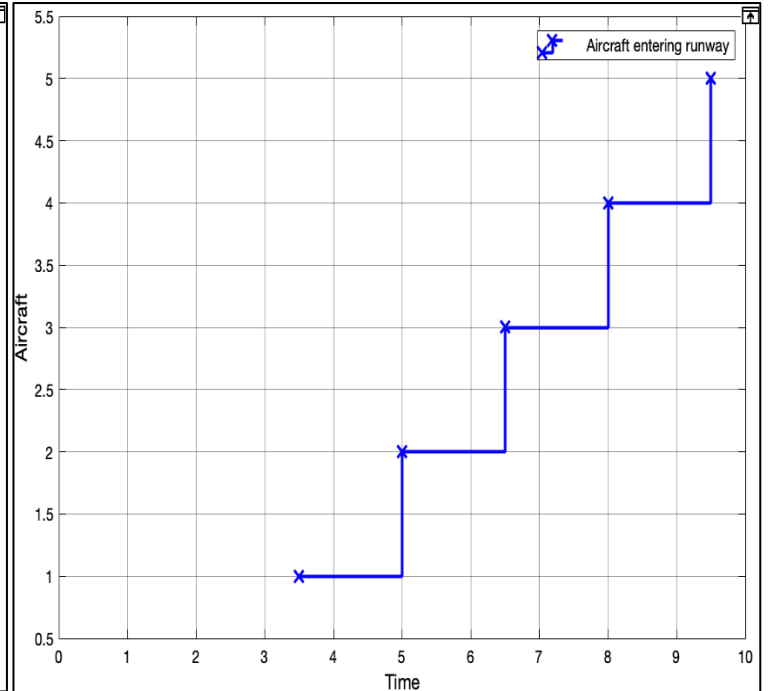


Fig.24-B. L-P (aircraft entering runway)

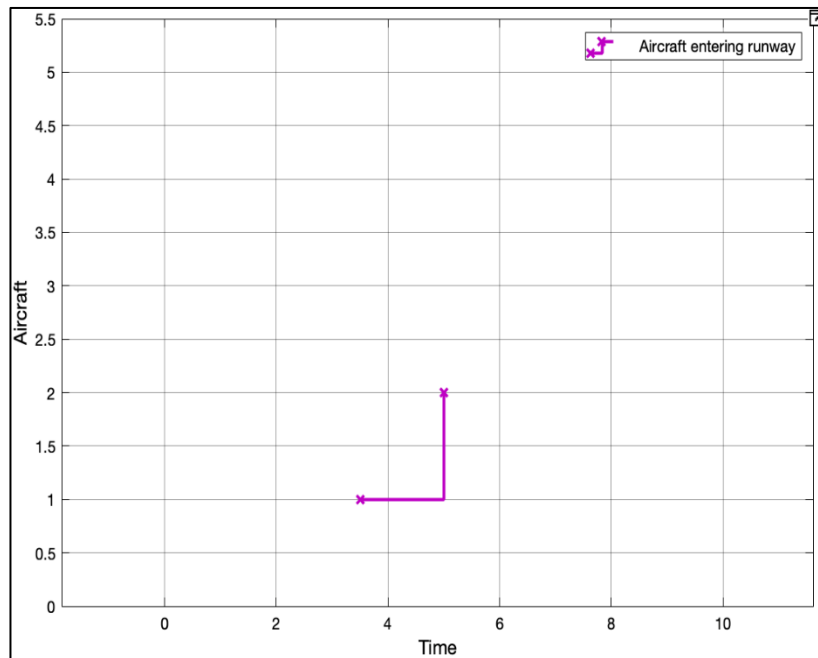


Fig.24-C. T-P (aircraft entering runway)

ii) Pre-Runway Queue

Before getting into the runway, there are two locations where aircraft are queued which is the runway server -- a place where the next aircraft that gets into the runway would be; and Pre-Runway entrance Queue

(PReQ) -- the final queue before the runway. In the model, the combination of these two short consecutive queues is named as the Pre-Runway Queue (PRQ). The total number of aircraft that made their way into PRQ is our second performance evaluation zone. **Figure 25-A** is the number of aircraft getting into the runway, and **25-B** is aircraft in the PReQ. Meanwhile **25-C, D, and E** contains charts showing the total number of aircraft that entered PReQ from a distance of 3 minutes, 2 minutes and 1 minute respectively.

The results show that most times, the runway server in all three simulated approaches is fully occupied as it functions to hold a single aircraft before letting it into the runway. However, in PReQ, MSTa and time-prioritization produced similar results with two aircraft remaining at the end of simulation, while for location-prioritization, no aircraft in the PReQ at the end of simulation.

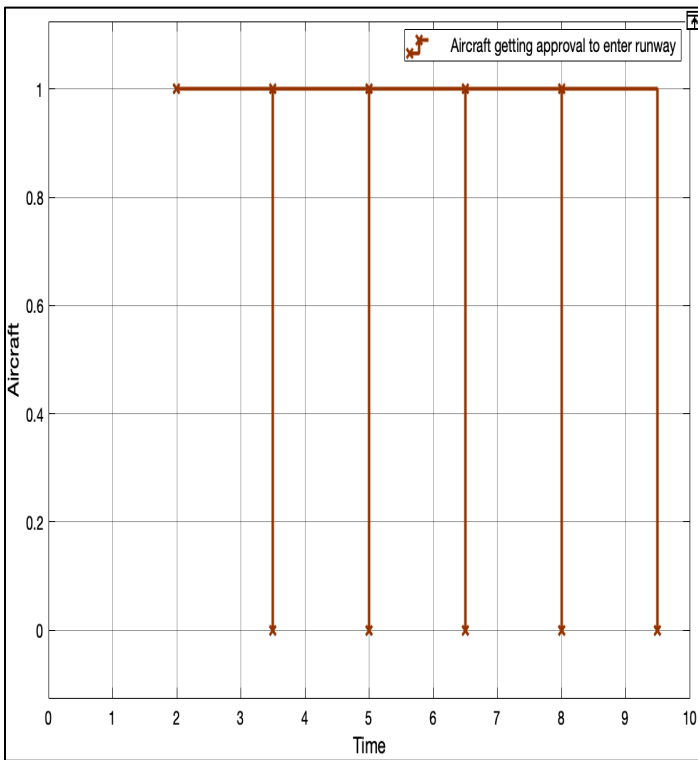


Fig.25-A. MSTa's Performance (in runway server)

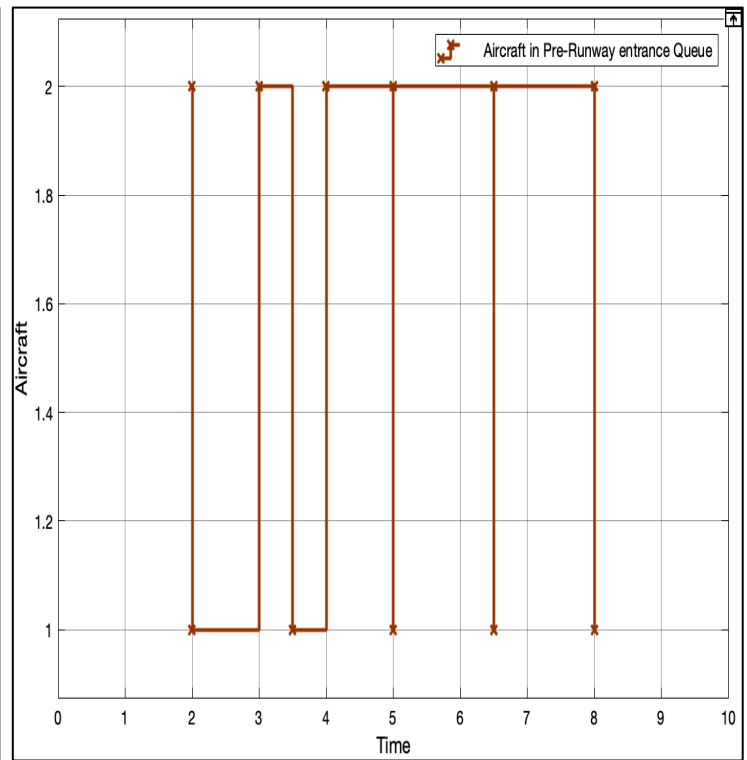


Fig.25-B. MSTa's Performance (in PReQ)

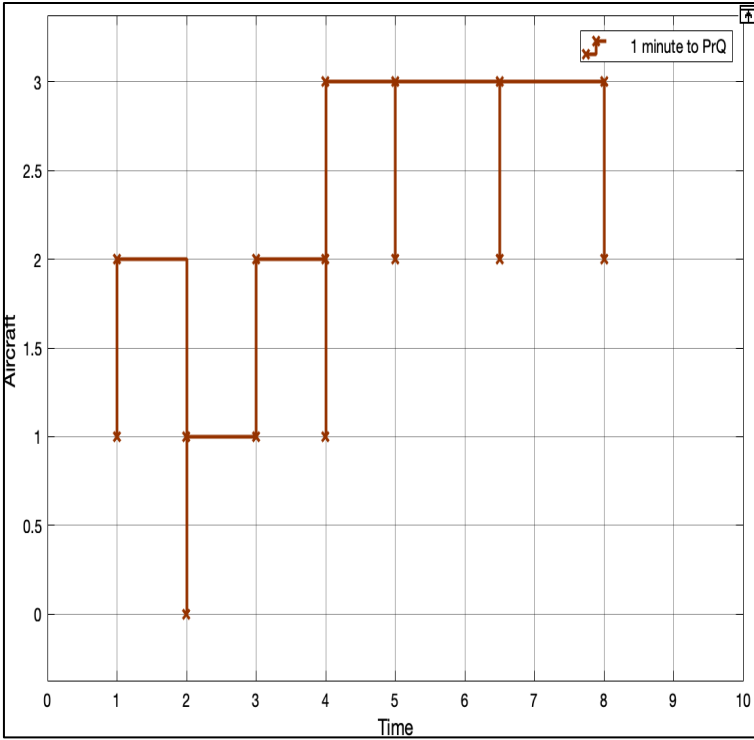


Fig.25-C. MSTA's Performance (1 minute to PRQ)

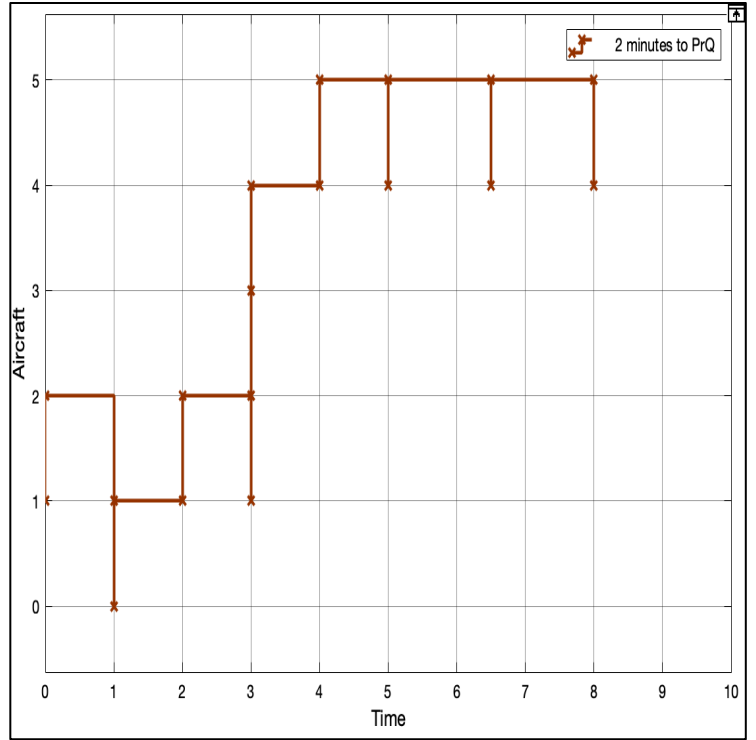


Fig.25-D. MSTA's Performance (2 min PRQ)

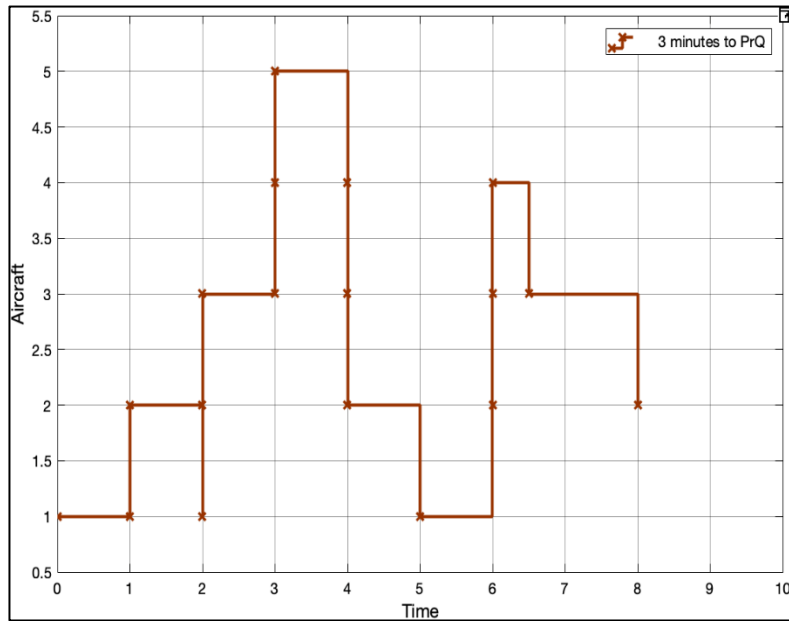


Fig.25-E. MSTA's Performance (2 min PRQ)

- iii) Aircraft Ratio of Farthest-Middle-Nearest-PRQ (excluding runway) Zones

Moving deeper into the taxiway zones, movement of aircraft within the three zones plus the PRQ is a significant factor in determining the performance of the taxiing approaches. Performance is determined by the difference between the ratios of aircraft within the three zones and PRQ at startup against the ratios at the end of simulation run time. For instance, statistical data by MSTA in **Figure 25-A** till **E** above - notably can be represented in progression ratio. By comparing the ratios, we can identify and differentiate the rate of aircraft progression of all the three approaches.

$$\text{Ratio, } R = \text{Farthest} : \text{Middle} : \text{Nearest} : \text{PRQ}$$

$$R = F : M : N : P$$

Thus, ratio at start is

$$R_{(start)} = F_{(start)} : M_{(start)} : N_{(start)} : P_{(start)}$$

while ratio at the end is

$$R_{(end)} = F_{(end)} : M_{(end)} : N_{(end)} : P_{(end)}$$

Based on the simulation results, the following **Table II-A** summarizes the situations of prior and after for each approach.

	MSTA	T-P	L-P
$R_{(start)}$	8:5:4:0		
$R_{(end)}$	0:0:10:2	7:2:3:3	7:2:2:1

TABLE II-A: Start and End Ratio of Farthest-Middle-Nearest-PRQ zone (peak period)

It is clearly shown that MSTA managed to bring all aircraft into the Nearest Zone. Meanwhile, between T-P and L-P, the former fared better as it enabled more aircraft to progress into Middle and Nearest Zone compared to the latter two approaches.

6.3.2 Non-Peak Period

i) Runway

For Non-Peak simulation, the discrete events that took place were less complex due to lesser aircraft involved. Using the number of aircraft that successfully entered the runway during the simulation run time of $T=10m$ as the primary performance index, MSTA recorded five aircraft, beginning at $T=3.5m$ while the last one entered at $T=9.5m$. Meanwhile L-P recorded similar statistics with the same number of aircraft that entered the runway and time intervals. For T-P, it only managed to fare sixty percent of the performance shown by the earlier two approaches with only three aircraft managed to get into the runway, specifically at $T=3.5m$, $T=7.5m$ and $T=9m$. This was mainly due to the dual factor of occurred perturbation together with the aircraft physical location. Progression charts for all three approaches can be viewed in the Aircraft Entering Runway charts as **Figure 26-A, B, and C**.

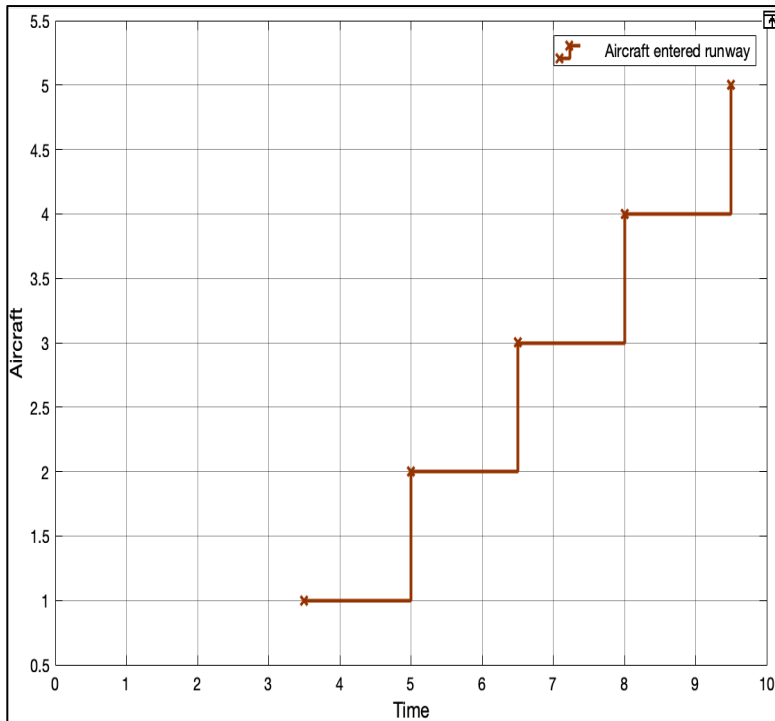


Fig.26-A. MSTA Non-Peak (aircraft entering runway)

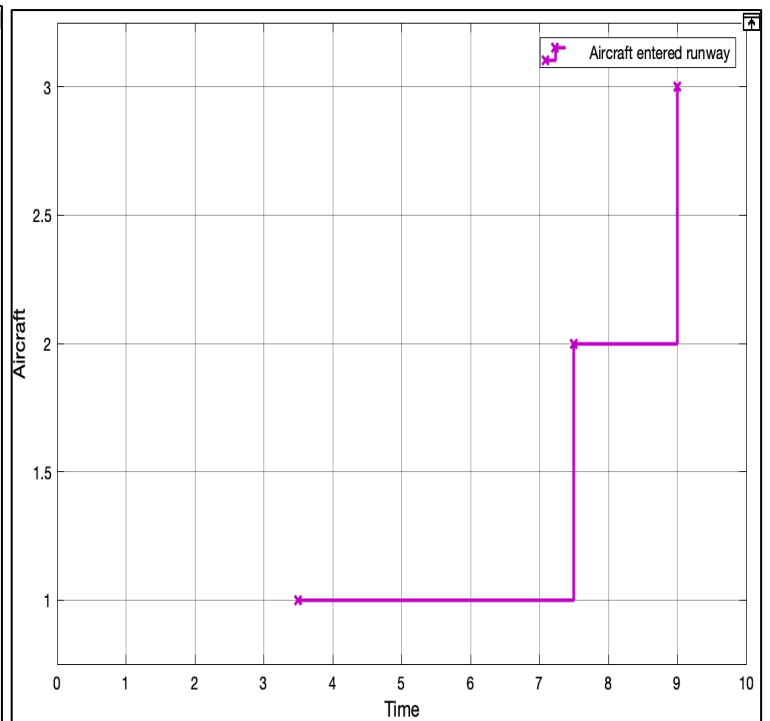


Fig.26-B. T-P Non-Peak (aircraft entering runway)

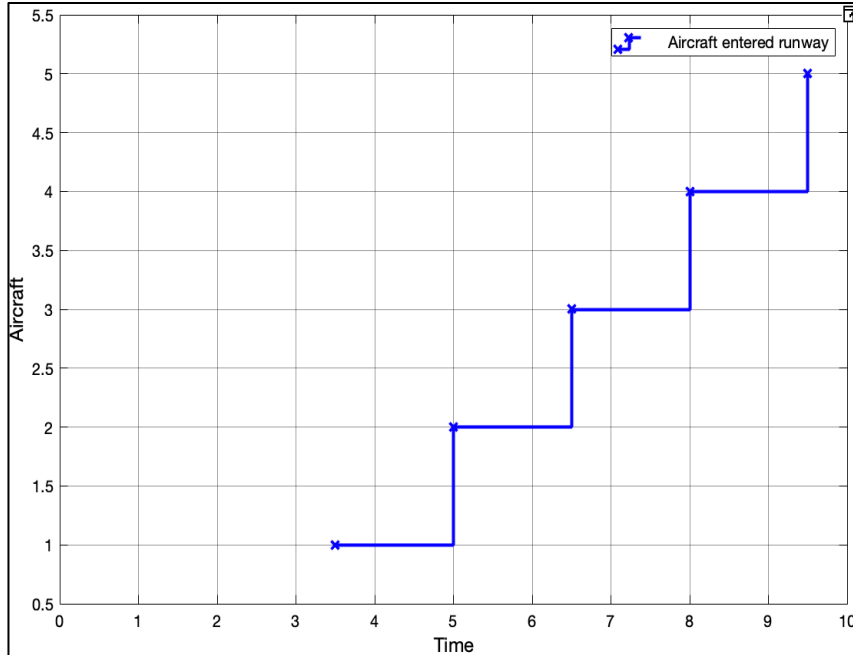


Fig.26-B. L-P Non-Peak (aircraft entering runway)

ii) PReQ

For the non-peak schedule, MSTA had this queue at the maximum capacity with two aircraft waiting to be allocated with the runway for takeoff at the end of simulation run time. For T-P, one aircraft is recorded in the queue while in L-P, PReQ records two aircraft.

iii) Zonal Ratios

Aircraft ratios within the three zones at the beginning and end of the simulation are as per the following **Table II-B**.

	MSTA	T-P	L-P
$R_{(start)}$	2:2:4:0		
$R_{(end)}$	0:0:0:3	0:1:3:1	1:0:0:2

TABLE II-B: Start and End Ratio of Farthest-Middle-Nearest-PRQ Zone (non-peak period)

6.4 Discussion

In general, the situational state of the taxiing can be denoted as total aircraft, α in its state of distribution according to the zones of the taxiway, S_n . For

$$\alpha = w + x + y + z$$

w = total number of aircraft in farthest zone

x = total number of aircraft in middle zone

y = total number of aircraft in nearest zone

z = total number of aircraft in PRQ

The state of taxiing at the beginning of simulation (prior perturbation) is:

$$S_{start} = w_0 : x_0 : y_0 : z_0$$

Based on the above starting distribution ratio, the state of taxiing at a particular instance (upon a perturbation) can be derived as:

$$S_n = w_n : x_n : y_n : z_n$$

for 3 attack instances in our simulation,

$$0 < n < 3$$

Thus, the end state, S_{end} of distribution ratio of the simulation is:

$$S_3 = w_3 : x_3 : y_3 : z_3$$

Based on series of simulation run of our proposed MSTTA, it is learnt that the factor of concurrent movement on the taxiway has enabled more aircraft to progress from their gates of origin under the period of perturbations caused by the cyberattacks. Both simulations for peak and non-peak schedule displayed similar traits. In the peak schedule simulation, five aircraft managed to enter the runway and the remaining at least are within the nearest zone of KLIA taxiway. The results of the non-peak schedule simulation echo the impressive performance in the peak schedule with all aircraft successfully entering the PRQ zone and five managed to enter the runway.

Different than MSTA, T-P and L-P approach does not fully practice concurrent movement of aircraft towards the runway. However, these two approaches adopt concurrent movement for aircraft that are located quite a distance from each other, purposely to prevent clashes of arrival time at the same location on the taxiway and so that their projected time of arrival at the PReQ will not compromise 1.5 minutes of separation rule, the rule which is of the essence for both T-P and L-P to conveniently prevent idling and long queues on taxiway.

6.4.1 Principle of Fairness and Equality

In L-P, aircraft which are located near the runway will benefit from the bias on preferential of this location-based cluster. Similar to SJF, this cluster only requires a short period of time to get into the PRQ. This is the main reason why L-P managed to record the number of aircraft entering the runway, similar to our proposed MSTA. However, L-P performance peaks mostly with proportionate number of aircraft within the nearest zone against the total simulation run time. Too many aircraft within nearest zone but with limited duration of simulation run time will not bear the same impressive results for majority of the aircraft. As more aircraft are located within the nearest zone, the required time for all aircraft to progress increases directly.

Mediocre or the least performance is shown by T-P approach in our series of simulations. The least number of aircraft that entered the runway and with ratios of significant number of aircraft left especially in the farthest and middle zone shows that time prioritization practices require more time on top of the separation time in abiding by the scheduled sequence. Fairness to aircraft which were scheduled to depart first would be served by T-P approach. However, this situation is not always true when concurrent movements are allowed for aircraft with non-contradictory time of arrival at PReQ. The reason is no other than to facilitate immediate progression during perturbations.

6.4.2 Close Monitoring and Increased Workload for the ATC

It is apparent that every time perturbation occurs (in case of our ghost spoofing attack), the taxiing sequence is disrupted, and the impact lies with the characteristics of the attack. Each time the attack pattern changes, or another airspace region is affected, the ATC have to recalibrate

its schedule to reflect the emergency situation and to follow suit the planned mitigation. The workload increase is the most with T-P approach sequencing as it aims to achieve fairness, uphold FIFO selection based on the original schedule prior perturbation and prevent idling and long queues before the runway. Meeting these three primary criteria requires thorough assessment especially if rescheduling depends solely on manual effort and non-automated recommended decision making. In L-P approach, the workload is a bit lesser when it comes to calibration, as the focus of the schedule is towards the cluster located at the nearest zone. Coupled with SJF, the ATC was able closely monitor with ease this cluster's progression while being aware of the possibility of concurrent moves by aircraft that are located towards bottom of the schedule. As for the least workload for the ATC, MSTA only requires the ATC to closely monitor the dynamics of the taxiway based on synchronous movements of aircraft. The ATC will definitely have to actively communicate with the involved aircraft to maintain safety especially when traffic is coming from multiple directions. However, they are cut short of the tedious schedule recalibrating task. Traffic on the ground would progress according to the defined queues leading to the PRQ.

6.4.3 Flexibility and Versatility

Throughout the entire simulation runs for both peak and non-peak schedule, the distribution of aircraft can be considered as ideally proportionate with more aircraft were located at the farthest zone in the peak schedule simulation while in the non-peak, most aircraft were in the nearest zone. Apart from the unique attributes of the schedule, our proposed approach stands out in terms of flexibility in managing high and low aircraft volume within a particular zone on the taxiway. This feature is not available in L-P approach as it only emphasizes cluster which is close to the runway while in T-P, time centered approach has little regards to number of aircraft in particular zone or which zone is denser than others. This is why certain aircraft which were located deep within the middle and farthest zone suffer from continuous halt in both T-P and L-P approach. Based on **Figure 25-A** till **25-E**, this circumstance did not occur in MSTA as all aircraft are progressing constantly based on spoofing situations. This shows how MSTA managed to facilitate the dynamics of the taxiway and capitalizing on the available time and queue capacity, enabling MSTA to bring forward 10 aircraft into the nearest zone.

6.4.4 Factor of Fixed Variables and Laid Assumptions during Simulations

Throughout the entire simulation, among the applied fixed variable is the movement speed of the aircraft on the airport taxiway. The movement speed of all aircraft regardless of the aircraft type is not affected by any factors and consistent throughout the progression towards the runway. Besides that, the simulation also assumes that aircraft that managed to takeoff are unaffected by the current interchanging pattern of GAS attacks.

Other than that, the unique features of KLIA is also a factor why the current form of MSTA simulation produced results as presented in this dissertation. The main idea of the methodology to model the time to progress to the runway can be generalized in any airports regardless of type. Queues can be formed at possible locations, based on the taxiing-out flow adopted by the civil aviation/airport authority.

6.4.5 Physical Airport Design

In the proposed MSTA, the physical layout determines the time nominator between the different zones (Farthest-Middle-Nearest-PRQ). This feature is critical to the proposed algorithm. Deployment in other airports either smaller, similar or larger in size requires a completely different value tuning of variable. It should reflect the exact time taken for an aircraft to reach the runway in the same condition as described in the scenario and considering all assumptions. Even though the results would be unique for each airport, we anticipate similar performance due to the capability of concurrent movement of the GAS attack-free aircraft with non-conflicting movement on the taxiway.

The proposed MTSA in this dissertation follows exactly the normal route of taxiing-out in KLIA. However, there may be changes to the taxiing-out route in the future. This could happen because of policy amendments to the departure operations or due to changes to the physical systems that are taking place on the airport ground which include apron management and allocation to other support services run by the ground crew. Moreover, if there are physical infrastructure changes, MSTA will have to adapt to these infrastructural changes and update the algorithm accordingly.

6.4.6 Drawbacks of MSTA in Peak Schedule Scenario

Even though the ratio of aircraft that managed to get to the Nearest Zone and PRQ in the Peak Schedule scenario outnumbered T-P and L-P, both of these queues are actually filled with lining aircraft. Full packed queues at both zones are similar to a typical congestion on the airport ground, with aircraft waiting to enter the runway one after another. If the simulation is prolonged, the anticipated results for takeoff time of each aircraft can be nominated in a simple arithmetic progression form of:

$$A_n = A_1 + (n-1) 1.5 \text{ minutes}$$

with A_n is the aircraft at the n turn.

Based on the above indicated time and due to the congestion build up in MSTA, the last aircraft in the queue, A_{12} will need to wait for 18 minutes before it can get into the runway.

7. Future Works

7.1 Minimizing Impact to AGMOD

Sticking to the results of the perturbation to AGMOD Dynamics shown by the simulation in this paper, the best optimization scheme would be by enabling takeoffs albeit ongoing spoofing attacks. The idea is to equally divide the TMA in two, based on the load capacity of approaching traffic. Next, a function to assess the intervals between the first and the last aircraft in the queue in terms of distance, velocity, trajectory, and synchronized time (if approaching airport airspace) would be beneficial for the ATC to gain adequate level of Situational Awareness (SA) of the current condition in the TMA. The level of SA adequacy that is going to support this function is based on overview of the affected air space, comprehension of the current attack, and projection of future states [51]. With adequate level of SA, capability to estimate the future dynamic space-time system states of the ATM, focusing on the affected airspace could be gained by refining the Kalman Filter associated algorithm such as what has been studied by [52]. These technical advantages can be complemented further

with a policy of satisfaction level criteria in maneuvering a takeoff through a 'Safe Passage' away from the lightly compromised airspace. The spoofed ADS-B in practical can be tracked by available tracking algorithms, but further studies are needed to integrate estimation algorithms like what [52] has done, with the deeply studied characteristics of a spoofed ADS-B in terms of its probable trajectory and velocity. If the calculated deviations of simulated scenarios are within the acceptable threshold, then this approach could be proved useful for the ATC during emergencies.

Assuming a case of a prioritized flight such as in **Figure 27** which intends to fly towards departure route of DR201, availability of automatic estimation of the trajectories and velocities of the ghost aircraft would likely enable the ATC to guide through the prioritized flight via the identified safe passage based on a defined set of criteria. The flight would rejoin the standard fixes once it has safely evaded the attacked airspace. Another method that can possibly safely guide the climbing aircraft is by deploying tactical benchmarking trajectory framework in climbing phase. However, this suggestion is difficult to implement as maneuverings of aircraft during climbing is limited, as the objective is to reach the designated altitude at a constant speed. The probability of needing to increase and decrease altitude during climbing phase to avoid GAS is more difficult to implement and seems impractical.

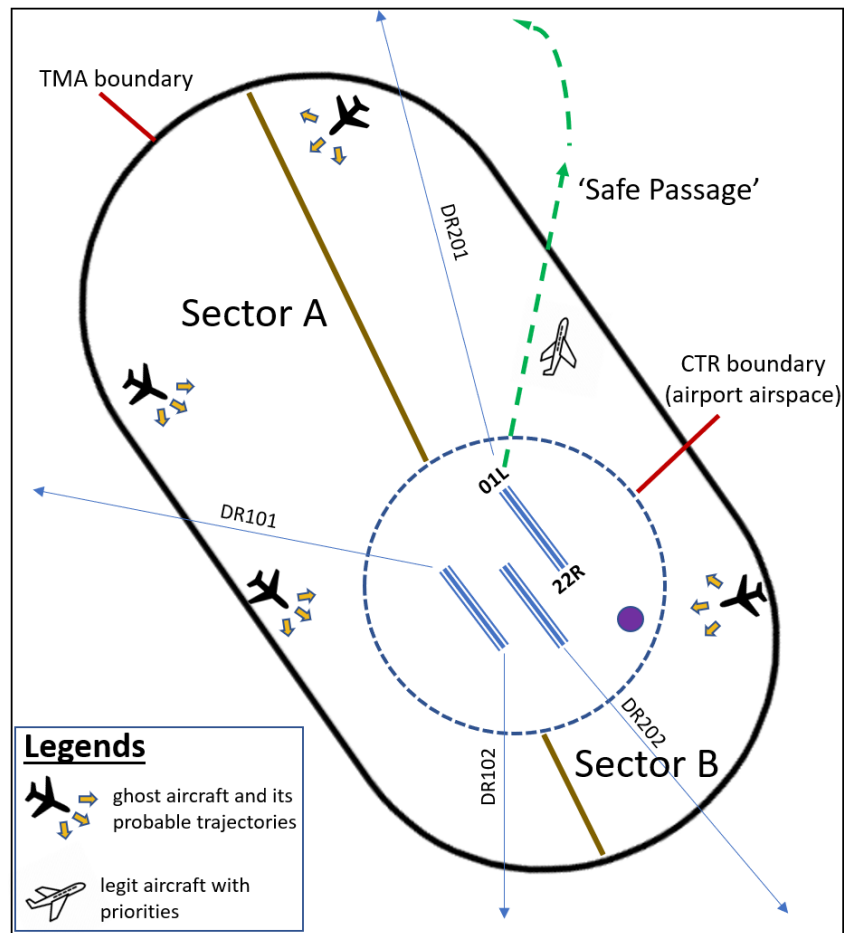


Fig. 27. Safe Passage Concept

7.2 Enhancing Implementation of MSTA

Among possible innovations in the future that could be explored to add value to MSTA are those that can promote its effective implementation.

7.2.1 Technical Changes

The addition of more significant variables into the simulation parameters, for example traffic pattern during emergency either in the air or on the airport ground will widen the scope of the modeled environment. Simulating a close to real system has always been a challenge to any system developer as it requires an adequate amount of meaningful and reliable data. As our approach is made up of several queues as the engine of our discrete events analysis, changes in queuing strategies in the future may work well in boosting the system dynamics of the taxiing-out process due

to physical changes on the airport ground. This is more relevant when more variables are introduced into the operational environment and if there are infrastructural expansions or renovations to the current ones. Noting that the current MSTA theoretically assumes that constant speed is observed by all aircraft during taxiing-out, congestion and longer queues may exist in MSTA when aircraft are heading towards the runway in droves especially in a scenario of a large size airports. However, with time-defined queues and segmentation of zones, breaking them into smaller zones might model the dynamics better. Besides a deep analysis on systems behavior during emergency need to be carried out, data representing taxiing movement dynamics at larger airport is required so that future studies on operational resiliency derived from this angle could offer better optimization.

7.2.2 Policy Harmonization and Integrated Communications

i) Complementing Regional Collaboration Framework

The concept of Airport Collaborative Decision Making (ACDM) is becoming more popular as more airports besides in Europe where it was established, have been embracing the concept of data sharing for optimizing airport operations. The primary objective of ACDM is to foster information sharing between airports for making pre-departure and the turn-around time processes more efficient and resilient. In support of the implementation of ACDM in terms of safety assessments, our proposed MSTA will fit as the local mitigation technique in dealing with delays due to systems failure.[53] highlights the assessment flow of generic and local failure case analysis. ACDM recognizes local mitigation techniques in lessening the overall impact on the flight operations. Manual of ACDM [54] indicates that technical failure experienced by the ATC may force the traffic control to be reverted to manual, or even worse, closure of the airport. Thus, we strongly believe that output from MSTA in the context of reducing departure delay time is in line with ACDM data sharing protocol and its objective.

ii) Service Level Fulfillment

Each airline has its own policy in handling delays and cancellations. Some countries such as The United States does not regulate the outcomes of any delays or cancellations of flights [55] However countries like Malaysia

through Malaysian Aviation Commission (MAVCOM) that acts as the mediation body between the air transportation users and the aviation service providers tend to create more conducive customer-driven air transportation sector through aviation customer's code of protection (MACPC (amendment)2019). The code emphasizes service quality in delivering punctual services in terms of flight departure and arrival [56]. The airline's policy also reflects their course of action whenever their aircraft is involved in incident as laid out in this study.

iii) Integration in Automation

In situations especially during emergency, the ATC has full discretion to manage and mitigate the situation to lessen the impact. However, with a structured automated recommendation for projecting aircraft taxiing scenario, our approach can be integrated as part of systems that facilitate compliance with the Standard Instrument of Departure (SID). The automation should recommend how specific taxiing approach such as MSTA should be executed to maintain compliance with SID and its objectives due to extraordinary events and unplanned changes to the inbound or outbound air traffic flow.

8. Conclusion

To assess the risks and impacts of GAS, this dissertation proposes a method to quantify cascading effects derived from spoofing attacks by using a discrete events model evaluating AGMOD Dynamics. From series of simulations with different set of parameters, the proposed model demonstrated how cascading effects of ADS-B spoofing attacks occur in the form of propagated flight delays and can be quantified starting from the response of ATC in verifying the ghost aircraft in TMA. In consequence, the legitimate aircraft behind the ghost aircraft were delayed and simultaneously, takeoffs were also suspended to make way for airport approaching aircraft, resulting to only a few aircraft that managed to take off. These events were clearly inferred from statistics recorded across the servers and queues during the simulated scenarios. The scale of the effects is theoretically correlated with the magnitude of the attack, which is in this paper, greater number of spoofed ADS-B introduced into the system will

cause longer delays to arrival, ground movements either inbound or outbound and continuous suspension of takeoffs.

Meanwhile the proposed ATC level tactical maneuvering in reducing delay to arrivals has shown results of an ideal framework in countering ADS-B false message injection cyberattack especially in situations whereby nature of such attacks could not be verified in the early stages as what the crafted high impact attack scenarios demonstrated. With safety as the utmost priority, adherence to safe distance and concurrently trying as best as possible not to deviate excessively from the original flight path has become the ATC agenda in dealing with such incidents. This can be achieved through consistent benchmarking of the ghost aircraft trajectory with defined separation thresholds so that ideal deviation in the proposed trajectory is sustained throughout the attack period.

For reducing delay during departure amid uncertainties of GAS, this dissertation's proposal of a novel of MSTA outperforms the conventional T-P and L-P in terms of number of aircraft that managed to enter the runway and with more aircraft progressed from farthest zone of the taxiway. Easy execution for MSTA compared to the conventional taxiing approaches during ADS-B spoofing attack enables the ATC to concentrate more on the nearest zone and PRQ where traffic build up is expected. Apart from that, the foundation of MSTA which is primarily developed based on time for aircraft to reach the runway and standard takeoff procedure during emergency is flexible for adoption in other airports with little modification. These features of MSTA provide opportunities to lessen delays in departures by capitalizing the available time amid uncertainties due to the ongoing cyberattacks.

This dissertation has demonstrated how queue formations and the sequencing algorithms were programmed to facilitate intervention to the interchangeable perturbed flows of aircraft arrival and departure caused by GAS cyberattacks. Another important aspect is the design of the methodologies that echo the procedures of air traffic management by the ATC and their contingency measures when incidences that jeopardize safety occur. Through the combination of advances of the computer science techniques and systems dynamics studies, this dissertation has shown how problems in the aviation domain can be investigated, analyzed and mitigated without compromising public safety.

References

- 1) William R. Richards, Kathleen O'Brien, Dean C. Miller; New Air Traffic Surveillance Technology, https://www.boeing.com/commercial/aeromagazine/articles/qtr_%02_%10/\%pdfs/AERO_%Q2-10_%article02.pdf, accessed on May 15 2022.
- 2) David Mumford, ADS-B Mandates 2023, <https://ops.group/blog/ads-b-mandates-in-2023/> accessed on September 23 2023.
- 3) Mohsen Riahi Manesh, Naima Kaabouch, Analysis of vulnerabilities, attacks, countermeasures and overall risk of the Automatic Dependent Surveillance-Broadcast (ADS-B) system, International Journal of Critical Infrastructure Protection, Volume 19, 2017, pages 16-31, ISSN 1874-5482, <https://doi.org/10.1016/j.ijcip.2017.10.002>.
(<https://www.sciencedirect.com/science/article/pii/S1874548217300446>)
- 4) Gopalakrishnan, K. K., "16.72 Security and vulnerabilities in the ADS-B architecture", MIT Report, pp. 1–15 (2018).
- 5) Lykou, G., Iakovakis, G., Gritzalis, D. Aviation Cybersecurity and Cyber-Resilience: Assessing Risk in Air Traffic Management. Advanced Sciences and Technologies for Security Applications, pp. 245–260, 2019. https://doi.org/10.1007/978-3-030-00024-0_%13
- 6) M. Monteiro, T. Sarmento, A. Barreto, P. Costa and M. Hieb, "An integrated mission and cyber simulation for Air Traffic Control," 2016 IEEE 19th International Conference on Intelligent Transportation Systems (ITSC), Rio de Janeiro, Brazil, 2016, pp. 2687-2692, doi: 10.1109/ITSC.2016.7795988.
- 7) Forster, P. et al. (2019). An Approach for Attribute- and Performance-Based Evaluation of Interdependent Critical Infrastructures. In: Electronic Navigation Research Institute (eds) Air Traffic Management and Systems III. EIWAC 2017. Lecture Notes in Electrical Engineering,

vol 555. Springer, Singapore. https://doi.org/10.1007/978-981-13-7086-1_3

- 8) Zhouyan, S.H.; Min, W.A.; Lu, Z.H.; Linzhi, M.A. Research on Track Deception Technology Based on Jamming of Flexible Lines by Jammers. MATEC Web Conf. 2018, 176, 01039.
- 9) Mehmood, S.; Malik, A.N.; Qureshi, I.M.; Khan, M.Z.; Zaman, F. A Novel Deceptive Jamming Approach for Hiding Actual Target and Generating False Targets. *Wirel. Commun. Mob. Comput.* 2021, 2021, 8844630
- 10) Wu, Z., Shang, T., Guo, A., "Security Issues in Automatic Dependent Surveillance - Broadcast (ADS-B): A Survey", *IEEE Access*, vol. 8, pp. 122147-122167, 2020, doi: 10.1109/ACCESS.2020.3007182.
- 11) Efe, A., Tuzlupinar, B. & Can Cavlan, A. (2019). Air Traffic Security against Cyber Threats. *Bilge International Journal of Science and Technology Research*, 3 (2), 135-143. DOI: 10.30516/bilgesci.405074.
- 12) Alexander E.I., Brownlee, Michal Weiszer, Jun Chen, Stefan Ravizza, John R. Woodward, Edmund K. Burke, 'A fuzzy approach to addressing uncertainty in Airport Ground', *Transportation Movement Optimisation*, Research Part C 92 p.p 150–175, 2018.
- 13) Yin J., Ma Y., Hu Y., Han K., Yin S., Xie H., 'Delay, Throughput and Emission Tradeoffs in Airport Runway Scheduling with Uncertainty Considerations', *Networks and Spatial Economics*, vol. 21(1), pp. 85–122, 2021. <https://doi.org/10.1007/s11067-020-09508-3>.
- 14) Shang, F., Wang, B., Li, T., Tian, J., Cao, K., Guo, R., Adversarial Examples on Deep-Learning Based ADS-B Spoofing Detection, *IEEE Wireless Communications Letters*, vol. 9, issue 10, pp. 1734-1737, 2020.
- 15) Meng, Q.; Hsu, L.T.; Xu, B.; Luo, X.; El-Mowafy, A., A GPS spoofing generator using an open sourced vector tracking-based receiver. *Sensors* 2019, 19, 3993.

- 16) Mirzaei, K.; Pessanha De Carvalho, B.; Pschorn, P. Security of ADS-B: Attack Scenarios. EasyChair Preprint No. 851. 2019. Available online: https://easychair.org/publications/preprint_open/DpM4. Accessed on 10 June 2022.
- 17) Sampigethaya K. "Aircraft cyber security risk assessment: Bringing air traffic systems and cyber-physical security to the front", AIAA Scitech 2019 Forum, 7-11 January 2019 San Diego, California <https://doi.org/10.2514/6.2019-0061>.
- 18) Naganawa, Junichi. "Improvement in RSSI-Based Distance Estimation for Aircraft ADS-B Signal by Antenna Diversity." In Multimedia University Engineering Conference (MECON 2022), pp. 358-366. Atlantis Press, 2022.
- 19) A. Tamimi, A. Hahn, S. Roy 'Cyber Threat Impact Analysis to Air Traffic Flows Through Dynamic Queue Networks', ACM Transactions on Cyber-Physical Systems, Volume 4, 2020.
- 20) Harison, E., Zaidenberg, N. (2018). Survey of Cyber Threats in Air Traffic Control and Aircraft Communications Systems. In: Lehto, M., Neittaanmäki, P. (eds) Cyber Security: Power and Technology. Intelligent Systems, Control and Automation: Science and Engineering, vol 93. Springer, Cham. https://doi.org/10.1007/978-3-319-75307-2_12.
- 21) Tabassum, Asma, Nicholas Allen and William Semke. "ADS-B message contents evaluation and breakdown of anomalies." 2017 IEEE/AIAA 36th Digital Avionics Systems Conference (DASC) (2017): 1-8.
- 22) Smolyak, A., Levy, O., Vodenska, I. et al. Mitigation of Cascading Failures in Ccomplex Networks. Sci Rep 10, 16124 (2020). <https://doi.org/10.1038/s41598-020-72771-4>.
- 23) Carré, Florence & Prats, Franck & Willot, Adrien & Cherkaoui, Auxane & Salmon, Romuald & osterlinck, Tom & Edjossan-Sossou, Abla & Sammels, Maurice & Tripelli, Giuliana & Lönnermark, Anders & Judek,

- Clément & Criel, Xavier & Maragos, Georgios & Van Heuverswyn, Kathleen. (2017). Incident Evolution Methodology: Methodology for creating a model of an incident with cascading effects for future threats. 10.13140/RG.2.2.21074.86729. 'Methodology for creating a model of an incident with cascading effects for future threats', *CascEff*, 2017.
- 24) N. Pyrgiotis, K. Malone, A. Odoni, 'Modelling Delay Propagation Within an Airport Network', *Transportation Research Part C: Emerging Technologies*, Vol. 27, pp.60-75, 2013.
- 25) A. Montlaur, L. Delgado, 'Flight and Passenger Delay Optimization Strategies', *Transportation Research Part C: Emerging Technologies*, Vol. 81, pp.99-117, 2017.
- 26) Z. Xing, H. Lu, 'Departure Taxiing Route Modelling and Optimization', *Proceedings - 11th International Conference on Natural Computation*, 2015.
- 27) Nieto F.J.S., 'Collision Risk Model for High Density Airspaces', In *Risk Assessment in Air Traffic Management*; Pérez Castán, J.A., Sanz, Á.R., Eds.; IntechOpen: Madrid, Spain, 2020; pp. 3–15.
- 28) Roy, S.; Sridhar, B. Cyber- Threat assessment for the air traffic management system: A network controls approach. In *Proceedings of the 16th AIAA Aviation Technology, Integration, and Operations Conference*, Washington, DC, USA, 13–17 June 2016.
- 29) Kamaruzzaman, M.R.; Sane, B.O.; Fall, D.; Taenaka, Y.; Kadobayashi, Y. Analyzing Cascading Effects of Automatic Dependent Surveillance-Broadcast (ADS-B) Spoofing Attacks Using Discrete Event Model of Air Traffic Control Response and AGMOD Dynamics. In *Proceedings of the IEEE Cyber Security and Resilience*, Rhodes, Greece, 26–28 July 2021.
- 30) Andreas Heidt, Hartmut Helmke, Manu Kapolke, Frauke Liers, Alexander Martin, 'Robust runway scheduling under uncertain conditions', *Journal of Air Transport Management*, pp. 1-10, 2016.

- 31) Gulsah Hancerliogullari, Ghaith Rabadi, Ameer H. Al-Salem, Mohamed Kharbeche b 'Greedy algorithms and metaheuristics for a multiple runway combined arrival-departure aircraft sequencing problem' *Journal of Air Transport Management*, pp. 39-48, 2013.
- 32) Ross Anderson, Dejan Milutinovic, 'An approach to optimization of airport taxiway scheduling and traversal under uncertainty', *Journal of Aerospace Engineering*, Vol. 227 (2) pp. 273-284, 2012.
- 33) Sureshkumar Chandrasekar, Inseok Hwang, 'Algorithm for Optimal Arrival and Departure Sequencing and Runway Assignment, *Journal of Guidance, Control and Dynamics*, volume 38, pp. 601-613, 2015.
- 34) Li, J., Zhang, H., Gong, M., Liang, Z., Liu, W., Tong, Z., Yi, L., Morris, R., Pasareanu, C., Koenig, S., Scheduling and airport taxiway path planning under uncertainty, *AIAA Aviation 2019 Forum*, pp. 1-7. <https://doi.org/10.2514/6.2019-2930>.
- 35) Shone, R., Glazebrook, K., Zografos, K. G., 'Applications of stochastic modeling in air traffic management: Methods, challenges and opportunities for solving air traffic problems under uncertainty', *European Journal of Operational Research* Vol. 292 issue (1), pp. 1-26, 2021. <https://doi.org/10.1016/j.ejor.2020.10.039>
- 36) Joseph A. Jackson, Jovan D. Boskovic 'Application of Airspace Encounter Model for Prediction of Intruder Dynamics', *AIAA Modeling and Simulation Technology Conference*, 2012.
- 37) A. Alsulami and S. Zein-Sabatto, "Resilient cyber-security approach for aviation cyber-physical systems protection against sensor spoofing attacks," in *Proc. IEEE 11th Annu. Comput. Commun. Workshop Conf. (CCWC)*, Jan. 2021, pp. 565-571.
- 38) Kamaruzzaman, Mohd Ruzeiny, Mohammad Delwar Hossain, Yuzo Taenaka, and Youki Kadobayashi. "ATC Level Tactical Manoeuvring during Descent for Mitigating Impact of ADS-B Message Injection Cyber Attack." *Engineering Proceedings* 28, no. 1 (2022): 14.

- 39) Kamaruzzaman Mohd Ruzeiny Bin, Doudou Fall, Md Delwar Hossain, Yuzo Taenaka, and Youki Kadobayashi. "Modulated Synchronous Taxiing: Mitigating Uncertainties Amid Ads-B Spoofing." In 2022 Integrated Communication, Navigation and Surveillance Conference (ICNS), pp. 1-13. IEEE, 2022.
- 40) M. R. Kamaruzzaman, M. D. Hossain, Y. Taenaka and Y. Kadobayashi, "Mitigation of ADS-B Spoofing Attack Impact on Departure Sequencing Through Modulated Synchronous Taxiing Approach," in IEEE Open Journal of Intelligent Transportation Systems, vol. 4, pp. 720-739, 2023, doi: 10.1109/OJITS.2023.3286881.
- 41) WMKK AD2.24: Charts Related to an Aerodome: AD-2-WMKK-4-1. Available online: <https://aip.caam.gov.my/aip/eAIP/2023-02-23-AIRAC/html/index-en-MS.html> (accessed on 5 June 2022).
- 42) Aviation Acts and Policy", Ministry of Transport Malaysia, <https://www.mot.gov.my/en/aviation/acts-and-policy>. Accessed on 16 January 2023.
- 43) Li, Jiahe & Zhou, Yazhou, 'Research on ADS-B spoof detection technology based on radio spectrum features'. Applied Mathematics and Nonlinear Sciences (2023), 10.2478/amns.2023.2.00848.
- 44) Saulius Rudys, Jurgis Aleksandravicius, Rimvydas Aleksiejunas, Andriy Konovaltsev, Chen Zhu, Lukasz Greda, 'Physical layer protection for ADS-B against spoofing and jamming', International Journal of Critical Infrastructure Protection, Volume 38 (2022), 100555, ISSN 1874-5482, <https://doi.org/10.1016/j.ijcip.2022.100555>.
- 45) Wafiuddin Suparman, Mariyam Jamilah Homam; Development of transmitter and receiver for fox hunting activity. AIP Conf. Proc. 11 (November 2019); 2173 (1): 020020.
- 46) Sudibya, B., Dermawan, D., Purnomo, M.J., & Irawaty, M. (2022). Radio Transmission Detection Using Doppler in UHF Frequency Band. AVITEC.

- 47) Samuel Chng, Han Yu Lu, Ayush Kumar, David Yau, Hacker types, motivations and strategies: A comprehensive framework, *Computers in Human Behavior Reports*, Volume 5, 2022, 100167, ISSN 2451-9588, <https://doi.org/10.1016/j.chbr.2022.100167>.
- 48) Moore, Ervin, Ahmed Imteaj, Shabnam Rezapour, and M. Hadi Amini. "A Survey on Secure and Private Federated Learning Using Blockchain: Theory and Application in Resource-constrained Computing." arXiv preprint arXiv:2303.13727 (2023).
- 49) K. Higasa and E. Itoh, "Controlling aircraft inter-arrival time to reduce arrival traffic delay via a queue-based integer programming approach," *Aerospace*, vol. 9, no. 11, p. 663, 2022.
- 50) X. Zhao, Y. Wang, L. Li, D. Delahaye, "A queuing network model of a multi-airport system based on point-wise stationary approximation," *Aerospace*, vol. 9, no. 7, p. 390, 2022. [Online]. Available: <https://doi.org/10.3390/aerospace9070390>
- 51) Munir, Arslan, Alexander Aved, and Erik Blasch. "Situational awareness: techniques, challenges, and prospects." *AI* 3, no. 1 (2022): 55-77.
- 52) Gite, L. K., and R. S. Deodhar. "Estimation of yaw angle from flight data using extended Kalman filter." *Aerospace Systems* 5, no. 3 (2022): 393-402.
- 53) Safety Assessment on Airport Collaborative Decision Making (A-CDM)", Eurocontrol, <https://www.eurocontrol.int/publication/safety-assessment-airport-collaborative-decision-making-cdm>. Accessed on 15 May 2023.
- 54) bibitem{ref44}"Airport-Collaborative Decision Making (A-CDM)", Eurocontrol, <https://www.eurocontrol.int/concept/airport-collaborative-decision-making>. Accessed on 15 May 2023.
- 55) "Flight Delays and Cancellations", US Department of Transportation, <http://www.transportation.gov/individuals/aviation-consumer-protection/flight-delays-cancellations>. Accessed on 26 December 2022.

56) Flight Delays and Cancellations", Malaysia Aviation Commission,
<https://www.mavcom.my/en/consumer/flight-delays-cancellations/>.
Accessed on 26 December 2022.

Appendices

1) Appendix 1-A

	Time (s)	X (m)	Y (m)	Altitude (m)	Course (°)	Ground Speed (m/s)	Descent Rate (m/s)	Roll (°)	Pitch (°)	Yaw (°)
1	0	-122	-14	7315	-170.15	246.45	6.35	0	-1.48	-170.15
2	60	-12,287	-1174	6927	176.63	201.66	6.60	9.01	-1.87	176.63
3	120	-24,287	-1174	6523	-160.22	201.15	3.12	-23.17	-0.89	-160.22
4	180	-32,550	-10,294	6401	-115.19	205.78	2.74	4.74	-0.76	-115.19
5	240	-37,115	-21,851	6149	-111.08	204.23	5.01	1.86	-1.40	-111.08
6	300	-41,142	-31,528	5776	-113.35	197.03	7.24	0	-2.10	-113.35

Table III. Trajectory Data for Legit Real Flight – *a*

2) Appendix 1-B

Table 2. Trajectory data for spoofed ghost aircraft.										
	Time (s)	X (m)	Y (m)	Altitude (m)	Course (°)	Ground Speed (m/s)	Descent Rate (m/s)	Roll (°)	Pitch (°)	Yaw (°)
1	0	1807	-10,479	7315	-170.22	246.45	22.53	0	9.17	130.49
2	20	-2572	-9577	6927	-164.64	201.66	13.77	25.39	0.03	151.51
3	60	-11,089	-6981	6523	-171.02	201.15	3.54	11.94	-0.37	-140.36
4	120	-25,691	-11,860	6401	-137.92	205.78	2.74	1.17	0.17	-117.76
5	180	-32,907	-28,655	6149	-87.47	204.23	5.01	17.75	0.66	-93.18
6	240	-30,186	-39,927	5776	-70.92	197.03	7.24	0	0.72	-68.07

Table IV. Trajectory Data for Ghost Aircraft – *b*

3) Appendix 1-C

Table 3. Trajectory data for proposed tactical diversion.										
Time (s)	X (m)	Y (m)	Altitude (m)	Course (°)	Ground Speed (m/s)	Descent Rate (m/s)	Roll (°)	Pitch (°)	Yaw (°)	
1	20	-5464	-952	7250	158.37	160.09	2.60	0	-0.93	158.37
2	47	-12,605	1425	7179	168.03	160.09	2.78	6.68	-0.99	168.03
3	150	-27,768	-975	6874	-149.19	180.09	3.06	9.46	-0.97	-149.19
4	207	-38,257	-14,133	6600	-112.05	200.09	3.07	5.92	-0.88	-112.05
5	303	-41,761	-25,765	6400	-105.01	200.09	3.06	-1.20	-0.88	-105.01
6	352	-44,382	-34,938	6247	-106.41	200.09	3.17	0	-0.91	-106.41

Table V. Trajectory Data for Proposed Tactical Diversion – c

4) Appendix 1-D

Table 4. Trajectory data for conventional simplistic diversion.										
Time (s)	X (m)	Y (m)	Altitude (m)	Course (°)	Ground Speed (m/s)	Descent Rate (m/s)	Roll (°)	Pitch (°)	Yaw (°)	
1	20	-5283	-221	7250	141.22	160	2.21	0	-0.79	141.22
2	46	-11,353	3818	7179	156.64	160	3.36	11.01	-1.20	156.64
3	110	-21,809	4531	6874	-167.48	180	4.00	8.26	-1.27	-167.48
4	190	-34,404	2598	6600	-134.98	180	2.52	6.29	-0.80	-134.98
5	292	-43,672	-18,045	6400	-110.32	200	1.86	3.27	-0.53	-110.32
6	378	-47,712	-33,730	6247	-99.21	200	2.37	2.32	-0.68	-99.21
7	424	-48,900	-42,760	6100	-96.64	200	3.73	0	-1.07	-99.64

Table VI. Trajectory Data for Simplistic Diversion – d

5) Appendix 2-A

	Simulation Periods in minutes (m)		
	$T=0 - T=2.9$	$T=3.0 - T=5.9$	$T=6.0 - T=10.0$
Closed Airspace	S	E	N
Open Airspace	E, N	S, N	E, S

Table VII. Attack Duration and Affected Airspace (peak schedule)

6) Appendix 2-B

	Simulation Periods in minutes (m)		
	$T=0 - T=2.9$	$T=3.0 - T=5.9$	$T=6.0 - T=10.0$
Closed Airspace	N	E	S
Open Airspace	S, E	S, N	E, N

Table VIII. Attack Duration and Affected Airspace (non-peak schedule)

7) Appendix 3-A

	Departure Time	Aircraft	Airspace to Fly Through	Gate	Time to Runway (minutes)
1.	0900	0175	S	C003	6
2.	0900	0750	E	C067	6
3.	0900	0754	E	G006R	2
4.	0900	0784	N	H006L	2
5.	0910	0193	S	C012	6
6.	0910	0141	S	C017	5
7.	0910	0072	E	H004	4
8.	0915	0520	E	C023	6
9.	0915	2610	E	B005	6
10.	0920	0129	S	C034	6
11.	0925	0170	N	G002	3
12.	0925	1051	S	A008	2
13.	0925	1268	E	C022	4
14.	0925	0070	N	C027	6
15.	0930	0611	S	H008	5
16.	0945	0740	N	H010	5
17.	0950	0004	N	C035	6

Table IX. Peak Schedule

8) Appendix 3-B

	Departure Time	Aircraft	Airspace to Fly Through	Gate	Time to Runway (minute)
1.	1800	0205	N	C031	6
2.	1805	0157	S	G004	3
3.	1810	1450	N	A006	2
4.	1810	2638	E	B009	6
5.	1825	1276	E	A008	2
6.	1835	0935	N	C031	5
7.	1845	0155	S	G002	3
8.	1850	0182	N	H008	5

Table X. Non-Peak Schedule

9) Appendix 4-A

No.	Departure Time	Aircraft	Airspace	Time from Gate (minute (m))	First attack ($T = 0 - 2.9$ m)	Second attack ($T = 3.0 - 5.9$ m)	Third attack ($T = 6.0 - 10.0$ m)	End of simulation ($T=10$ m)
					Time to begin movement / Location (end of attack) / Planned time to enter runway	Time to begin movement / Location (end of attack) / Planned time to enter runway	Time to begin movement / Location (end of attack) / Planned time to enter runway	
1.	0900	0715	S	6		Moved at $T = 3.0$ m / Stopped at 3.0 m from PRQ / $T = 10.5$	Moved at $T = 6.0$ m / Stopped at 0.5 m from runway / $T = 10.5$	In runway server
2.	0900	0750	E	6	Moved at $T = 0$ m / Stopped at 3.0 m from PRQ / $T = 7.5$ m		Moved at $T = 6.0$ m / Stopped at 1.5 m from runway in PReQ (second) / $T = 12.0$	Second position in PReQ
3.	0900	0754	E	2	Moved at $T = 0$ m / Stopped at 0.5 m from runway / $T = 3.5$ m	Moved at 3.0 m / Entered runway at $T = 3.5$ m*	- / - / -	First to enter runway at $T = 3.5$ m*
4.	0900	0784	N	2	Moved at $T = 1.5$ m / Stopped at 0.5 m from PRQ / $T = 5.0$ m	Moved at 3.0 m / Entered runway at $T = 5.0$ m	- / - / -	Second to enter runway at $T = 5.0$ m
5.	0910	0193	S	6		Moved at $T = 4.5$ m / Stopped at 4.5 m from PRQ / $T = 12.0$	Moved at $T = 7.5$ m / Stopped at 2.0 m from PRQ / $T = 13.5$ m	2.0 m to PRQ
6.	0910	0141	S	5		- / - / -	Moved at $T = 8.5$ m / Stopped at 3.5 m from PRQ / $T = 15.0$	3.5 m to PRQ
7.	0910	0072	E	4	Moved at $T = 1.0$ m / Stopped at 3.0 m from PRQ / $T = 6.5$ m		- / - / -	3.0 m from PRQ
8.	0915	0520	E	6	Moved at $T = 0.5$ m / Stopped at 3.5 m from PRQ / $T = 8.0$ m		- / - / -	3.5 m to PRQ
9.	0915	2610	E	6	- / - / -		- / - / -	- / - / -
10.	0920	0129	S	6		- / - / -	- / - / -	- / - / -
11.	0925	0170	N	3	- / - / -	Moved at $T = 3.0$ m / Stopped at 1.5 m from runway - in PReQ (First) / $T = 7.5$ m		First position in PReQ
12.	0925	1051	S	2		Moved at $T = 5.5$ m / Stopped at 1.5 m from PRQ / $T = 9.0$ m	- / - / -	1.5 m to PRQ
13.	0925	1268	E	4	- / - / -		- / - / -	- / - / -
14.	0925	0070	N	6	- / - / -	- / - / -		- / - / -
15.	0930	0611	S	5		- / - / -	- / - / -	- / - / -
16.	0945	0720	N	5	- / - / -	- / - / -		- / - / -
17.	0950	0004	N	6	- / - / -	- / - / -		- / - / -

Table XI: T-P Sequencing Results for $T = 10$ m (peak schedule)

10) Appendix 4-B

No.	Departure Time	Aircraft	Airspace	Time from Gate (minute (m))	First attack ($T = 0 - 2.9$ m)	Second attack ($T = 3.0 - 5.9$ m)	Third attack ($T = 6.0 - 10.0$ m)	End of Simulation ($T=10$ m)
					Time to begin movement / Location (end of attack) / Planned time to enter runway	Time to begin movement / Location (end of attack) / Planned time to enter runway	Time to begin movement / Location (end of attack) / Planned time to enter runway	
1.	0900	0715	S	6	- / - / -	- / - / -		- / - / -
2.	0900	0750	E	6	- / - / -		Moved at $T = 7.5$ m / Stopped at 3.5 m from PRQ / $T = 14.0$ m	3.5 m to PRQ
3.	0900	0754	E	2	Moved at $T = 0$ m / Stopped at 0.5 m from runway / $T = 3.5$ m	Moved at 3.0 m / Entered runway at $T = 3.5$ m*	- / - / -	First to enter runway at $T = 3.5$ m*
4.	0900	0784	N	2		Moved at 3.0 m / Stopped at 0.5 m from runway / $T = 6.5$ m	Moved at 6.0 m / Entered runway at $T = 6.5$ m	Third to enter runway at $T = 6.5$ m
5.	0910	0193	S	6	- / - / -	- / - / -		- / - / -
6.	0910	0141	S	5	- / - / -	Moved at $T = 3.0$ m / Stopped at 2.0 m from PRQ / $T = 9.5$ m		2.0 m to PRQ
7.	0910	0072	E	4	Moved at $T = 1.0$ m / Stopped at 2.0 m from PRQ / $T = 6.5$ m		Moved at $T = 6.0$ m / Entered runway at 9.5 m /	Fifth to enter runway at $T = 9.5$ m
8.	0915	0520	E	6	- / - / -		Moved at $T = 8.0$ m / Stopped at 4.0 m from PRQ / $T = 15.5$ m	4.0 m to PRQ
9.	0915	2610	E	6	- / - / -		Moved at $T = 9.5$ m / Stopped at 5.5 m from PRQ / $T = 17.0$ m	5.5 m to PRQ
10.	0920	0129	S	6	- / - / -	- / - / -		- / - / -
11.	0925	0170	N	3		Moved at $T = 3.5$ m / Stopped at 0.5 m from PRQ / $T = 8.0$ m	Moved at $T = 6.0$ m / Entered runway at $T = 8.0$ m	Fourth to enter runway at $T = 8.0$ m
12.	0925	1051	S	2	Moved at $T = 1.5$ m / Stopped at 0.5 m from PRQ / $T = 5.0$ m	Moved at $T = 3.0$ m / Entered runway at $T = 5.0$ m	- / - / -	Second to enter runway at $T = 5.0$ m
13.	0925	1268	E	4	Moved at $T = 2.5$ m / Stopped at 3.5 m from PRQ / $T = 8.0$ m		Moved at $T = 6.0$ m / Stopped at 1.0 m from runway / $T = 11.0$ m	In runway server
14.	0925	0070	N	6		- / - / -	- / - / -	- / - / -
15.	0930	0611	S	5	- / - / -	- / - / -		- / - / -
16.	0945	0720	N	5		- / - / -	Moved at $T = 6.0$ m / Stopped at 1.0 m from PRQ / $T = 12.5$ m	1.0 m to PRQ
17.	0950	0004	N	6		- / - / -	- / - / -	- / - / -

Table XII: L-P Sequencing Results for $T = 10$ m (peak schedule)

11) Appendix 5-A

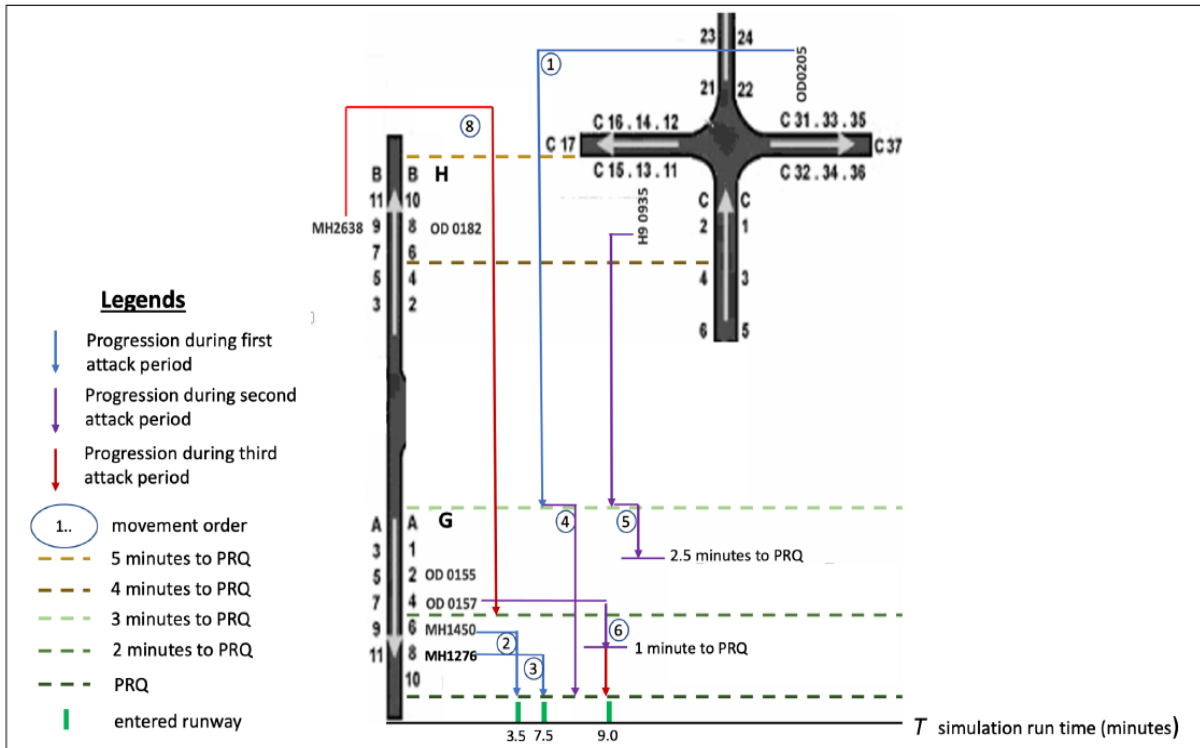


Fig.22. T-P Sequencing Results for Non-Peak Schedule

12) Appendix 5-B

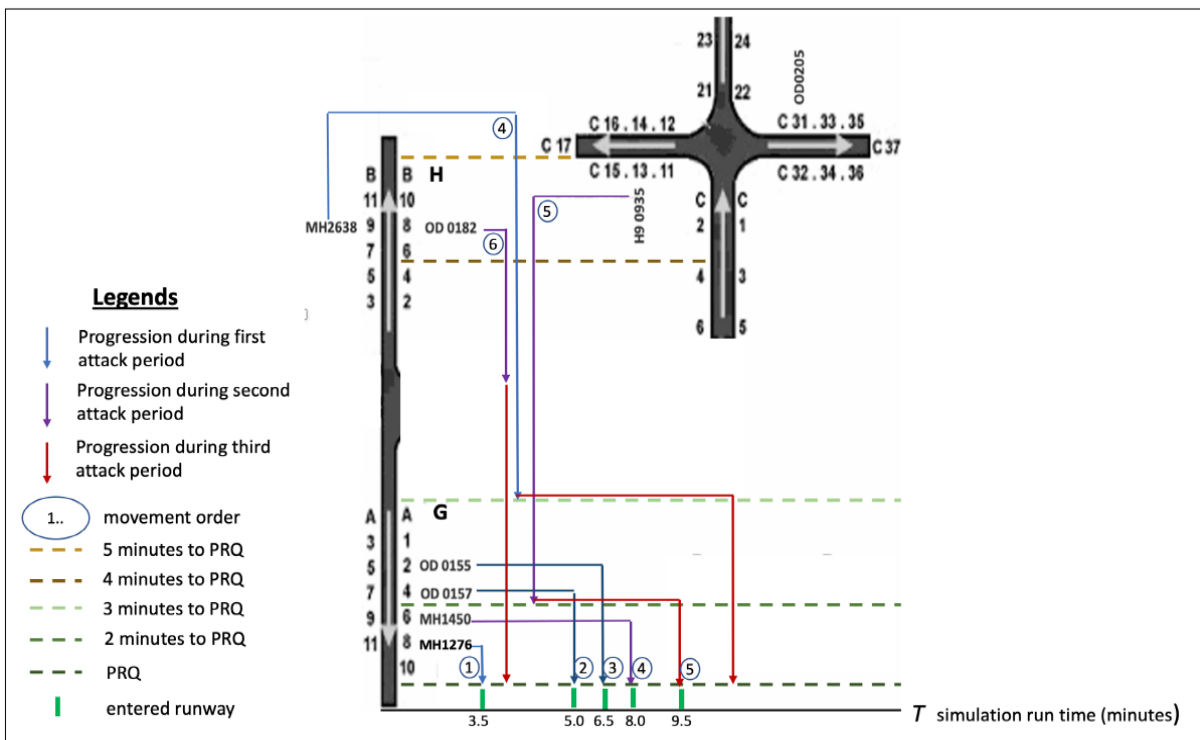


Fig.23. L-P Sequencing Results for Non-Peak Schedule

13) Appendix – Source Codes

13.1 AGMOD Discrete Events Model (screenshots)

13.1.1 Real Aircraft Generation

Block Parameters: Real Aircraft

Entity Generator

Generate entities using intergeneration times from dialog or upon arrival of events. Optionally, specify entity types as anonymous, structured, or bus.

Entity generation Entity type Event actions Statistics

Generation method: Time-based

Time source: Dialog

Period: 3

Entity generation Entity type Event actions Statistics

Entity type: Structured

Entity priority: 100

Entity type name: Aircraft

Define attributes

+ - ↑ ↓

	Attribute Name	Attribute Initial Value
1	ADSB	1
2	TimeOfServiceStart	1
3	TimeOfServiceEnd	1

Entity type	Event actions	Statistics
Generate action:		
Called after entity is generated. To access attribute use: entity.ADSB		
<pre> 1 entity.ADSB = 1; 2 3 % Unused 4 entity.TimeOfServiceStart = 0; 5 entity.TimeOfServiceEnd = 0; </pre>		

13.1.2 Ghost Aircraft Generation

Block Parameters: Ghost Aircraft
✕

Entity Generator

Generate entities using intergeneration times from dialog or upon arrival of events. Optionally, specify entity types as anonymous, structured, or bus.

Entity generation	Entity type	Event actions	Statistics
-------------------	-------------	---------------	------------

Generation method: Time-based ▼

Time source: MATLAB action ▼

Intergeneration time action:

```

1 persistent idx;
2 if isempty(idx)
3     idx = 1;
4 end
5 N = 1;    % Read from workspace
6 IGT = 5; % Read from workspace
7 if idx < N
8     dt = 0;
9     idx = idx + 1;
10 else

```

Entity generation	Entity type	Event actions	Statistics
Entity type: Structured			
Entity priority: 100			
Entity type name: Aircraft			
Define attributes			
<input type="button" value="+"/> <input type="button" value="X"/> <input type="button" value="↑"/> <input type="button" value="↓"/>			
	Attribute Name	Attribute Initial Value	
1	ADSB	2	
2	TimeOfServiceStart	2	
3	TimeOfServiceEnd	2	

13.1.3 Pause/Resume Server source codes (identical for Pushback, Taxiing Out, Runway Out, and Taking Off servers) adapted from Matlab Pause/Continue® server example.

```
classdef (StrictDefaults)PushbackServerPause < matlab.DiscreteEventSystem
```

```
    properties (Nontunable)
        Capacity = 10;
    end
```

```
    properties (DiscreteState)
        IsPaused;
        ResidualTime;
        TimeOfServiceStart;
    end
```

```
    methods (Static, Access=protected)
        function header = getHeaderImpl
            header = matlab.system.display.Header(...
                'PushbackServerPause', ...
                'Title', 'Pushback');
        end

        function groups = getPropertyGroupsImpl
            firstGroup = matlab.system.display.SectionGroup(...
                'Title', 'General', ...
                'PropertyList', {'Capacity'});
            groups = firstGroup;
        end
    end
```

```
    methods (Access = protected)
        function icon = getIconImpl(~)
```

```

        icon = sprintf('Pushback');
    end

    function num = getNumInputsImpl(~)
        num = 2;
    end

    function num = getNumOutputsImpl(~)
        num =1;
    end

    function [name1, name2] = getInputNamesImpl(~)
        name1 = 'Aircraft';
        name2 = 'HaltCmd';
    end

    function name = getOutputNamesImpl(~)
        name = 'Aircraft';
    end

    function [sz, dt, cp] = getDiscreteStateSpecificationImpl(~, ~)
        sz = 1;
        dt = 'double';
        cp = false;
    end

    function entityTypes = getEntityTypesImpl(obj)
        entityTypes = [obj.entityType('entity')...
            obj.entityType('pause')];
    end

    function [input, output] = getEntityPortsImpl(~)
        input = {'entity', 'pause'};
        output = {'entity'};
    end

    function [storageSpec, I, O] = getEntityStorageImpl(obj)
        storageSpec = [
            obj.queueFIFO('entity', obj.Capacity)...
            obj.queueFIFO('pause', 1)...
            obj.queueFIFO('entity', 1)];
        I = [1 2];
        O = 3;
    end

    function resetImpl(obj)
        obj.IsPaused = 0;
        obj.ResidualTime = 0;
        obj.TimeOfServiceStart = 0;
    end
end

methods
    function [entity, events] = pauseEntry(obj, ~, entity, ~)

```

```

events = obj.eventDestroy();

if entity.data ~= 0
    if obj.IsPaused
    else
        obj.IsPaused = 1;
        events = [events obj.eventIterate(3, 'stopTimer',10)];
    end
else
event=obj.eventIterate(1, 'moveFromStorageOneToStorageThree',10);
    events = [events event];

    if obj.IsPaused
        obj.IsPaused = 0;
        events = [events,obj.eventIterate(3, 'startTimer',10)];
    else

    end
end
end

function [entity,events,next] =
entityIterate(obj,storage,entity,tag,~)

    events = obj.initEventArray;

    if storage == 1
        events = obj.eventForward('storage', 3, 0);

    elseif string(tag) == 'startTimer'

        obj.TimeOfServiceStart = obj.getCurrentTime();
        events = obj.eventTimer('service_complete',
obj.ResidualTime);

    elseif string(tag) == 'stopTimer'

        TimeOfServiceEnd = obj.getCurrentTime();
        obj.ResidualTime = obj.ResidualTime-(TimeOfServiceEnd-
obj.TimeOfServiceStart);
        events = obj.cancelTimer('service_complete');

    end
    next = false;
end

function [entity, events] = entityEntry(obj, storage, entity, ~)

    events = obj.initEventArray;

```

```

obj.ResidualTime=entity.data.ADSB;

if storage == 1
    if(obj.IsPaused == 0)
        events = obj.eventForward('storage', 3, 0);
    end

elseif storage == 3

    if obj.IsPaused == 0
        obj.TimeOfServiceStart = obj.getCurrentTime();
        events = obj.eventTimer('service_complete',
entity.data.ADSB);
    end
end

end

function [entity, events] = entityTimer(obj, storage, entity, ~)
    assert(storage == 3);
    events = obj.eventForward('output', 1, 0);
end
end
end
end

```

13.2 Benchmarking Trajectory of Ghost Aircraft

```

scenario = createScenario();
[tp, platp] = createPlotters();

while advance(scenario) && ishghandle(tp.Parent)
    truePosition = readData(scenario);

    plotPlatform(platp,truePosition);

    drawnow
end

function position = readData(scenario)

truePoses = platformPoses(scenario);
position = vertcat(truePoses(:).Position);
end

function [tp, platp] = createPlotters
tp = theaterPlot('XLim', [-52831.7102569078 5763.45550733099], 'YLim', [-
48164.9121816939 10430.2535825449], 'ZLim', [-54663.455507331
3931.7102569078]);
set(tp.Parent,'YDir','reverse','ZDir','reverse');
view(tp.Parent, -17.707, -32.5566);

```

```

platp = platformPlotter(tp, 'DisplayName', 'Platforms', 'MarkerFaceColor', 'k');
end

function scenario = createScenario
scenario = trackingScenario;
scenario.StopTime = Inf;
scenario.UpdateRate = 1;

% Create platforms
Aircraft = platform(scenario, 'ClassID', 5);
Aircraft.Dimensions = struct( ...
    'Length', 40, ...
    'Width', 30, ...
    'Height', 10, ...
    'OriginOffset', [0 0 0]);
Aircraft.Signatures = {...
    rcsSignature(...
        'EnablePolarization', false, ...
        'Pattern', [20 20;20 20], ...
        'Azimuth', [-180 180], ...
        'Elevation', [-90;90], ...
        'Frequency', [0 1e+20], ...
        'FluctuationModel', 'Swerling0'});
Aircraft.Trajectory = waypointTrajectory( ...
    [-122.2 -14 -7315.2;-12286.6 -1173.6 -6926.58;-24206.6 -1173.6 -6522.72;-
    32549.5 -10294.1 -6400.8;-37115.3 -21850.6 -6149.34;-41142 -31527.7 -5775.96],
    ...
    [0;60;120;180;240;300], ...
    'GroundSpeed', [246.448;201.662;201.148;205.778;204.234;197.032], ...
    'ClimbRate', [-6.35;-6.60155769230769;-3.1216231884058;-2.73697959183674;-
    5.00875609756098;-7.239], ...
    'AutoPitch', true, ...
    'AutoBank', true);

Aircraft1 = platform(scenario, 'ClassID', 5);
Aircraft1.Dimensions = struct( ...
    'Length', 40, ...
    'Width', 30, ...
    'Height', 10, ...
    'OriginOffset', [0 0 0]);
Aircraft1.Signatures = {...
    rcsSignature(...
        'EnablePolarization', false, ...
        'Pattern', [20 20;20 20], ...
        'Azimuth', [-180 180], ...
        'Elevation', [-90;90], ...
        'Frequency', [0 1e+20], ...
        'FluctuationModel', 'Swerling0'});
Aircraft1.Trajectory = waypointTrajectory( ...
    [1807 -10479 -7315.2;-2572 -9577 -6926.8;-11089 -6981 -6522.72;-25691 -
    11860 -6400.8;-32907 -28655 -6149.34;-30186 -39927 -5775.96], ...
    [0;20;60;120;180;240], ...
    'GroundSpeed', [246.448;201.662;201.148;205.778;204.234;197.032], ...

```

```

        'ClimbRate', [-22.526;-13.7735202433887;-3.54040427733701;-
2.73697959183674;-5.00875609756098;-7.239], ...
        'Orientation', quaternion([0.417424181478757 -0.0726227617877987
0.0334910126475973 0.905185803721502;0.240150898508418 0.0537991498862794
0.213070381890925 0.945533822651505;0.337576742173227 0.0322193607659498 -
0.0989382956096471 -0.935529299165666;0.516788397160763 0.00658080615541569 -
0.00796259891410639 -0.85605084111219;0.678345036373647 0.110136881013535 -
0.10817186145047 -0.718343043022055;0.828656973918375 0.00353755901021746
0.00523736056466132 -0.55972106920055]));

Aircraft3 = platform(scenario, 'ClassID', 5);
Aircraft3.Dimensions = struct( ...
    'Length', 40, ...
    'Width', 30, ...
    'Height', 10, ...
    'OriginOffset', [0 0 0]);
Aircraft3.Signatures = {...
    rcsSignature(...
        'EnablePolarization', false, ...
        'Pattern', [20 20;20 20], ...
        'Azimuth', [-180 180], ...
        'Elevation', [-90;90], ...
        'Frequency', [0 1e+20], ...
        'FluctuationModel', 'Swerling0');
Aircraft3.Trajectory = waypointTrajectory( ...
    [-5464 -952 -7250;-12605 1425 -7179;-27768 -975 -6874;-38257 -14133 -
6599.5;-41761 -25765 -6399.5;-44382 -34938 -6247], ...

[20;46.6408721715107;149.55721959673;236.626968977025;303.423328504102;352.307
574820005], ...
    'GroundSpeed',
[160.088213124411;160.088213124411;180.09;200.09;200.09;200.09], ...
    'ClimbRate', [-2.60369853606302;-2.77750416885901;-3.05781412587475;-
3.0678935356862;-3.05884720358685;-3.17262248419207], ...
    'AutoPitch', true, ...
    'AutoBank', true);

Aircraft2 = platform(scenario, 'ClassID', 5);
Aircraft2.Dimensions = struct( ...
    'Length', 40, ...
    'Width', 30, ...
    'Height', 10, ...
    'OriginOffset', [0 0 0]);
Aircraft2.Signatures = {...
    rcsSignature(...
        'EnablePolarization', false, ...
        'Pattern', [20 20;20 20], ...
        'Azimuth', [-180 180], ...
        'Elevation', [-90;90], ...
        'Frequency', [0 1e+20], ...
        'FluctuationModel', 'Swerling0');
Aircraft2.Trajectory = waypointTrajectory( ...
    [-5283 -221 -7250;-11353 3818 -7179;-21809 4531 -6874;-34404 -2598 -6600;-
43672 -18045 -6400;-47712 -33730 -6247;-48900 -42760 -6100], ...

```

```

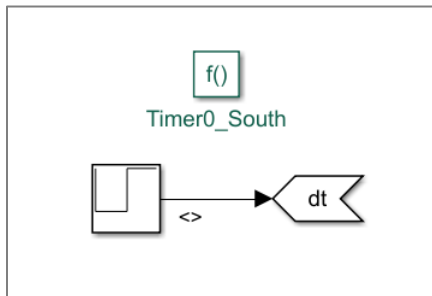
[20;45.6562350603005;110.190411216396;189.926910496395;292.329702644527;377.99
8261626929;423.537724279078], ...
'GroundSpeed', [160;160;180;180;200;200;200], ...
'ClimbRate', [-2.21013814584002;-3.36438208748171;-4.00154511598806;-
2.51935035612005;-1.86330739557206;-2.36905917588612;-3.72846238106949], ...
'AutoPitch', true, ...
'AutoBank', true);

```

end

13.3 MSTA – Peak Schedule Discrete Events System

13.3.1 Timer function block: dt= Timer0_South()



Block Parameters: Repeating Sequence Stair

Repeating Sequence Stair (mask) (link)

Discrete time sequence is output, then repeated.

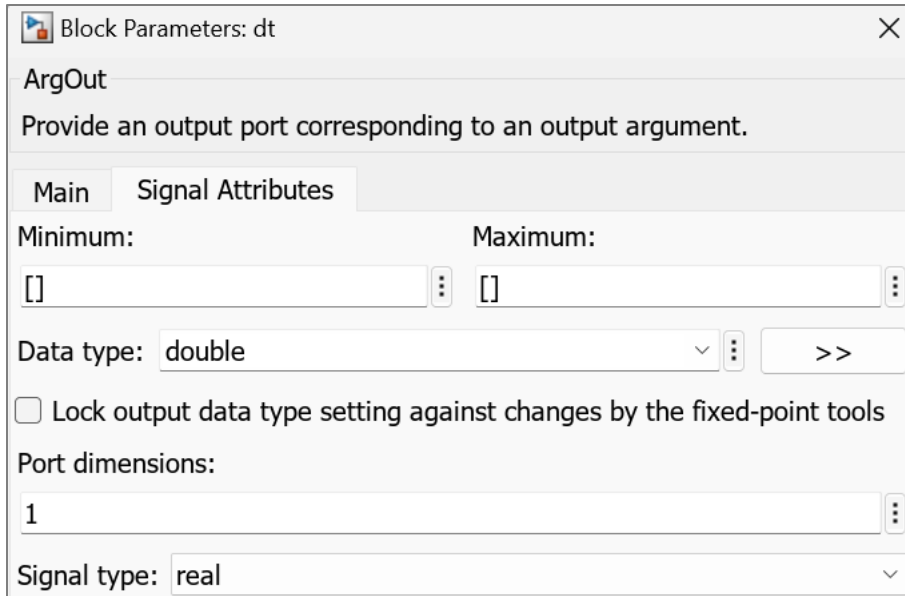
Main Signal Attributes

Vector of output values:

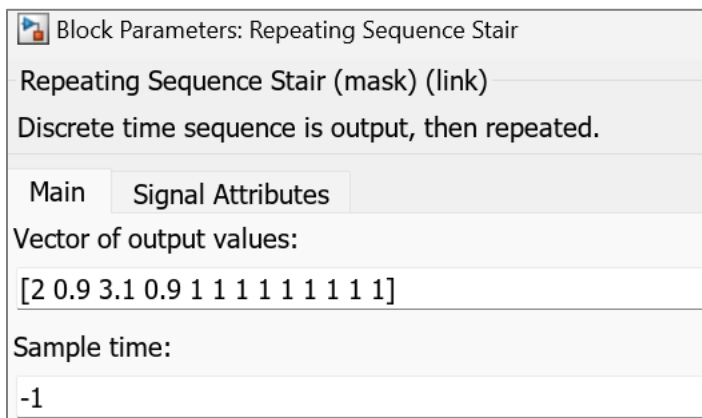
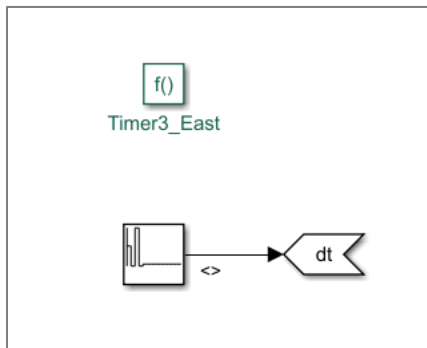
[3 8] [3,8]

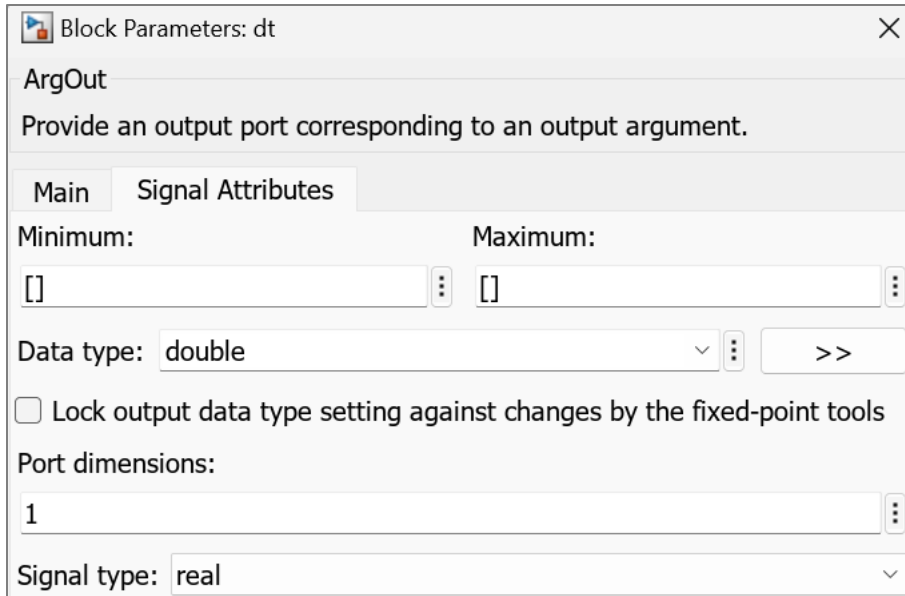
Sample time:

-1

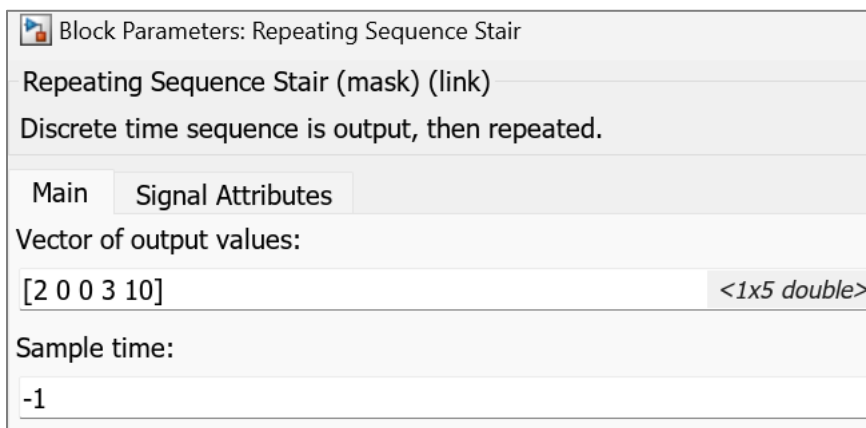
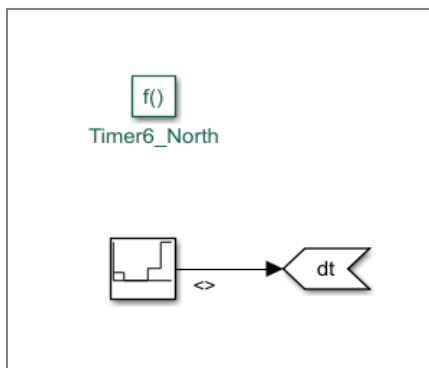


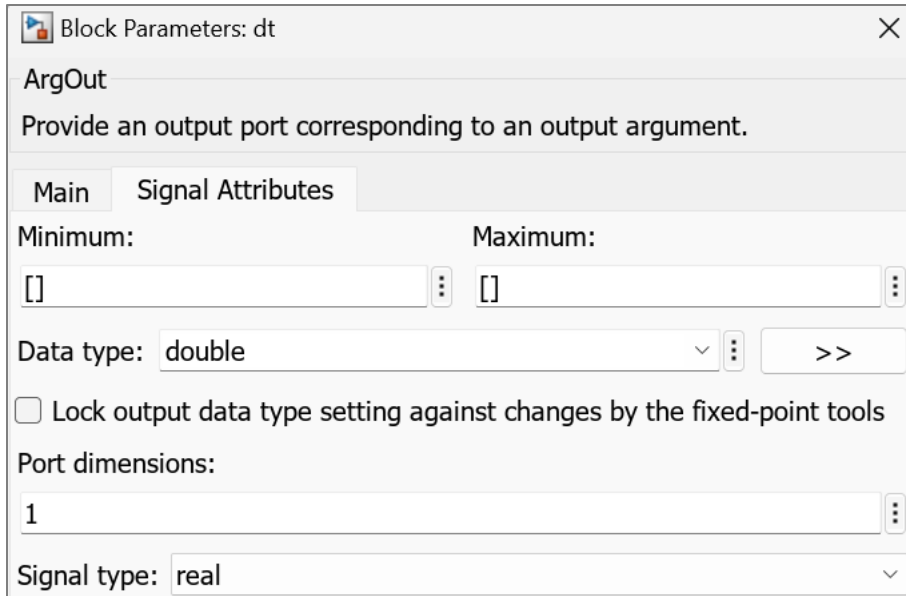
13.3.2 Timer function block: dt= Timer3_East()





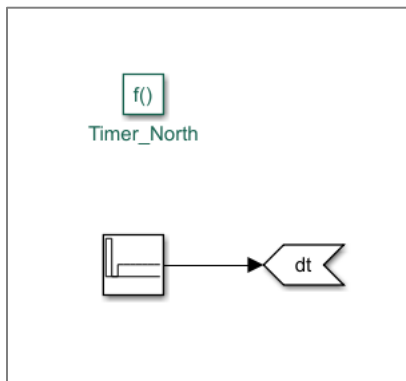
13.3.3 Timer function block: dt= Timer6_North()





13.4 MSTA – Non-Peak Schedule Discrete Events System

13.4.1 Timer function block: dt= Timer_North()



Block Parameters: Repeating Sequence Stair

Repeating Sequence Stair (mask) (link)

Discrete time sequence is output, then repeated.

Main Signal Attributes

Vector of output values:

[3 0 1 1 1 1 1 1 1] <1x9 double>

Sample time:

-1

Block Parameters: dt

ArgOut

Provide an output port corresponding to an output argument.

Main Signal Attributes

Minimum: [] Maximum: []

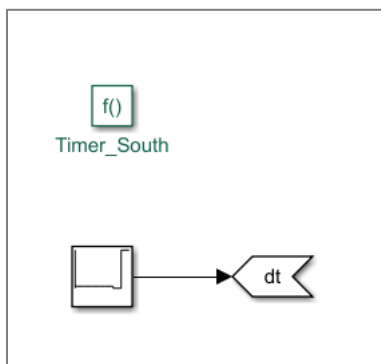
Data type: double >>

Lock output data type setting against changes by the fixed-point tools

Port dimensions: 1

Signal type: real

13.4.2 Timer function block: dt= Timer_South()



Block Parameters: Repeating Sequence Stair

Repeating Sequence Stair (mask) (link)

Discrete time sequence is output, then repeated.

Main Signal Attributes

Vector of output values:

[1 1 1 1 1 0.9 4.1] <1x7 double>

Sample time:

-1

Block Parameters: dt

ArgOut

Provide an output port corresponding to an output argument.

Main Signal Attributes

Minimum: [] Maximum: []

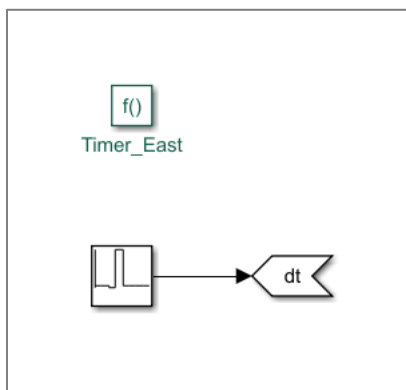
Data type: double >>

Lock output data type setting against changes by the fixed-point tools

Port dimensions: 1

Signal type: real

13.4.3 Timer function block: dt= Timer_East()



Block Parameters: Repeating Sequence Stair

Repeating Sequence Stair (mask) (link)

Discrete time sequence is output, then repeated.

Main Signal Attributes

Vector of output values:

[1 1 0.9 3.1 1 1 1 1] <1x8 double>

Sample time:

-1

Block Parameters: dt

ArgOut

Provide an output port corresponding to an output argument.

Main Signal Attributes

Minimum: [] Maximum: []

Data type: double >>

Lock output data type setting against changes by the fixed-point tools

Port dimensions: 1

Signal type: real